Valuing Protective Services of Mangroves in the Philippines

Technical Report

Wealth Accounting and the Valuation
of Ecosystem Services
www.wavespartnership.org

IH cantabria

The Nature
Conservancy

Team at the Institute of Hydraulics at the University of Cantabria

ÍÑIGO J. LOSADA RODRÍGUEZ

PELAYO MENÉNDEZ FERNÁNDEZ

ANTONIO ESPEJO HERMOSA

SAÚL TORRES ORTEGA

PEDRO DÍAZ SIMAL

FELIPE FERNÁNDEZ PÉREZ

SHEILA ABAD HERRERO

NICOLÁS RIPOLL CABARGA

JAVIER GARCÍA ALBA

Team at The Nature Conservancy

MICHAEL W. BECK

SIDDHARTH NARAYAN

DANIA TRESPALACIOS

ANGELA QUIROZ

Suggested Citation:
Losada, I.J., M. Beck, P. Menéndez, A. Espejo, S. Torres, P. Díaz-Simal, F. Fernández, S. Abad, N. Ripoll, J. García, S. Narayan, D. Trespalacios. 2017. Valuation of the Coastal Protection Services of Mangroves in the Philippines. World Bank, Washington, DC.

Points of contact:
Michael W. Beck, mbeck@tnc.org
Íñigo J. Losada Rodríguez, inigo.losada@unican.es

WAVES - Global Partnership for Wealth Accounting and the Valuation of Ecosystem Services

Wealth Accounting and the Valuation of Ecosystem Services (WAVES) is a global partnership led by the World Bank that aims to promote sustainable development by mainstreaming natural capital in development planning and national economic accounting systems, based on the System of Environmental-Economic Accounting (SEEA). The WAVES global partnership (www.wavespartnership.org) brings together a broad coalition of governments, United Nations agencies, nongovernment organizations and academics for this purpose. WAVES core implementing countries include developing countries—Botswana, Colombia, Costa Rica, Guatemala, Indonesia, Madagascar, the Philippines and Rwanda—all working to establish natural capital accounts. WAVES also partners with UN agencies—UNEP, UNDP, and the UN Statistical Commission—that are helping to implement natural capital accounting. WAVES is funded by a multi-donor trust fund and is overseen by a steering committee. WAVES donors include—Denmark, the European Commission, France, Germany, Japan, The Netherlands, Norway, Switzerland, and the United Kingdom.

Table of Contents

EXECUTIVE SUMMARY

Mangroves and other coastal ecosystems act as natural defenses that protect people and property from storms, floods, erosion, and other coastal hazards, reducing coastal risk. Mangroves protect coastlines by decreasing the risk of flooding and erosion. The roots of mangroves retain sediments and prevent erosion, while the prop roots, trunks and canopy reduce the force of incoming wind and waves and reduce flooding. Yet the value of these ecosystems is often not fully accounted for in policy and management decisions, and thus they continue to be lost at alarming rates, increasing the risk faced by coastal communities. Between 1980-2005, the world lost 19% of its mangroves. The Philippines has lost hundreds of thousands of hectares of mangroves in the last century. When mangroves are degraded or destroyed, the coast line becomes more exposed to the destructive impacts of waves and storm surge, and coastal communities have greater risks from the impacts of storms, floods, and sea level rise.

The Philippines is at high risk from coastal hazards and natural defenses can help reduce these risks. Between 2005 to 2015, 2,754 natural hazards affected the Philippines: 56% of property damage was caused by typhoons and storms, and another 29% was caused by floods. Due to a recognition of these increasing risks, and of the potential role of natural defenses to reduce these risks, the Government of the Philippines has committed to restoring mangroves as part of its risk reduction strategy, and the Philippines WAVES program on natural capital accounting is helping the Philippines incorporate the value of mangroves into their national accounts.

This Technical Report, and its accompanying Policy Brief, provide a social and economic valuation of the flood protection benefits from mangroves in the Philippines. This work aims to support decisions across development, aid, risk reduction and conservation sectors as they seek to identify sustainable and cost-effective approaches for risk reduction.

This Technical Report applies the Expected Damage Function approach recommended by the World Bank to quantify the risk reduction benefits from mangroves in the Philippines. Using high-resolution flooding models, the Report examines the flooding that would occur with and without mangroves under different storm conditions throughout the Philippines, and estimates the annual expected benefits of mangroves for protecting people and property in social and economic terms. The report examines flooding under regular storms and under extreme conditions (e.g. typhoon) and compares the people and property damaged under 3 different scenarios of mangrove cover: historical mangrove cover (1950), current mangrove cover (2010), and no mangrove cover. The protection services of mangroves are valued nationally across the Philippines using national models. The values obtained from these national models are compared to values from sensitivity analyses in a few locations (i.e., Pagbilao and Busuanga) calculated with very high-resolution data and models, so that the results of the national models may be verified.

In summary, the key findings are:

- In the Philippines, if the current mangroves (data from 2010) were lost, 24% more people would be flooded annually, i.e., an additional 613,000 more people many of whom live in poverty.

- Damages to residential and industrial property would increase by 28% to more than US $1 billion annually; and 766 km of roads would be flooded.

- One hectare of mangroves in the Philippines provides on average more than US $3200/ year of direct flood reduction benefits.

- Based on the Philippines's current population, the mangroves lost between 1950 and 2010 have resulted in increases in flooding to more than 267,000 people every year. Restoring these mangroves would bring more than US $450 million/year in flood protection benefits.

- Mangroves provide the most protection for frequent lower intensity storms (for example, 1-in-10 year storm events). For more catastrophic events, such as the 1-in-25 year storm, they provide more than US $1.6 billion in averted damages throughout the Philippines. When combined with built infrastructure, mangroves provide an effective defense against storms and coastal flooding.

- The results are presented in maps that show the spatial variation in the flood reduction benefits provided by mangroves to identify the places where mangrove management may yield the greatest returns.

Incorporating the value of these ecosystem services into a country's system of natural capital accounts can ensure that these ecosystems are accounted for in policy and management decisions. Currently, only a subset of the benefits provided by ecosystems is valued, usually extractive services such as fish and timber harvests. Many critical services that rely on keeping ecosystems intact, such as flood protection and climate mitigation, are rarely valued. This encourages short-term over-exploitation and reduces the quantity and quality of the goods and services provided by natural capital. Better valuations of the protection services of coastal habitats may halt the loss of our natural capital and ensure the provision of ecosystem services- what gets measured, gets managed.

Mangrove conservation and restoration can be an important part of the solution for reducing coastal risks. By valuing these coastal protection benefits in terms used by finance and development decision-makers (e.g., annual expected benefits), these results can be readily used alongside common metrics of national economic accounting, and can inform risk reduction, development and environmental conservation decisions in the Philippines.

1 | Introduction

1.0   Section Overview

This section provides the context and background for the modelling of the protective services of mangroves in the Philippines. This Technical Report was commissioned by the World Bank Wealth Accounting and the Valuation of Ecosystem Services (WAVES) program in the Philippines. The program is intended to support the Philippine government strategy for incorporating the value of ecosystem services, including coastal protection, into their natural capital accounting system. To support the government's strategy, the Philippines WAVES program on natural capital accounting includes a component on the ecosystem services of mangroves, including the coastal protection services of mangroves. The objective of this Technical Report is to help the Philippine WAVES program and the Philippine government construct these mangrove accounts by providing a methodology for quantifying the protective role of mangroves.

The Philippines is among the most at-risk countries in the world (Beck 2014, World Risk Report 2016). Typhoons, storms and floods account for around 80% of the total losses from disasters, with estimates of annual average losses totaling nearly US $3 billion (NEDA 2017, UNISDR 2015a). More than 60% of the country's 101 million people live on the coastline[1] and are heavily dependent on its natural ecosystems for resources and livelihoods. The Philippines has lost approximately half of their mangrove habitat over the past century, thereby losing the protective benefits of these coastal ecosystems. Realizing the risk reduction role of mangroves, the Government of the Philippines has committed to restoring mangroves as part of its coastal protection strategy. There is now broad interest in incorporating the value of ecosystem benefits into natural capital accounting

frameworks to ensure better management, and in green investments for risk reduction.

To assess the coastal protection services of mangroves, this Report follows a five-step methodology recommended by the World Bank (World Bank 2016). The five steps involve: estimation of offshore dynamics; estimation of nearshore dynamics; the influence of habitats; estimation of coastal impacts with and without habitats; and estimation of the resulting flood damages to people and property with and without habitats. (More detail will be found in Section 1.6.) The methodology evaluates the protective services of the habitats – in this case, mangroves –in terms of avoided flood damages to people and property. This Report uses two national scale analyses and one local scale analysis. The national scale analyses look at flooding from waves and from historical tropical cyclones using a simplified one dimensional (1-D) numerical model. The local scale analysis uses a higher resolution, two dimensional (2-D) model to look at flooding from an extensive synthetic database of tropical cyclones. All the analyses assess habitat values under three scenarios: historic mangrove cover (i.e. mangrove cover in 1950); current mangrove cover (i.e., mangrove cover in 2010); and an 'extreme' future scenario where all mangroves are lost.

The report examines the role of mangroves in reducing the flooding risks from 'regular' climate conditions (including daily ocean waves and sea level conditions) and from extreme conditions (including local and specific extreme events and tropical cyclones). It measures the protective services that mangroves offer today under existing mangrove cover, and the protection services that have been lost over the past half century due to mangrove degradation and loss. It calculates the people and property that would be affected by flooding under these

---

[1] http://sdwebx.worldbank.org/climateportalb/home.cfm?page=country_profile&CCode=PHL&ThisTab=Dashboard

scenarios, including the people under poverty affected by flooding. The protection services of mangroves are valued nationally across the Philippines, and locally in Pagbilao; the local study serves to validate the accuracy of the national results.

1.1 Coasts at Risk

The 2011 Global Assessment Report (GAR) on Disaster Risk Reduction highlights that the risk of economic loss due to tropical cyclones, storm surge and floods is growing as the exposure of economic assets increases and the health of coastal ecosystems degrades. Already, the proportion of the world's GDP annually exposed to tropical cyclones has increased from 3.6 % in the 1970s to 4.3 % in the first decade of the 2000s (UNISDR 2011). In 2011, insured losses from natural disasters (especially coastal and riverine hazards) reached an all-time high. Erosion, flooding, and extreme weather events affect hundreds of millions of vulnerable people, important infrastructure, and economic activity, and cause significant losses to national economies. The impacts of coastal hazards such as tropical cyclones can be devastating to coastal economies. These impacts will continue to worsen with continued climate change.

The Philippines is one of the most at risk nations to the impacts of coastal storms. It ranks as the nation with the third highest number of recorded landfalls of tropical cyclones and the second most landfalls over the past 5 decades[2]. The Philippines are also socially vulnerable to storm exposure: they rank third, after Vanuatu (1st) and Tonga (2nd), for countries with the highest disaster risk in the world (World Risk Report 2016). The National Economic and Development Authority (NEDA) identifies that coastal hazards contribute significantly to the population's vulnerability, and that storms such as Super Typhoon Yolanda (Haiyan) have slowed progress in poverty alleviation (DRR Platform 2014).

The Philippines has extensive experience with disaster risk reduction. Government policies mandate assistance to local communities that conduct vulnerability and risk assessments. Between 2006-2011, the Philippine government launched the READY Project, a multi-agency initiative led by the National Disaster Coordinating Council (NDCC) to address disaster risk management at the local level in 27 high risk Philippine provinces. Building on the outputs of the READY Project, the National Operational Assessment of Hazards (NOAH) Program, led by the DOST, provided enhancements to existing geo-hazard vulnerability assessments and maps through sophisticated, scenario-based mapping which integrate probabilistic climate modelling and simulation.

The Philippine Development Plan of 2017-2022 includes strategies to rehabilitate and restore degraded natural resources, protect fragile ecosystems and improve the welfare of resource-dependent communities (NEDA 2017). However, efforts to integrate disaster risk reduction and climate change adaptation in to comprehensive land use and development plans are hampered by many factors, including the limited availability of appropriately-scaled probabilistic hazard maps and the lack of capacity to use this geospatial information when it is available. Funding for adaptation and hazard mitigation is limited particularly as much of the available resources are needed for relief and recovery.

1.2 The Role of Mangroves in Coastal Protection

Coastal and marine habitats, particularly coral reefs and mangroves, can substantially reduce vulnerability and risk, providing natural protection from waves, wind and storm surge. Both mangroves and reefs are now regularly cited in both conservation and development literature for their role in natural coastal protection; i.e. for their value in reducing the impacts of coastal erosion

---

[2] http://www.aoml.noaa.gov/hrd/tcfaq/E25.html

and inundation during storms, as well as providing important co-benefits for fisheries production, tourism, and in the case of mangroves, carbon sequestration.

Seagrasses were not included in this study because data on the national distribution of seagrasses in the Philippines does not exist, and because this team currently lacks an operational model for the flood reduction benefits of sea grasses. It is also true that this team has not prioritized these models because the flood reduction benefits of seagrasses are much lower than those of mangroves and reefs.

Mangroves are particularly effective at providing coastal protection to people and property. The aerial roots of mangroves retain sediments, and prevent erosion. The mangrove's roots, trunks and canopies significantly reduce the drag force from incoming wind and waves. The entire structure can reduce the force of wind waves and flood waters. If mangroves are degraded or destroyed, the loss of their aerial roots leads to erosion, coastal regression, soil destruction and increasing water depth. The more exposed coastline is more vulnerable to the destructive impacts of waves and storm surge, and is at higher risk of coastal flooding and erosion. As mangroves are degraded and lost, more people and property are directly

at risk from the impacts of storms, floods, and sea level rise.

Despite the myriad of ecosystem services that they provide, the value of mangroves as 'green infrastructure' is still not fully recognized, and they continue to be lost and degraded. Global losses of coastal habitats are high: 30-50% of the world's wetlands have been lost (Zedler and Kercher 2005), 19% of mangroves were lost just between 1980-2005 (Spalding et al. 2010), and 75% of the world's coral reefs are rated as threatened (Burke et al. 2011). Often, the loss of these habitats is greatest around large populations- the places were the impacts of coastal degradation are greatest, and where the most people stand to benefit from coastal ecosystems. Sixty percent of the world population is expected to live in urban areas by 2030, with greater concentration around coastal areas[3]. This means that rates of coastal development will be increasing with heavy investments in coastal infrastructure and potential of loss of more coastal habitats.

1.3 Taking Nature into Account

There is a growing need for policies that encourage the conservation and restoration of habitats that provide coastal protection, in the places that yield the greatest protection benefits and are most cost effective
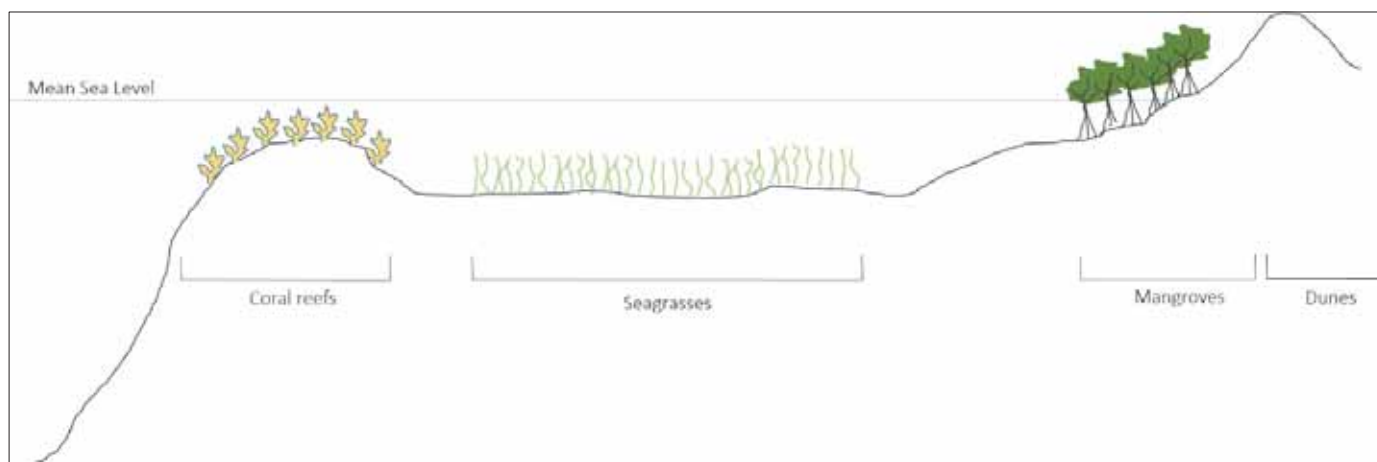

Figure 1 A conceptual representation of the distribution of natural infrastructure along a beach profile. Coral reefs, sea grasses, mangroves and dunes provide coastal protection services.

[3] http://www.who.int/gho/urban_health/en/

compared to other coastal protection strategies. Better valuations of the protection services from coastal habitats could inform decisions to meet multiple objectives in risk reduction and environmental management. One important pathway through which these services may be considered is in national economic accounts. The United Nations has identified a general approach for assessing ecosystem services in these accounts. To assist the development of these policies, the World Bank WAVES Policy and Technical Experts Committee commissioned "Managing coasts with natural solutions: Guidelines for measuring and valuing mangroves and coral reefs" (World Bank 2016). These guidelines show how to assess and value the coastal protection services of mangroves, seagrasses and coral reefs. The Guidelines recommend using process-based approaches, in particular the Expected Damage Function (EDF) approach for spatially explicit valuation of the coastal protection services from mangroves. The EDF is adapted from approaches commonly used in engineering and insurance to assess risks and benefits.

1.4 Mangroves in the Philippines

Mangroves in the Philippines provide a variety of ecosystem services to adjacent coastal populations, including food, timber, other livelihood activities, and coastal protection. Traditionally, rural Filipinos intensively used mangroves for fuelwood, construction, shellfish collection, fishing, and settlement (Walters 1997). Mangroves have significant economic importance for the poor and the most vulnerable coastal inhabitants, particularly the landless and women (Walters 1997).

In the Philippines, rates of mangrove deforestation have been among the highest in the world (Myers 1998) (Hamilton et al. 1989, Primavera 1991, 1995), and many of the remaining mangroves are highly degraded (Walters 1997). From 1950 to 2010, around 50,000 ha of mangroves were lost. In addition, the distribution of mangrove cover

has changed throughout the whole country. Figure 2 illustrates these two trends of mangrove loss and redistribution.

Many mangrove areas have been converted to aquaculture ponds or development despite the fact that these lands at low elevation are the most at risk to coastal hazards. The restoration of mangroves through conversion of abandoned fish ponds has been problematic due to land tenure issues as well as biogeochemical changes including acid sulfide build-up in the sediments (Primavera 1991). Some communities have left a small but critical strip of mangroves on the coastline, in part to help reduce erosion and to provide barriers for aquaculture ponds, in other parts to encourage sediment retention that may lead to new land. For example, Figure 1.1 (see Annex 1) shows land cover and land use change in a part of Pagbilao Bay.

The Philippines have a history of planting coastal mangrove trees in densely populated, highly degraded coastal watersheds. Research has shown that socioeconomic factors were more important than ecological factors in determining the relative success of restoration efforts (Walters 1997). One example is the Talabong Mangrove Sanctuary in Bais Bay, which has 200 hectares of nationally recognized nursery habitat for wildlife and fish. The Bais local government unit spearheaded restoration and rehabilitation efforts through a 'household planting' program, where coastal communities were encouraged to plant multi-species mangrove trees. Residents started small, private mangrove plantations to provide wood and other products (Walters, 1997). In another example, the Philippines Department of Environment and Natural Resources (DENR) encouraged planting and conservation of mangroves by local residents through 25-year private leases on intertidal land to encourage mangrove stewardship (Walters 1997).

Among the greatest challenges for mangrove conservation and restoration in the Philippines are population growth and coastal development. Between 2017 and 2022, there will be an additional 8.3 million Filipinos. Some regions, such as Metro Manila, will become denser, and increased concentrations will encourage land conversion. It is difficult to effectively enforce environmental laws. There is a lack of sustainable financing, and limited access to funding for climate change adaptation, disaster and risk reduction and insurance products for local governments. Furthermore, there is a lack in capacity to use science-based information. The private sector, which could complement government efforts by providing risk transfer mechanisms, has so far been minimally involved.

1.5 Measuring the Protective Services of Mangroves in the Philippines

In the wake of several destructive typhoons, the Government of the Philippines has committed to restoring mangroves as part of its coastal protection strategy under the National Greening Program. A recently issued Executive Order "Expanding the Coverage of the National Greening Program" (EO 193 s. 2015) further identified the critical role of forests including mangroves.

To support the government's strategy, the Philippines WAVES program on natural capital accounting includes a component on the ecosystem services of mangroves, including carbon sequestration, ecotourism, and coastal protection services. The development of mangrove accounts, and their inclusion into the Philippines System of National Accounts, will enable the government to consider the protection services of mangroves, and will ultimately inform decisions surrounding disaster risk management, coastal zone management, and climate change adaptation.

To help the Philippine WAVES program and the Philippine government construct these mangrove accounts, this Technical Report provides a methodology for quantifying the protective role of mangroves in the Philippines. It examines the role of mangroves in reducing the flooding risks from 'regular' climate conditions (including daily ocean waves and sea level conditions) and from extreme conditions (including local and specific extreme events and tropical cyclones). It measures the protective services that mangroves offer today under existing mangrove cover, and the protection services that have been lost over the past half century due to mangrove degradation and loss. It calculates the people and property that would be affected by flooding under these scenarios, including the people under poverty affected by flooding. The protection

Figure 2 An illustration of mangrove loss and redistribution. The image on left shows the loss of mangrove cover in Roxas. The image on the right shows the redistribution of mangrove cover between 1950 and 2010 in Samar Island.

services of mangroves are valued nationally across the Philippines, and locally in Pagbilao; the local study serves to validate the accuracy of the national results.

1.6   Methods at a Glance

The methods used in this study for evaluating the protection services of habitats against coastal flooding follow the recommendations in the Guidelines for the Valuation of Natural Coastal Protection (World Bank 2016). Figure 3 visually summarizes the methods (see Annex 1 Figure 1.2 for more detail). First, an understanding of offshore dynamics is constructed from the historic databases generated by the Institute of Hydraulics at the University of Cantabria, which include historical time series of waves, astronomical tide, storm surge, mean sea level and wind. Then, using hydrodynamic models (SWAN and DELFT 3D), waves and water levels are propagated from offshore to nearshore, and over habitats (mangroves and coral reefs). In the fourth step, waves and water level are propagated on shore, and the flooding impacts are calculated. In the final fifth step, the coastal assets damaged by flooding under different habitat conditions (i.e with and without mangroves) are compared, and the benefits provided by mangroves are calculated.

In this report, we do not consider freshwater flooding. We only analyze coastal flooding due to ocean events and the role of mangroves in reducing these events. The models for freshwater catchment flooding are very different from the coastal flooding models. In the future it would be useful to combine models on freshwater and coastal flooding.

1.6.1   National and Local Scales

We examined flood risks and benefits at two different scales. At the national scale, we applied high resolution models across the country. For key test locations (e.g., Pagbilao) where better data (particularly bathymetric data) was available, we applied

the highest resolution models. The results of the national and local scales were compared to ascertain the accuracy of the national models with the higher resolution local models.

1.6.2 Assessing Flooding Under Two Conditions

A critical part of this work is the assessment of the extent of flooding from regular storms and tropical cyclones (also referred to as TC). To estimate this flood risk, we considered flooding data from two types of events, which we refer to as 'regular conditions', and 'extreme conditions' or 'tropical cyclones'. The first data set, for regular conditions, considers 30+ years of wave and water level data from the Philippines, which captures significant events of waves and storm surge, but does not capture the most extreme events produced by tropical cyclones. The second dataset considers the effects of tropical cyclones, the most extreme events, across the Philippines.

We use the following data for regular and extreme wave and surge conditions at local and national scales:
1- Regular Conditions:

   a. <u>National Scale</u>: Historical wave climate and Sea Level (from 1992 to 2015), 30m resolution of DTM and Hydraulically connected bathtub approach for coastal flooding using GIS algorithm.

   b. <u>Local Scale 1</u> (Pagbilao): Historical wave climate and Sea Level (from 1992 to 2015), 5m resolution of DTM and Hydraulically connected bathtub approach for coastal flooding using GIS algorithm.

2- Tropical Cyclones:

   a. <u>National Scale:</u> Historical Tropical Cyclones (from 1951 to 2015), 30m resolution of DTM and Hydraulically connected bathtub approach for coastal flooding using GIS algorithm.

Figure 3 Methodology to evaluate coastal protection services of ecosystems like coral reefs and mangroves. 1: Oceanographic data are combined to assess offshore sea states. Stage 2: Waves are modified by nearshore hydrodynamics. Stage 3: Effects of habitat on wave run-up and surge are estimated. Stage 4: Flood heights are extended inland along profiles (every 200 m) for four locally generated, storm events (10, 25, 50, 100-yr events) with and without mangroves. Stage 5: The land, people and built stock damaged under the flooded areas are estimated (see World Bank 2016).

b. Local Scale 1 (Pagbilao): Historic Tropical Cyclones (from 1951 to 2015), 5m resolution of DTM and Hydraulically connected bathtub approach for coastal flooding using GIS algorithm

c. Local Scale 2 (Pagbilao): Historic and Synthetic Tropical Cyclones (5000 years), 5m resolution of DTM and high resolution model for coastal flooding (RFSM-EDA).

Additional details may be found in the Annex.

1.6.3 Scenarios for Mangrove Cover

We analyze flooding in the Philippines under three different scenarios of mangrove cover in the Philippines:

1. Mangrove cover in 1950 (Defense Mapping Agency DMA): The first 'Historical Mangroves' scenario considers the mangrove cover that existed in 1950, when approximately 360,000 ha of the Philippines were covered by dense mangrove forests. This is the earliest comprehensive cover data available.

2. Mangrove cover in 2010 (DENR): The second 'current mangroves' scenario considers the mangrove cover that existed in the Philippines in 2010. This is the most recent comprehensive mangrove cover data available. Since 1950, there has been an evident loss of mangrove cover, and significant reduction in mangrove density. Mangrove cover in the Philippines

decreased from 360,000 ha in 1950 to 310,000 ha in 2010.

3. Without mangroves: The third scenario, 'No Mangroves', assumes a hypothetical situation in which all mangrove forests in the Philippines have been completely destroyed.

Figure 4 represents the three different mangrove cover scenarios in Pagbilao. Pagbilao, located on the northern shore of Tayabas Bay in Quenzon province, exemplifies the rapid mangrove lost that has characterized much of the Philippines: the loss of mangrove extent is evident between scenarios 1 and 2. The images also show a redistribution of mangrove cover, particularly visible in the middle of the bay.

1.6.4 People & Property Flooded

The analysis calculates the people and property affected by flooding, including the total population flooded, and the number of people below poverty affected. This study uses data from the 2015 Global Assessment Report on Disaster Risk Reduction (GAR15, UNISDR 2015a) on the economic value of residential and industrial stock. The GAR15 provides a global exposure database with a standard 5 km spatial resolution and a 1 km detailed spatial resolution on coastal areas, estimating the economic value of the exposed assets, as well as their physical characteristics in urban and rural

agglomerations. The variables included in the database are number of residents, and economic value of residential, commercial and industrial buildings (De Bono et al., 2015). The GAR15 database follows a top-down approach using geographic distribution of population and gross domestic product (GDP) as proxies to distribute the rest of socio-economic variables (population, income, education, health, building types) where statistical information including socio-economic, building type, and capital stock at a national level are transposed onto the grids of 5x5 or 1x1 using geographic distribution of population data and gross domestic product (GDP) as proxies (UNISDR, 2015c).

Our estimation of benefits from mangroves considers only the direct effects of mangroves on flood reduction, it does not consider the many other benefits from mangroves (e.g., fisheries, timber, livelihoods) and indirect impacts (e.g., business disruption from storms) on the local economies.

Figure 4 Mangroves scenarios in Pagbilao region: (1) Historical, (2) Current and (3) No mangroves scenario.

2 | Data Sources

2.0 Section Overview

The following section describes the data and the sources of data used in this study. Most of the hydrodynamic and coastline analyses use the latest, freely available, global data of the best possible resolution for climate and sea-level projections, tropical cyclone tracks, bathymetry, coastlines, topography and mangrove and coral reef cover. Additionally, the local scale analysis use a locally available 5 meter resolution IFSAR DTM for topography and a synthetic analysis of cyclone tracks based on historical tropical cyclones in the region. Exposure data on the number of people, property and roads were obtained from a mix of global databases and data provided by local authorities. The economic values of residential and industrial stock nationwide were estimated based on these datasets.

2.1 Coastline Data

The coastline is obtained from the NOAA database GSHH (Global Self-consistent, Hierarchical, and High-resolution Geography Database). Out of the 5 different resolutions provided in this database (i.e. full resolution (0.1 km), high resolution (0.2 km), intermediate resolution (1 km), low resolution (5 km) and coarse resolution (25 km)), this study uses the full resolution. Islands smaller than 2 km in perimeter are not considered. This study considers 32,859 km of coastline spread across 1,311 islands ranging in perimeter from 4,763 km to 1.98 km.

2.2 Bathymetry and Topography Data

Good bathymetry and topography are critical for these flooding analyses (Beck et al. In review, World Bank 2016). The availability and quality of bathymetry and topography datasets varied greatly across the Philippines- we used the best available data at both local and national scales.

For bathymetry, we used ETOPO 1:1.6 km resolution (1 arc min) global topo-bathy database, and SEAWIFS 1km resolution of coral reefs bathymetry worldwide. The global ETOPO bathymetry database is commonly used in regional and global flooding analyses. In tropical countries such as the Philippines, the bathymetry of shallow, nearshore coral reefs is critical for predicting flooding, because coral reefs play a critical role in wave energy dissipation by reducing waves reaching mangrove shorelines. However this type of bathymetry is currently not accounted for in ETOPO data or in other national and global flooding models (Beck et al. In review). We approached this problem by combining the ETOPO data with data from SeaWiFS project (NASA) that includes information about water depth over the coral reefs. With a spatial resolution of 1km, SeaWiFS bathymetry is the most accurate database that may account for a coral reef´s location and depth.

For topography, we used ETOPO 1: 1.6 km resolution (1 arc min) worldwide topo-bathy database, and SRTM 30 PLUS: 30 m across The Philippines. Adequate flooding analyses require high resolution topography data, or digital terrain model (DTM). For the national level analyses, the 30x30m horizontal resolution DTM elevation SRTM30M-PLUS (Shuttle Radar Topography Mission) was the best available data. For regional scale analysis using higher resolution flooding modelling approaches, IFSAR topography (available in Pagbilao) was used. It provides a DTM with a resolution of 5m. Figure 2.1 (see annex 1) illustrates the resolution of some of the different bathy-topo data that we used locally and nationally.

2.3 Mangrove Cover

This study used two different datasets for mangrove cover:

1. Historical Mangroves (1950): Topographic Maps at 1:50,000 Scale originally published by the US Army Service and compiled from aerial

photographs taken from 1947 to 1953 (http://www.namria.gov.ph/download.php). This is the earliest comprehensive mangrove cover data available.

2. Current Mangroves (2010): The most recent mangrove cover data available is from the 2010 Land Cover Mapping Project, which used high resolution satellite imageries such as the Advanced Very Near Infra-Red (AVNIR), Panchromatic Remote Sensing for Stereo Mapping (PRISM) and Satellite Pour l'Observation de la Terre (SPOT 5) to generate the land cover data for the Philippines. A total of 245 AVNIR images with 10 m resolution were used. For areas without AVNIR images, SPOT images with 10 m resolution were used.

2.4 Coral Reef Cover

In the Philippines, as in many tropical environments, coral reefs often exist alongside mangroves. Coral reefs are submerged natural structures which break waves and dissipate wave energy through friction, thus reducing the volume and force of water reaching coastlines. To adequately measure the water reaching mangroves, the effect of coral reefs must be taken into account. Our wave propagation model takes into account both the friction and wave breaking provided by coral reefs in the Philippines (see Figure 5).

This study uses the 2010 Millennium Reef Map Project, released by the United Nations Environmental Programme World Conservation Monitoring Center (UNEP-WCMC), to obtain a global spatial distribution of tropical and subtropical coral reefs. The data draws from multiple sources, including University of South Florida's Millennium Coral Reef Mapping Project Seascape database and the World Fish Centre in collaboration with WRI and TNC.

2.5 Climate Data

2.5.1 Wave Climate and Sea Level

Historical wave climate and sea level time series are required to evaluate the coastal protection role provided by mangrove forests in the Philippines. Most of the existing databases are hourly or 6-hourly averaged,

Figure 5 The coral reef cover (green) and mangrove cover (red) in Pagbilao, Luzon, in 2010.

i.e., regular wave climate, and do not capture peak extreme events like Tropical Cyclones.

We used GOW 2.0 (Global Ocean Waves), GOT (Global Ocean Tides) and DAC (Global Storm Surge) to obtain datasets for waves and sea level (See Table 1 and 2). We combined these three datasets to build a 36-year time series (1979-2015), which yielded results in 315,360 1-hourly measures of sea states.

The GOW 2.0 (Perez et al. 2017) database comes from CFS (http://cfs.ncep.noaa.gov/cfsr/) reanalysis which provides reliable time series of atmospheric pressure and the induced wind field worldwide with 0.25º resolution from 1979 to 2015 (http://ihpedia.ihcantabria.com/wiki/IH_DATA). The main data for the Philippines from GOW 2.0 database was wave height, peak period and

wave direction. The latest version of Global Ocean Waves improves the previous existing datasets with improved spatial resolution from 1.5º to 0.25º; and better captured local extreme events (see Table 2).

The DAC (Dynamic Atmospheric Correction) dataset is the worldwide water surface elevation induced by a pressure gradient and wind in the period 1992-2014 (Carrère and Lyard 2003). The model is forced by the pressure and wind speeds at 10m altitude provided by the European Centre for Medium-Range Weather Forecasts (http://www.ecmwf.int/en/research/climate-reanalysis) reanalysis. The storm surge database was recently extended for the period 1871-2010 (Cid et al. 2014, Cid Carrera 2015) by using the 20th Century Reanalysis ensemble (Compo et al. 2011) as a predictor to reconstruct global 20th century surge

	Forcing Method	Spatial coverage	Spatial resolution (latitude by longitude)	Time resolution	Time interval
Waves (GOW 2.0)	CFS	Global	0.25º	1h	1979 - 2015
Astronomical Tide (GOT)	TPX07+T-Tide	Global	0.25º	1h	1900-2099
Storm Surge (DAC)	ECMWF	Global	0.25º	6h	1979-2015

Table 1 Datasets for waves and sea level.

	Forcing Method	Spatial coverage	Spatial resolution (latitude by longitude)	Time resolution	Time interval
Waves (GOW 2.0)	CFS	Global	0.25º	1h	1979 - 2015
Astronomical Tide (GOT)	TPX07+T-Tide	Global	0.25º	1h	1900-2099
Storm Surge (DAC)	ECMWF	Global	0.25º	6h	1979-2015

Table 2 Oceanographic datasets used as input for the propagation model and their spatial and temporal resolution and historical time series.

levels. The Storm Surge time series (DAC) does not detect Tropical Cyclones events because storm surge is averaged every 6 hours, infra-estimating the peak of sea level during a TC event.

For the Mean Sea Level dataset, we assumed a constant sea level across the Philippines.

2.5.2 Tropical Cyclones

2.5.2.1 Historical Tropical Cyclone Tracks

This study used the International Best Track Archive for Climate Stewardship (IBTrACS) v03r08 (Knapp et al., 2010) provided by NOAA to characterize the tropical cyclone climate (typhoons) in the Philippines. This file contains ensemble mean data from observations performed by different institutions using various methods. Data contains 6-hourly information about tropical cyclone center location (latitude and longitude in tenths of degrees) and intensity

(maximum 1-minute surface wind speeds in knots and minimum central pressures in milibars) for all Tropical Storms and Cyclones observed from 1951 to date. Despite global satellite based observations started in 1966, the IBTrACS database covers from 1950 to 2014, thus existing some uncertainties and non-homogeneities before the 60s. In Figure 6, the historical tropical cyclone tracks making landfall in the Philippines from 1951 to 2014 are shown.

Historical tropical cyclone occurrence rates coincide with those obtained in previous works such as Cinco et al., 2016, with an average of 19.8 TCs/year in the Philippines Area of Responsibility and only 7.8 TCs/year making landfall.

A climatology frequency analysis indicates that tropical cyclones in the Philippines can occur in every calendar month, with the greatest tropical cyclone activity concentrated in July, September, October
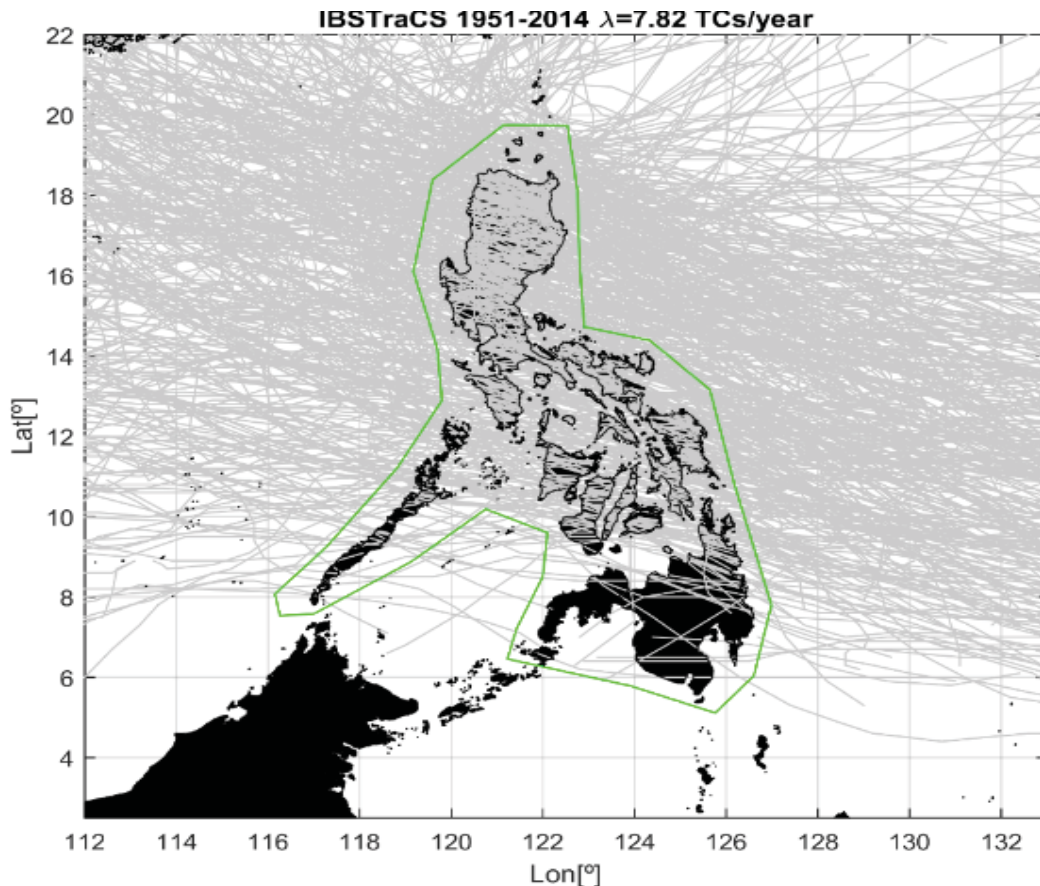

Figure 6 Historical Tropical Cyclone tracks (gray lines) making landfall in the Philippines from 1951 to 2014. The green polygon represents the coastal buffer used to identify land falling events.

and November (see Figure 7 and Figure 2.2 in the annex for more details). This is true for all categories of typhoons, form Category 1 tropical storms to violent Category 5 typhoons. Figure 10, also shows the spatial distribution of tropical cyclone activity, which indicates a strong latitudinal gradient with increasing number of tropical cyclones in north Luzon (nearly 1 tropical cyclone/year).

Typhoon activities in the Philippines are greatly influenced by monsoons and sea surface temperature in the Southern Pacific ocean. Many typhoons enter the Philippine Area of Responsibility (PAR) during the months of July to November when sea surface temperature is warmer compared

with the other months of the year. Typhoons usually make landfall between December and February, when the northeast monsoon is active.

2.5.2.2 Synthetic Tropical Cyclone Tracks

The amount of damage caused by tropical cyclones depends not just on the intensity of the cyclone, but also on its track. Therefore, observation data is not sufficient to properly define return periods for different associated hazards. To adequately capture the possible number of tropical cyclones that could impact a particular region, we use a stochastic method. Stochastic methods are
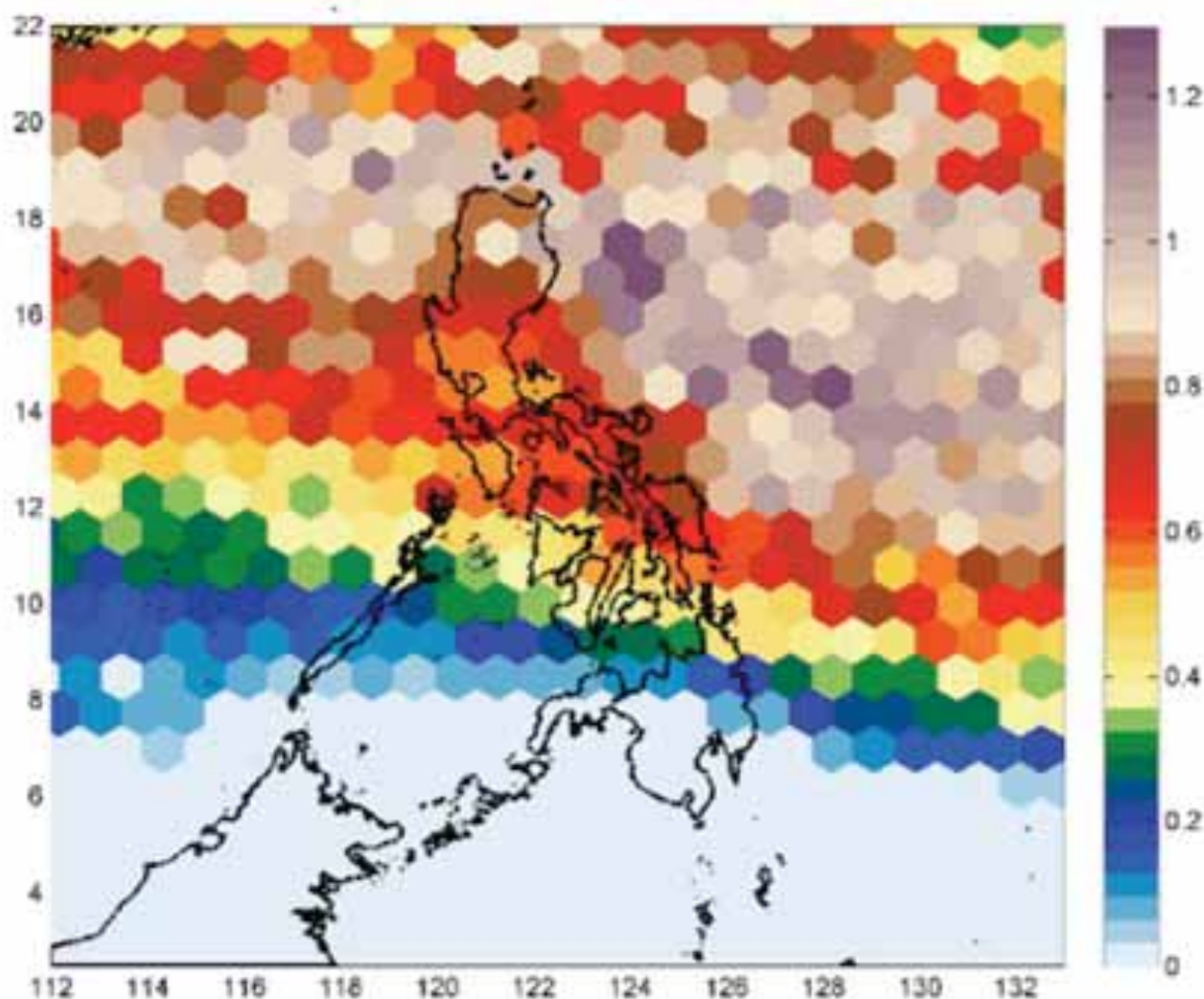

Figure 7 Spatial distribution of the tropical cyclone activity. The legend marks the number of cyclones per year passing through each grid cell, from 0 (light blue) to >1.2 (purple .The axes mark latitude and longitude.

based on Monte Carlo simulations in which the sequential development of tropical cyclones is calculated statistically from given statistical parameters of tropical cyclone data. The model used in this work is based on the work of Nakajo et al., 2014. Three tropical cyclone parameters are stochastically modeled: translation direction, speed, and minimum sea level pressure (see Figure 2.3 in Annex 1).

2.5.3 Tidal Gauges

To calibrate and validate the hydrodynamic model, data from six tide gauges was used, downloaded from the Global Sea level Observing System (GLOSS, http://www.gloss-sealevel.org) (see Figure 2.4 in Annex 1).

2.6 Exposure

The assets susceptible to damage were classified into five categories:

1. Population
2. Population below poverty
3. Residential stock
4. Industrial stock
5. Roads network

2.6.1 Population

The number and distribution of people in The Philippines was obtained from the WorldPop database (http://www.worldpop.org.uk/), which provides, globally, the number and location of people per hectare (100mx100m) residing in low and middle income country.
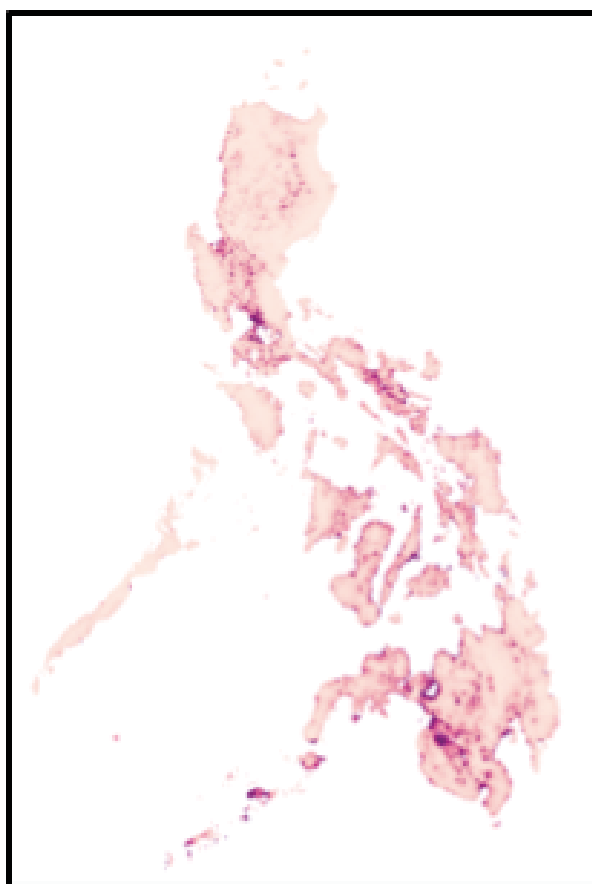
Figure 8 The spatial distribution of number of people living below poverty. Higher values are in darker shades.
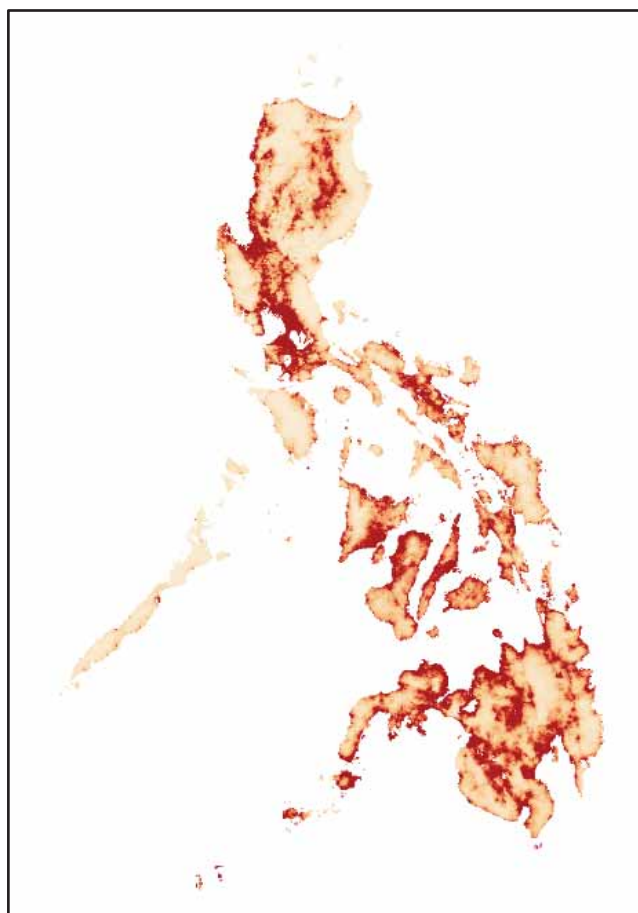
Figure 9 Residential stock distribution (US $ millions). Darker shades indicates higher values.

This project used the WorldPop 2010 population distribution layer. In addition to mapping population counts, WorldPop produces high resolution estimates of population demographics and characteristics which cover a range of factors, including age and sex structures, births, pregnancies and poverty. An example of the WorldPop database in The Philippines is shown in Figure 2.5 (see Annex 1).

2.6.2 Population Below Poverty

The data for the percentage of population below poverty was provided by local authorities. This information was disaggregated at the municipal level (see Figure 8). The data were transformed from shape layer to raster, then the resulting raster was multiplied by the total population layer

(previous section) to obtain the number of person per grid below poverty with the same 100m grid resolution of the original population layer.

2.6.3 Residential Stock

This study uses data from GAR15 (UNISDR 2015b), which includes the economic value of residential, commercial and industrial buildings, as well as hospitals and schools, the number of residents and the type of labor activities. GAR15 provides this data at 5km spatial (see Figure 9). GAR15 combines different sets of data to obtain its socio-economic information: population distribution (LandScan), night time light intensities (Visible Infrared Imaging Radiometer Suite, VIIRS), capital stock (Perpetual Inventory Method (PIM) and
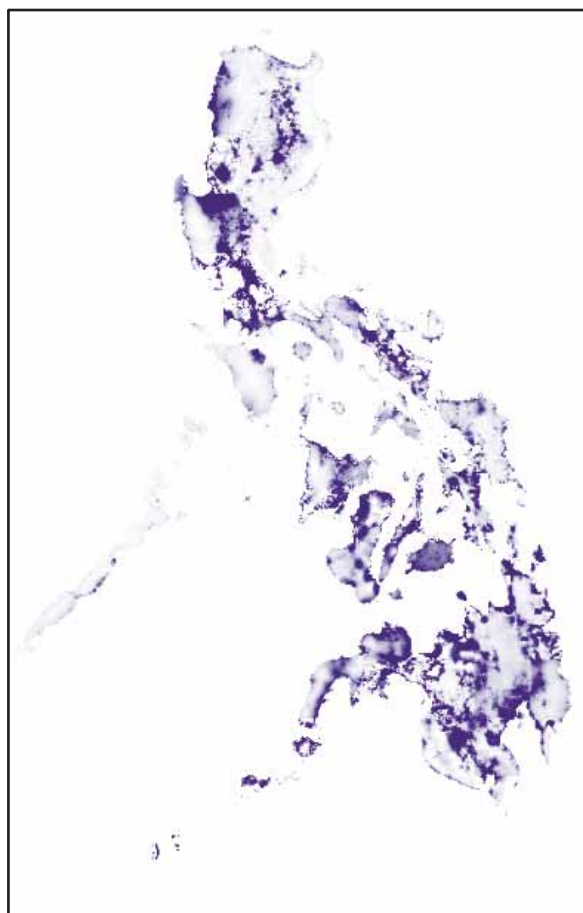
Figure 10 Industrial stock distribution (US $ millions). Darker blue indicates higher values.

historical Gross Capital Formation (GCF) data from World Bank), Gross Regional Product (GRP) distribution (from several sources) and different socio economic indicators (economic level, commercial, industrial, public, education and health data) as proxies to estimate the use of the building stock. (UNISDR, 2015c)

The study downscaled residential stock data in the following process:

1. For each point of GAR layer, the total population was calculated. Eight fields were summed: high, medium high, medium low and low income for both rural and urban population. GAR data is referenced to 2014, so an adjustment to 2015 WorldPop estimates was performed.

2. In each point of GAR layer, total residential stock was calculated. Eight

fields were summed: high, medium high, medium low and low income for both rural and urban residential stock.

3. In each point of GAR layer, residential stock per capita was calculated by dividing residential stock and adjusted population.

4. A raster layer was created for residential stock per capita. Inverse distance weighted interpolation was used for the creation of this raster.

5. Finally, using the population raster (from WorldPop, 100m resolution) the residential raster layer was calculated by multiplying residential stock per capita and population. A scale verification was done, checking that sum of residential stock from GAR layer was the same that the sum of residential stock raster layer created.
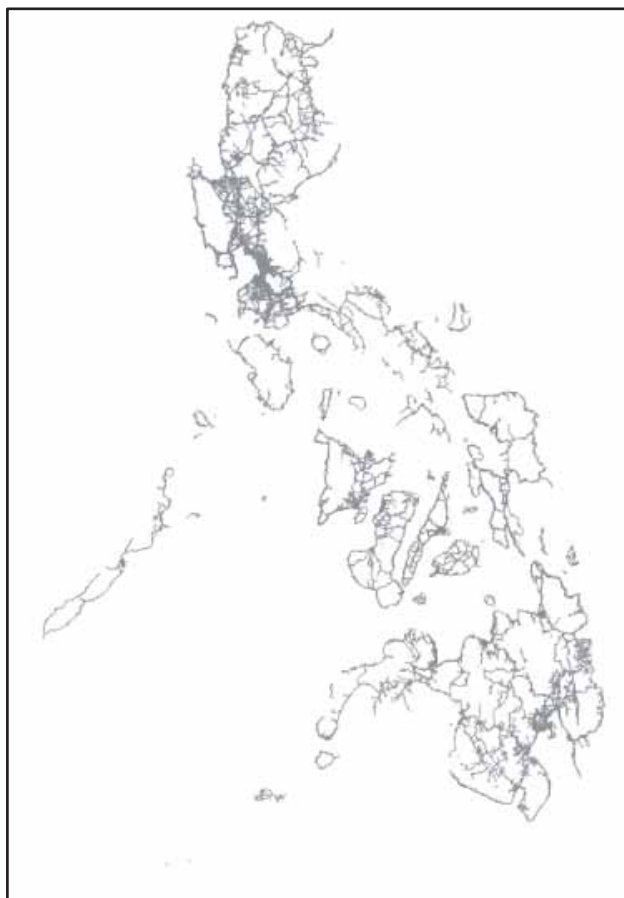
16

Figure 11 Road network distribution.

2.6.4 Industrial Stock

Mirroring the process used for the residential stock, the study used GAR data to calculate industrial stock.

1. In each point of GAR layer, total industrial stock was calculated. Two fields were summed: rural and urban industrial stock.

2. A distance to roads network raster layer was created with a 100m resolution. This layer shows for each cell the distance in meters to the nearest road.

3. A kriging technique was used to obtain a raster layer analyzing the relationship between industrial stock (from GAR points), population and distance to roads network.

4. The previous step can place some stock in places where there should not be (lakes, offshore), so the obtained distribution of industrial stock was cut with the administrative national borders.

5. A scale verification was done, checking that sum of industrial stock from GAR layer was the same that the sum of industrial stock raster layer created. (see Figure 10.)

2.6.5 Roads Network

The study used OpenStreetMap to characterize the roads network for the Philippines (see https://www.openstreetmap.org/export). This data includes categories from motorways to footways. We used data only for motorways, trunk, primary and secondary roads. This information was then transformed into a raster layer with 100m resolution. (see Figure 11.)

3 | Constructing the Coastal Profiles

3.0 Section Overview

This section describes the construction of cross-shore coastal profiles, used to estimate the propagation of waves and surge levels from the ocean to the inland extent of the floodplain. A profile was created at every 200 m along the Philippines' ~30,000 km coastline. Multiple steps were taken to ensure that the profiles were accurate, ran parallel to the bathymetric gradient (i.e. wave direction) and were limited to depths of less than 50 meters. The profiles were then paired with the nearest, most representative data points

for offshore dynamics, bathymetry and habitat cover. To reduce computational effort in estimating flooding along all these profiles, the profiles were grouped into 250 representative 'families' and the flooding was then estimated for each of these families.

3.1 Constructing the Coastal Profiles

To measure the flooding that occurs throughout the Philippine coast, we divide the coastline into equal sections, or 'profiles', every 200m. The resolution of the profiles chosen depends on the scale of this particular project. For example, a 2 km
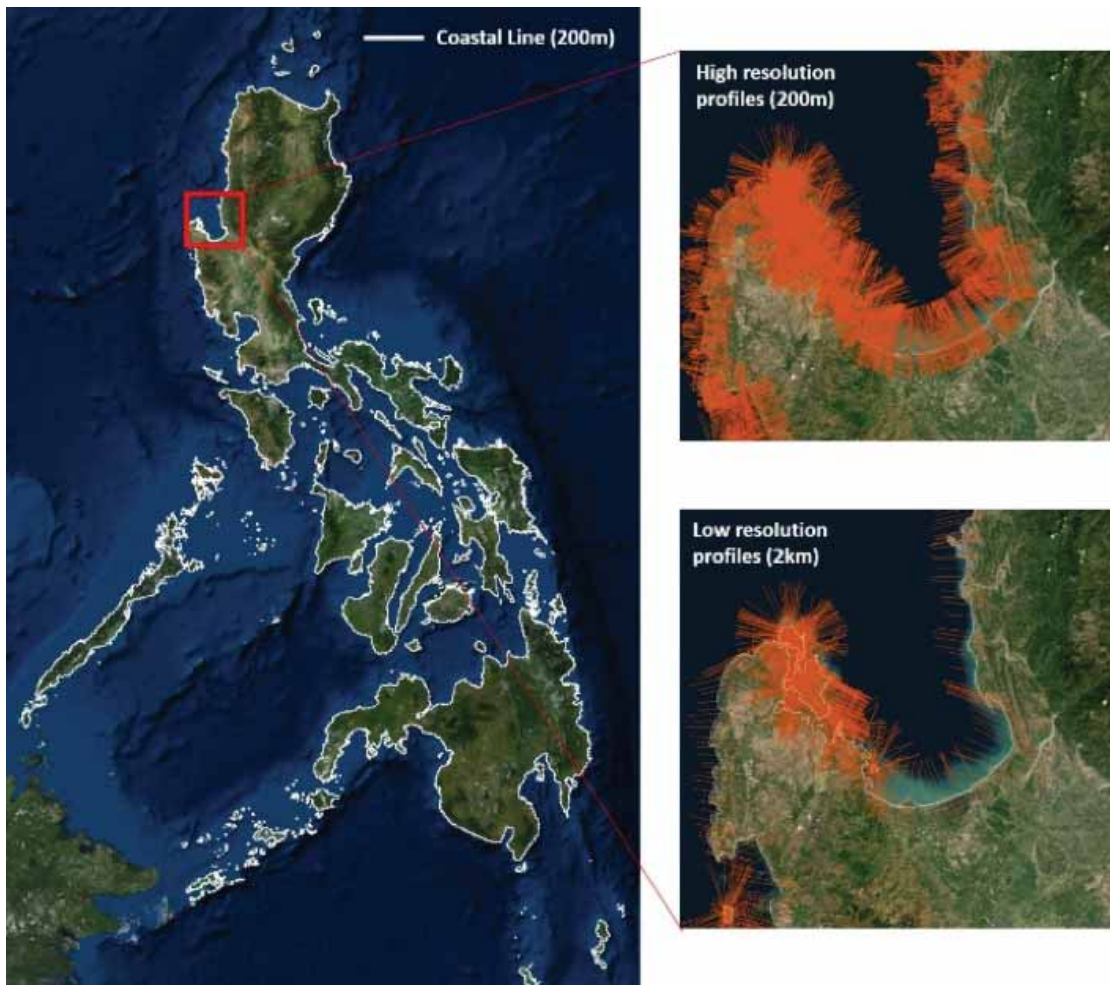

Figure 12 Coastline for Lingayen Gulf, derived from NOAA data. The left shows a 200m resolution, the top right shows a high resolution of 200m, the bottom right shows a low resolution of 2km

resolution is reasonable for global scale projects, however for national scale projects the resolution may be fine-tuned to 200 m. The advantage of having one profile for every 200 m is that the potential errors resulting from a two dimensional wave propagation process are reduced, and that more realistic values of coastal Total Water Levels may be generated. The disadvantage of using such a fine scale is that it requires a huge computational effort and the use of statistical tools to simplify a huge amount of profiles into representative clusters (see Section 4: Profile classification). An example of two different resolutions of coastal profiles (2 km vs 200 m) is shown in Figure 12 in Lingayen Gulf (Luzon).

The high resolution coastline obtained from the NOAA database GSHH (see section 2.1) allows the analysis of the Philippines coast at a 200 m resolution. The accuracy of these data will determine the accuracy of the hydrodynamic transformation of waves and sea level (astronomical tide + storm surge). Profiles are traced starting from offshore and moving towards the coastline. Care is taken to trace the profiles parallel to the bathymetric gradient, so that each profile tracks the main direction of waves as closely as possible. Since we are tackling a two dimensional problem using multiple one dimensional solutions, we omit a few important processes of wave transformation associated with wave direction (refraction and diffraction, for instance). To reduce the loss of information resulting from this omission, we orient profiles parallel to the expected wave´s direction (perpendicular to the contour lines) and with the highest resolution possible (every 200 m).

To obtain mean bathymetry gradients for each profile, we tested two methodologies.

1. Sector method: We generated an average value of the gradients within a 60 degree range on either side of the seaward transect perpendicular to the coastline of each centroid.

2. Circular method: We generated the average value of the gradients within a circle (diameter=10km) around each centroid.

The sector method reduces the number of incorrect profiles (that is, profiles that do not follow the wave direction) by 40% when compared to the circular method. Furthermore, on coastlines dominated by small islands and non-linear configurations, like those of the Philippines, the errors generated with circular method are greater because of the chaotic distribution of bathymetry gradients in these areas. We applied a few further corrective steps to the profiles. First, we eliminated profiles that started on land. Second, we eliminated profiles that followed the sequence 'sea-land-sea' from the coastline, seaward. These profiles generally occur in a bay or estuary and correspond to areas protected from waves. Thus, we assumed that no wave-induced flooding would occur at these coastlines, and eliminated the corresponding transects.

The final step was to limit the profiles to water depths of 50 m or less: at depths greater than 50 m, waves propagate differently, and the propagation model is no longer valid.

3.2 Profile Classification

In total, 171,888 profiles were drawn along 32,859 km of Philippine coastline. After creating profiles for every 200 m of coastline, and then refining them, we

intersected each profile with three data layers:

1. Bathymetry: SeaWifs (NASA) with 1 km resolution + ETOPO 1 (1.6km resolution)

2. Mangrove coverage in 1950 (DMA) and 2010 (LandCover) scenarios.

3. Coral reef coverage (Millenium Reef Map 2010, UNEP-WCMC)

The high computational effort required to analyze the propagation of waves over the ecosystems of such a huge number of profiles forced us to reduce the number of profiles to a few representative 'families' of profiles. We used a clustering technique, K-MEANS, to group or classify the profiles into 250 representative families of profiles in the Philippines. To build these families, we considered the water depth along the whole profile for every kilometer (resulting in 20 water depth values), and the type of bottom cover for every kilometer for three types of bottoms: sand, coral reef, and mangrove (resulting in 20 bottom cover values).

K-MEANS is a clustering method which aims to partition 'n' observations (171,888 profiles defined by their water depth and bottom type) into 'k' clusters (250 representative profiles, also defined by their water depth and bottom cover) in which each observation belongs to the cluster with the nearest mean. Although this is a challenging computational problem, there are efficient heuristic algorithms that converge quickly to a local optimum via an iterative refinement approach.

Three different K-MEANS classifications are performed, for the 3 mangrove coverage scenarios, resulting in 750 families of coastal transects profiles (3 scenarios x 250 profiles/ scenario).

4 | Modeling Coastal Habitats: Numerical Model DELFT 3D

4.0 Section Overview

This section describes the setup and validation of the Delft 3D numerical model suite used for these analyses. The suite comprises models simulating flow and wave conditions. The models use information on offshore hydrodynamics, bathymetry, topography and land cover and accounts for various physical processes. This section also describes the setup of the model and cross-shore profiles, inclusion of habitats as land-cover type inputs, model validation for offshore and nearshore regions, and some analyses of sensitivity to hydrodynamic inputs. More information on the physics behind the models, including the relevant equations, may be found in Annex 2.

4.1 Numerical Set-Up for 1D Simulations

For the study case, waves and flow were propagated over 1D profiles. To simulate 1D propagations with Delft 3D, a 2D mesh with 3 cells in Y-direction was created. X-direction is assumed to be perpendicular to the coast and was divided in 10 m spaced cells. Profiles are 20 km long and they extend 10 km shoreward and 10 km landward. In total the numerical mesh will have 2000 x 3 cells (X and Y directions). For an explanation of the physics and governing equations see Annex 2.

4.2 Modelling Coastal Habitats: Mangroves and Coral Reefs

Coastal habitats like coral reefs or mangroves are modeled by means of introducing a roughness value based on the corresponding Manning coefficient. Different values of Manning coefficient were adopted:

- Sand soil: n=0.02 (Zhang et al 2012)

- Mangroves: n=0.15 (Zhang et al 2012)

- Coral reefs: n=0.05 (Prager 1991)

4.3 Validation and Sensitivity Analysis

Two validations and two sensitivity analysis were implemented before applying DELFT 3D model for waves and storm surge propagation:

1- Offshore validation. A national scale mesh grid was tested with the aim of validating the capacity of the model of deep water sea level propagations.

2- Nearshore validation. One specific event (Tropical Cyclone in August 1987) was simulated and propagated over different mangrove forests typologies 2D and 1D.

3- Sensitivity analysis of DELFT 3D against storm surge intensity and duration in presence of mangroves (1D profile approach).

4- Sensitivity analysis of DELFT 3D against coral reef and mangrove presence or absence (1D profile approach).

These are further described in the following sections.

4.3.1 Offshore Validation

A numerical mesh of 5 km resolution was created. It covers all the Philippines (302x352 cells). ETOPO bathymetry was used in this first validation. Total Water Level and storm surge are the output variable validated with historical instrumental data.
To validate the Total Water Level induced by the previous mentioned forcing methods, six locations with bouys were chosen: Manila, Legaspi, Davao, Subic Bay, Curmao and Lubang. Additionally, two tropical cyclone events were simulated and validated: Typhoon Haiyan (November 2013), and Tropical Cyclone Nesat (September 2011).

The following forcing methods were tested:
a) Astronomical Tide

21

b) Wind

c) Astronomical Tide + wind

d) Astronomical Tide + wind + waves (swell conditions)

e) Astronomical Tide + wind + waves (wind conditions)

f) Wind + waves (wind conditions)

Two validation cases are shown as an example of the whole generated tests. It should be noted that no significant differences were observed between "wind" and "wind+waves" cases. Also, swell waves do not modify the Total Water Level due to the low intensity of the swell component in The Philippines with respect to wind components. In Annex 1 Figure 4.1 and Figure 4.2 show the high capacity of the model to reproduce offshore sea level induced by tropical cyclones.

4.3.2   Nearshore Validation

To carry out this analysis a simulation was run in the large-scale mesh of the Philippines for the tropical cyclone of August 1987. The simulation began one day after the start of the cyclone to stabilize the model. The simulations modeled the period from August 6, 1987 to August 15, 1987. The model was forced with the boundary conditions mentioned in the previous section. Results of the coarse mesh were stored at points with a time resolution of 1 minute for the coast of Pagbilao.

We performed 1D and 2D simulations of the cyclone. The 2D mesh has 468x234 cells of 100 meters of side. The time step is 30 seconds and the turbulent viscosity has been considered constant at 0.4 m^2/ s. In this mesh, we assumed that all boundaries are closed except the offshore boundary that has been modeled as a level condition. Based on the sea levels obtained at the boundary points in the coarse mesh, we assumed a constant sea level throughout the nearshore model domain. In

contrast, SWAN boundaries were divided into 5 parts of equal length to account for changes in wave height between the right and left side.

To simulate bottom induced friction, we considered 3 scenarios with spatially variable roughness: (1) without mangrove, (2) with the current mangrove extension and (3) with the historic mangrove extension. Manning's coefficients adopted the following values according to the soil type:

- Landward bottom type: n=0.033

- Seaward bottom type: n=0.02

- Mangroves: n=0.15

When comparing the 1D and 2D simulations, we found that the model can not show the effect of the mangroves due to the short length of the mangrove profile and the wave period. In the 2D model, the total water level slightly increases without mangroves, resulting in lower flood speed but larger flood extents.

In conclusion, in order to capture the effect of mangroves when using the DELFT 3D model, greater mangrove cover and higher model resolution (i.e. decreasing cell size 100 m to 10 m) is required. In other words, the smaller cell size, the better the model will be able to simulate wave and sea level propagation in mangrove areas.

4.3.3 Sensitivity Analysis: Storm Surge Intensity and Duration

We performed a set of theoretical simulations of a storm-surge event on a 1D grid of 5001 cells of 5 m sides, and we analyzed the following parameters:

- Length of area covered by mangrove: 0, 2, 4, 6, 8, 10, 12 and 15km.

- Storm-surge duration: 2, 4, 6 and 8 hours.

- Maximum level (m) reached by storm-surge: 0.5, 1, 2 and 3m. All storm-surge have been generated as a Gaussian pulse.

Mangrove cover was assigned a Manning coefficient of 0.15. And any other bottom type is assigned a coefficient of 0.02 (i.e., in essence assumed to be bare bottom).

The coastline is located at x=12.5 km. Mangroves extend seaward from x=12.5km until the corresponding mangrove length.

The following conclusions are derived from the analysis:

- For the same storm surge, longer pulse durations and lower friction result in more flooding.

- Storm surge duration is the most critical variable affecting flooding level.

- Larger mangroves decrease water level (dissipation) and, consequently, the flooding extension.

To ascertain how the DELFT 3D model is able to provide the Total Water Level for different bottom types, four cases were run in a 1D numerical mesh:

1. A profile with mangroves and with coral reefs

2. A profile only with mangroves

3. A profile only with coral reefs

4. A profile without mangroves and without coral reefs

The Total Water Level in the coast was obtained for each case. Results show that the presence of both coral reefs and mangroves provide more than a 149% reduction in flood height as compared to case 4, with no mangroves and no coral reef. We also find that mangroves alone provide more than a 102% reduction in flood height (relative to the no habitat case), while coral reefs provide an additional reduction in flood height of 8%. Figure 13 shows the results of the sensitivity analysis for storm surge duration of 2 and 8 hours. Annex 3 provides the computational costs for these DELFT 3D simulations.

In conclusion, mangroves contribute significantly to storm surge reduction; reefs do not contribute greatly to storm surge reduction. Reefs however contribute primarily to flood reduction through wave (not surge) attenuation.
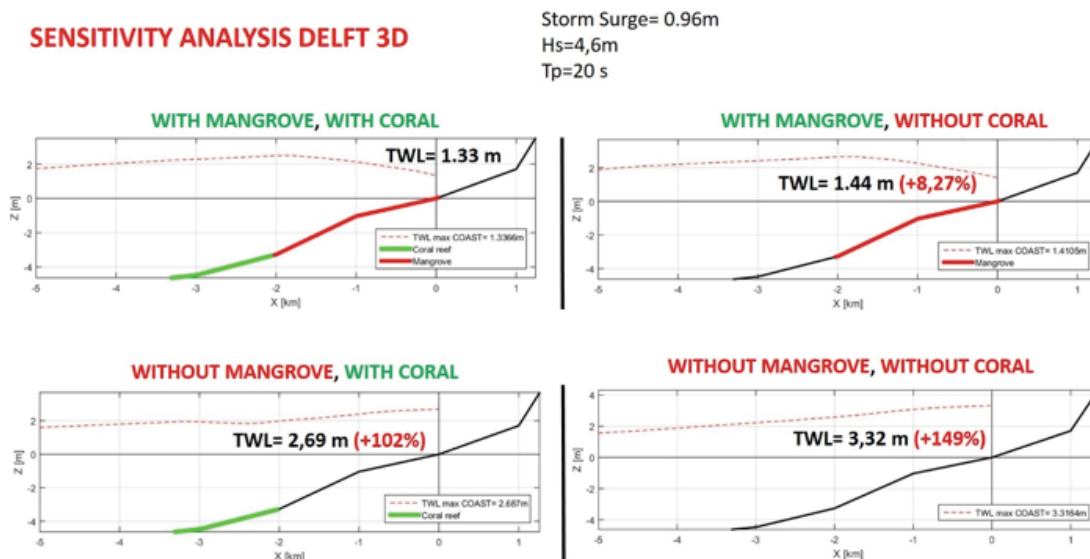
Figure 13 Sensitivity analysis of the effects of habitat on the reduction of flood height in DELFT 3D. Four cases are examined considering water level or flood height (z) with and without reefs mangroves. The black lines represents the elevation profile above (z>0) and below water. The green and red lines indicate where reefs and mangroves occur along the profile respectively. The red dashed line indicates the water level (flood height) across the profile.

5 | Regular Wave Climate

5.0 Section Overview

This section describes the process for estimating the coastal flooding that occurs under 'regular conditions'. First, data on hourly offshore wave conditions are associated with each cross-shore profile. Next, after excluding any wave conditions that occur due to tropical cyclones to avoid double counting (see Section 6), the maximum values of specific wave parameters are selected. The final selection of offshore waves is then grouped into representative families of wave-climate to reduce computational effort. The waves from each of these families are propagated to the

coastline over the profiles using the Delft 3D modelling suite, for each of the three mangrove scenarios (historic, current and total loss). The final total water levels at the shoreline determine the 'flood height' for each scenario. The difference between these results indicates the protective capacity of mangroves for wave-induced flooding.

5.1 Offshore Dynamics

The total water level due to regular hourly wave conditions is estimated for 171,888 profiles perpendicular to the shore across the entire country. Each profile is associated with a coastline point (see Figure 14). First,
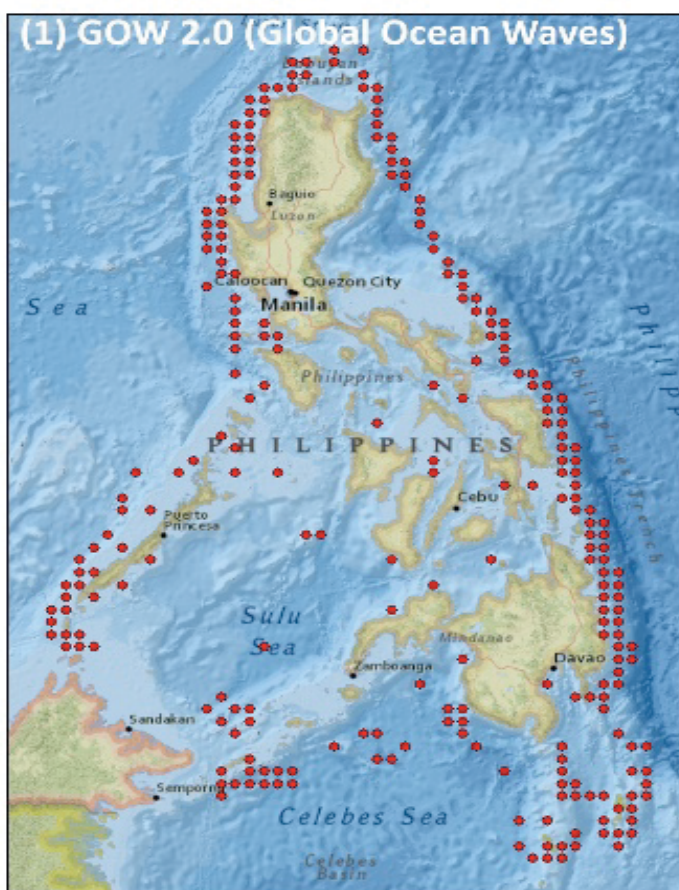
Figure 14 Spatial distribution of offshore data points. To calculate offshore ocean dynamic, a global ocean waves database was used to obtain data on for tides, storm surge and wind for each of the red points. Mostly, the distribution of the points is constant. (See Annex 1 Figure 5.1 for the distribution of data points for the other offshore databases).

offshore hydrodynamic measurements are assigned for each coastline point based on global data, and are used to estimate nearshore wave heights. Based on these measurements, the total water level at each coastal point is obtained. Then, the effect of vegetation on the total water level is assessed for 3 mangrove scenarios (see Section 4).

Offshore wave climate and sea level statistics are obtained for all of Philippines to have an overview of the national distribution of

waves, astronomical tide, storm surge and wind. Sea level rise projections for an RCP 8.5 scenario for the end of the century are also included (Slangen 2014) to indicate areas that could be vulnerable future climate change (see Figure 15).

The nearest offshore measurements of waves (GOW 2.0), astronomical tide (GOT) and storm surge (DAC) are identified and assigned to each coastline point in the Philippines. The mesh resolution of the national model at the coastline is 200 m.
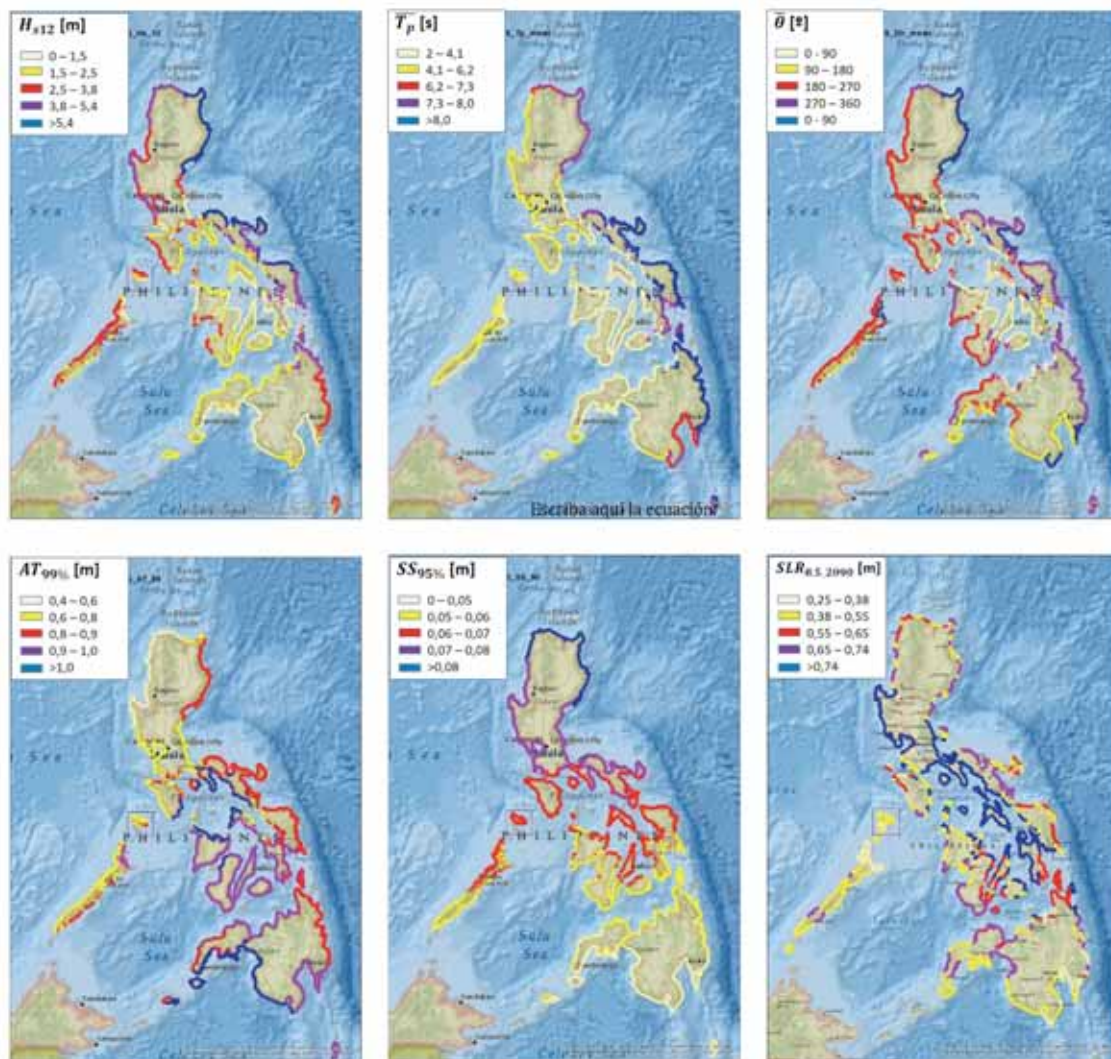
Figure 15 Statistics of Ocean Dynamics and Sea Level: (1) Significant wave height exceeded 12h/year, (2) Mean Peak Period, (3)Mean Wave Direction, (4) Astronomical Tide exceeded 1% of the time, (5) Storm Surge exceeded 5% of the time and (6) Sea Level Rise in 2090 according to RCP 8.5 (Slangen 2014)

However, the resolution of the global offshore datasets is 25 km (0.25°). Therefore, every 25 km of the coastline uses the same offshore measurements. Figure 14 and Figure 5.1 in Annex 1 shows the spatial distribution of the offshore database points in The Philippines.

To reduce errors in translating the offshore data into nearshore values, two conditions are followed in assigning these points: (1) the offshore point must be inside the influence area of the coastal point, which is defined by a triangle oriented +/-30° seaward; (2) where there are multiple points within a triangle, the nearest point to the coastline point is chosen. This method minimizes errors in choice of appropriate offshore points that can be critical in island regions where the directionality of waves is highly conditioned by which side of the island is being considered (see Annex 1 Figure 5.2).

5.2 Wave climate selection process

Each of the 171,888 coastline point and profiles is associated with a 36-year time series (1979-2015) of hourly sea state (wave and sea level) measurements, making a total of 315,360 hourly sea states (see Section 2.5). To assess flooding from regular wave climates, and to avoid double-counting of extreme conditions in subsequent analyses of tropical cyclones, the time-series is filtered to remove extreme sea-state measurements that represent tropical cyclones (tropical cyclone induced flooding is calculated in Section 6). 207 tropical cyclones (TCs) are detected between 1979 and 2015 and filtered out of the record using information from the cyclone occurrence databases (see Figure 16). The filtered sea states are then grouped into 120 families by applying a K-MEANS algorithm. Each family has information on the following parameters:

- Significant wave height (Hs)

- Peak Period (Tp)

- Wave´s direction (θ)

- Sea Level (SL), which is the summation of the Storm Surge and Astronomical Tide

In total, there are 3,225 offshore points that contain hourly time series data for the parameters Hs, Tp, θ and SL. The closest sea states to the coastline, as defined in the national numerical mesh (5km X 5km), are used as inputs to the 1D Delft-3D model to simulate the propagation of waves over mangroves and coral reefs.
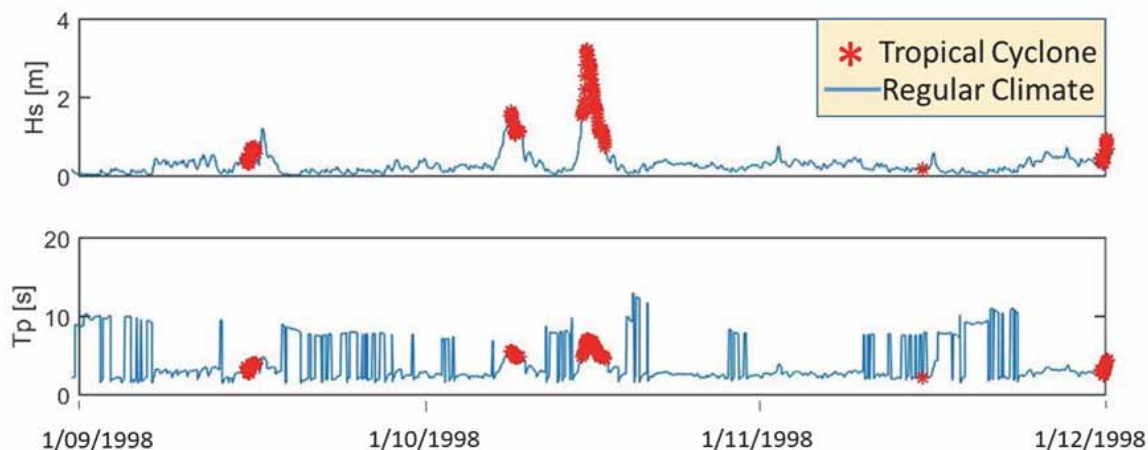

Figure 16 Example of the process for identifying tropical cyclones (red dots) within regular wave climate (Hs, Tp), Sea Level and Wind speed time series

5.3 Habitat pathway: 1D propagation

Next, we simulate wave propagation from offshore to the shoreline, over vegetation. This is done for 120 representative sea states at each of the 250 theoretic profiles (see Section 4), and for each of the 3 mangrove scenarios, making a total of 90,000 simulations. These simulations are performed in Delft-3D. The Flow and Wave modules are coupled (i.e. run simultaneously) for a simulation time length of 60 minutes. The numerical boundary conditions assume a non-stationary process with a triangular time-evolution of Hs and a constant SL within each sea state.

The output of each simulation provides the Total Water Level time series for every 10 m. However, we are only interested in the maximum Total Water Level at the shoreline (henceforth, referred to as "Flood Height"). From the outputs of the 90,000 simulations, 750 "look-up tables" or "interpolation tables" of Flood Height are created. Each one of the 750 profile families thus have their own interpolation table with 120 sea-state parameter combinations of Hs, Tp, SL and θ and the associated output, Flood Height.

These look-up tables can now be used to quickly estimate wave and surge dissipation by mangrove forests. The input variables needed to make these estimates would be the sea state parameters (i.e. Hs, Tp, SL and θ) and the vegetation characteristics (i.e. mangrove length and average water depth in the mangroves)

5.4 Flood height reconstruction

The simulations of wave and sea level propagation over the 1D representative profiles result in 90,000 theoretical values of Flood Height. However, the goal is to reconstruct the Total Water Level in the whole coast of The Philippines. To do this, we first generated a look-up table to estimate the Total Water Level for each representative profile for each mangrove scenario. The interpolation tables allow estimation of Total Water Level based on the 4 sea-state parameters for each of the 120 representative sea states. Using these tables, a Total Water Level is obtained for every profile across the country for the entire period (hourly from 1979-2015).

Extreme values of Total Water Level for the average wave climate simulations are obtained using a Peak-Over-Threshold method with the threshold set at 98% (i.e. the top 2% of all values are defined as extreme). To ensure time-independence of the selected data points, values that occur within 3 days of a previous value are excluded. A Pareto-Poisson distribution is then applied to the selected values to obtain a return period distribution for the extreme Total Water Levels. Since the collected data only span 36 years, the maximum return period should not exceed this order of magnitude. Here, we assumed that 36 years of data allows us to obtain 50 years return period events. The Flood Height is thus estimated every 200 m across the entire country's coastline for four return periods of 1, 10, 25 and 50 years and three mangrove scenarios. An example of a 25 years return period Flood Height for regular wave climate is shown in Figure 17. The increase in Flood Height is more significant under the no mangrove scenario, particularly when compared with the increase in Flood Height under the current mangrove scenario. In other words, a greater loss of protection benefits occurs when moving from current mangroves to no mangroves, compared to
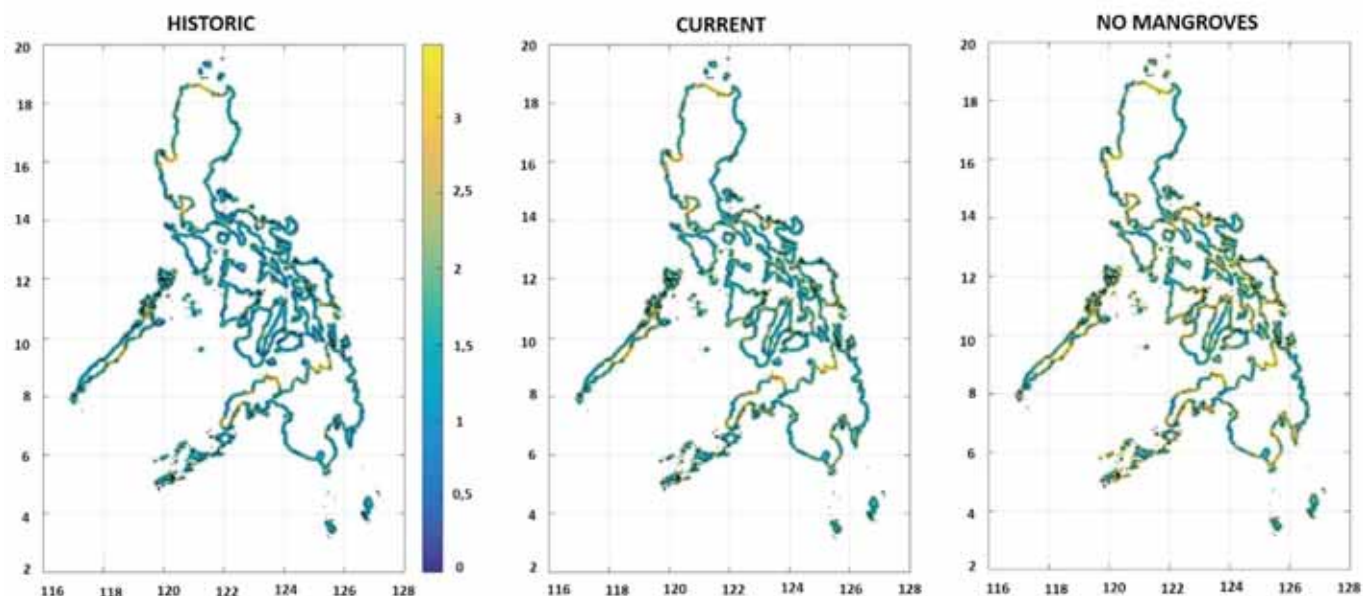
Figure 17 Flood height (m) at the shore for a 1 in 25 year event in the regular wave climate data set, under three scenarios: historic mangrove cover in 1950, current mangrove cover in 2010, and a hypothetical no mangrove cover. The increase in Flood Height is more significant under the no mangrove scenario, particularly when compared with the increase in Flood Height under the current mangrove scenario.

the loss that occurs when moving from historical mangroves to current mangroves.

5.5 Comparing Flood Height for different scenarios

The loss in protection from flooding due to mangrove degradation over the last half century and the potential future loss in protection in case of complete destruction of this ecosystem are shown in the following figures for different return period events (see Figure 18 and Figure 19). The figures show the differences in Flood Height to demonstrate the relevance and potential of mangroves in reducing flooding.

Several conclusions can be drawn from these results:
- The complete loss of mangroves will result in a loss of protection greater than what has already been lost due to degradation since 1950.

- For events with a return period greater than 10 years, mangrove protection does not increase with increasing return periods. This implies that mangroves are more efficient at protecting the coast for less intense storms.

- In general, the effect of losing mangroves produced the same percent increment in Flood Heights across the country, except in few critical areas like the South Islands or north Palawan Island which experienced greater increments in Flood Height due to mangrove loss.
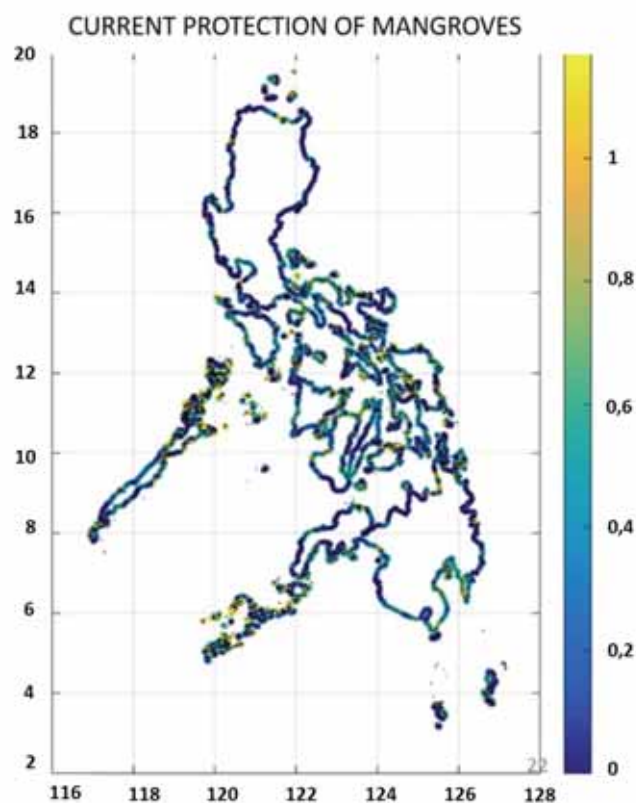
Figure 18 Difference in Flood Height (m) with (current) and without mangroves. For a 1 in 10 year return period event. Areas in yellow represent where mangroves have the most significant effects on flood height.
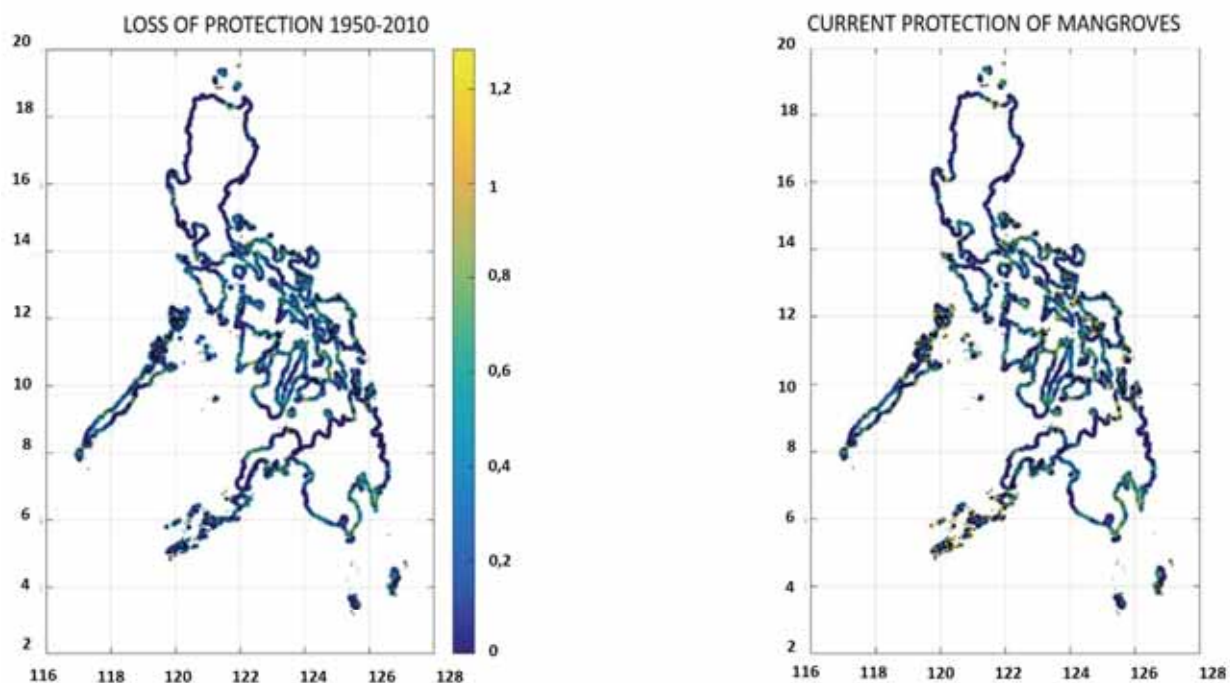
Figure 19 Increment of Flood Height (m) (1) Between 1950 and 2010 and (2) Between now and a theoretical case of no mangroves scenario. 50 years return period event

6 | Tropical Cyclones

6.0   Section Overview

This section describes the process for estimating the coastal flooding that occurs due to tropical cyclones. First, data on historical tropical cyclones in the region are used to reconstruct the offshore dynamics relevant to cyclone-induced storm surge. This involves reconstructing wind and sea-level pressure fields for historical tropical cyclones, setting up the numerical model to simulate the resulting waves and sea levels at the national scale, and validating the model based on historically available observations of sea level during extreme events. The tropical cyclone conditions are grouped into 548 representative families. Next, these waves and sea levels are propagated to the coastline over nearshore bathymetry and habitats, for the three mangrove scenarios (historic, current and total loss) using the Delft 3D model. From this, Total Water Levels (or Flood Heights) are obtained all along the nation's coastline, for multiple return periods (10, 25 50 and 100 years). Comparing the Flood Heights for each scenario indicates the protective capacity of mangroves for storm surge-induced flooding.

This analysis is then repeated using an extended database of synthetic tropical cyclones for the higher resolution local scale analyses in Pagbilao. Here, 1,462 synthetic tropical cyclones nationwide are generated, of which 456 are specific to the Pagbilao region. These events are then used to estimate Flood Heights at the Pagbilao coastline for multiple return periods (7 to 200 years) using the same process used for the national model. The final Total Water Levels at the shoreline determine the 'Flood Height' for each mangrove scenario. The

difference between these results indicates the protective capacity of mangroves for surge-induced flooding in Pagbilao.

6.1 Modelling Tropical Cyclones

To determine the role of the mangroves in attenuating storm surge at both the national and the local scale, a set of processes of different spatial scales must be tackled. There are several large scale factors concerning tropical cyclone characteristics and the general shape of the coast that contribute to the amount of storm induced surge at a given location:
- Central pressure: lower the pressure higher the surge
- Storm intensity: stronger winds will produce a higher surge
- Storm size: larger the storm, higher the surge
- Storm forward speed: faster storms increase surges on open coasts, slower storms increase surges in bays
- Landfall angle and approach: storms approaching perpendicular to the coast are more likely to produce higher surges
- Shape of the coastline: concave coastlines will experience higher surges
- Tide amplitude and phase: concurrent high tides will increase storm surges

Storm surge is also highly dependent on local features, such as coral reef barriers, wetlands or mangrove forests that will affect the flow of water. Moreover, it is at the local scale where nonlinearities between waves, sea levels and currents have a greater effect

30

on the Total Water Level. Storm surge reduction by mangroves is expected to depend on a number of mangrove forest characteristics and on the flood process itself. These factors include:

- Mangrove width: the rate of flood reduction of mangroves appears to range from 5-15 cm/km (Krauss et al., 2009) to 50 cm/km (Zhang et al. 2012).

- Mangrove vegetation characteristics: the density of the mangrove vegetation and the diameter of aerial roots and stems are expected to affect the mangroves' capacity to reduce storm surge. However, few data are available to support this assumption.

- Storm surge height and storm forward speed: depending on the height of the surge, it will interact with different parts of the mangroves (aerial roots, trunks and leaves). Consequently, the flow will experiment different friction rates, and thus different attenuations of the water level. Depending on the forward speed, the surge can occur for anywhere between a few hours to more than a day. Numerical simulations (Zhang et al. 2012) indicate that mangroves are more effective at attenuating faster surges than slower ones.

Due to the different processes involved, a two-step methodology has been adopted to evaluate the role of mangroves in attenuating storm surge at the national scale. The first step consists on determining offshore dynamics (waves and sea levels) produced by all the historical available records of tropical cyclones that have impacted the country. The second step is focused on solving the local scale processes where mangrove extent, coral reef presence and seafloor bathymetry must be accounted for. Due to the reduced depths at the local scale, nonlinear interactions are produced between waves and sea level. Dingemans et al. (1987) demonstrated that the wave radiation stress contributes to wave-driven flow in shallow waters where wave dissipation due to bottom friction and wave breaking take place. To account for these interactions, a coupled modeling approach is adopted in which the modification of the wave field due to variations in sea level during a given tropical cyclone are considered simultaneously with wave setup contributions to the Total Water Level.

The coastal risk assessment will be conducted at the national scale and at a local study site in Pagbilao, in south Luzon. Existing frameworks to assess risk from tropical cyclone hazards can be broadly summarized in three categories:

- Worst case scenario: the goal of this approach is to find the maximum possible flood extent. A set of worst case tropical cyclones are proposed (generally category 3 or higher) that make landfall with different angles and at different distances respective to the study site. Proposed scenarios are based on expert judgment or historical knowledge.

- Based on historical best track data: even though the worst possible event has not been recorded, if there are enough numbers of tropical cyclones that have crossed within a distance of the study site, it is possible to obtain realistic estimations of the hazard in term of probabilities or return periods.

- Based on synthetic tropical cyclone tracks: this approach is based on the idea that storm surge damage is sensitive to both the intensity and the track of the tropical cyclone. Based on the available historical information about tropical cyclone activity in the area, a stochastic Monte Carlo simulation is used to generate thousands of synthetic cyclones that are in statistical agreement with observations. A large set of events (i.e. spanning several years) is then available for the extreme value analysis, thus reducing uncertainties.

In the present work, the national scale assessment is based on historic storm track information, and the local scale assessment at the Pagbilao site is based on modeling a large number of synthetic events. A fully probabilistic coastal flood risk assessment approach is unaffordable at the national scale, which encompasses more than 7,000 islands and islets and more than 30,000 km of coastline. For this reason and due to the large number of land fall events found in the historical tropical cyclone record (548 events), the national assessment is based solely on historical track information. At the local scale in Pagbilao, the risk assessment has been achieved by modelling a large number of events (1,462 synthetic tropical cyclones whose tracks cross less than 300 km from Pagbilao) that represent 5,000 years of plausible tropical cyclone activity.

In all cases, three mangrove scenarios have been considered: mangrove extent in 1950, mangrove extent in 2010, and a hypothetical scenario where all mangroves are lost. Modeling waves and sea levels is usually an efficient and reliable method for estimating risks in coastal areas. A number of storm surge modeling systems such ADCIRC (Lin et al., 2010), FVCOM (Weisberg and Zeng, 2008) or Delft3D (Veeramony et al., 2014) have been used to model surge inundation in coastal areas due to tropical cyclones, obtaining good estimations of both flood depth and extent. Figure 6.1 in Annex 1 shows the general scheme of the methodology used to obtain offshore total water level estimations.

Regardless of what tropical cyclone track data is used in the risk assessment (historical or synthetic), the statistical storm surge estimation can be summarized in six steps:

1. Selecting tropical cyclone events to be simulated

2. Obtaining tropical cyclone wind and sea level pressure fields

3. Grid design and models setup

4. Calibration and validation

5. Running the models

6. Extreme value analysis

Even though not all tropical cyclone events will produce significant surges, all historical tropical cyclones that made land fall in the Philippines between 1951 and 2014 have been considered to determine annual expected benefits in terms of the reduction of flooding by mangroves at the national scale. In Pagbilao, both historical and synthetic tropical cyclones have been used to obtain the offshore dynamics and statistics in order to test uncertainties derived from a limited number of events.

6.2 Offshore Dynamics

The first step to run the wave and hydrodynamic models is to obtain the wind fields corresponding to each of the events to be simulated. Generally, there are three basic

approaches to reconstruct tropical cyclone wind fields: measurements, high resolution atmospheric models, and parametric/analytical simplified models (Holland et al., 1980, 2010; Emanuel and Rotunno, 2011; etc.). In this study, for each selected storm, the surface axisymmetric wind field is estimated by calculating the wind velocity at the gradient level with the analytical wind profile of Emanuel and Rotunno (2011) which has yielded relatively good results (Lin and Chanvas, 2012). The wind speed (V) is determined as follows:

$$V(r) = \frac{2r(R_m V_m - 0.5 f R_m^2)}{R_m^2 + r^2} - \frac{fr}{2} \tag{7.1}$$

where r is the radius, f the Coriolis parameter, R_m the radius of maximum winds, and V_m the maximum wind speed. To force the wave and hydrodynamic models, a reduction factor of 0.9 is used. The asymmetry of the wind field is accounted for by adding 60% of the storm translation velocity. The surface pressure P is

estimated from the parametric model of Holland (1980):

$$P(r) = (P_n - P_c) exp\left(-\left(\frac{R_m}{r}\right)^B\right) + P_c \tag{7.2}$$

where P_c is the core pressure (minimum pressure), P_n the pressure at infinite radius, and B the Holland parameter:

$$B = \frac{\rho e V_m^2}{(P_n - P_c)} \tag{7.3}$$

As an example, Figure 20 shows the wind footprint of the Super Typhoon Haiyan which devastated the city of Tacloban in November 2013, including a time step of the parametric wind model for November 8th at 20:00 UTC. The hourly wind and sea level pressure fields generated with the parametric model are the forcing of the Delft 3D model (https://oss.deltares.nl/web/delft3d), in which the processes of tide, wind setup, inverse barometers and wave setup are simulated
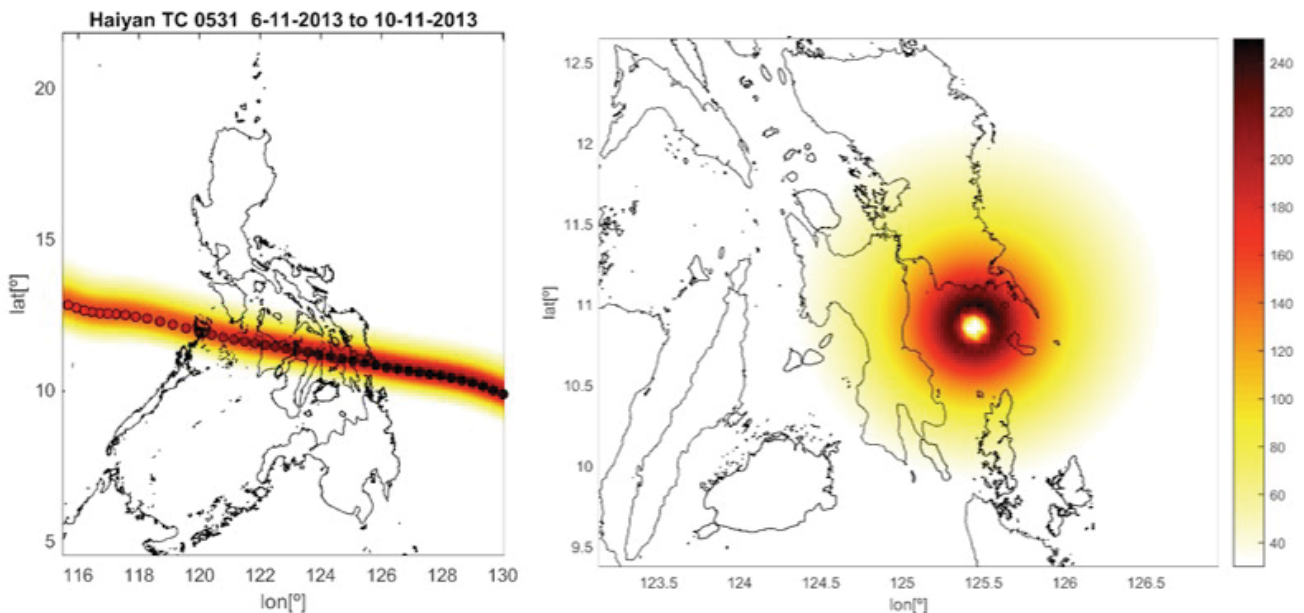
Figure 20 Wind footprint of the Super typhoon Haiyan which devastated the city of Tacloban in November 2013 (left), parametric wind field for the November 8th at 20:00 UTC (left). Wind speeds in legend are in km/h.

together, conserving the nonlinear interaction between them. The Delft3D modeling suite is composed of several modules of which this study utilizes the Delt3d-FLOW and Delft3d-WAVE modules (see section 5).

The computational domain extends from 111.5-130.5° E and 4-21.5° N which has been found to be sufficiently wide to model the sea states generated by tropical cyclones traveling long distances from the east. This achieves a compromise between the quality of the desired results and the required computational effort and allows the model to capture distant waves and the interactions between extreme water levels and waves closer to the coastline.

The resolution of the numerical grid is set at 5 km X 5 km as an effective compromise between computational cost and the ability to capture surge patterns. Simulated sea level validations of different tropical cyclones indicate that the 5 km grid reasonably reproduces storm surges in most locations,

and this grid is chosen for the baseline study. Increased model resolution should produce more realistic surges and waves near the coast though this will increase the computational cost. As an example, Figure 21 shows the differences of the simulated Haiyan storm surge in Tacloban using a 5 km or 2 km grid resolutions. Both grids produce similar storm surge patterns, with the 2 km grid doing a better job of capturing small scale processes such the long wave amplification in the Gulf of Leyte.

Figure 6.2 in Annex 1 displays the grid used for the baseline storm surge study together with the coastal points where waves and sea levels are obtained. Seafloor bathymetry and elevation data are extracted from the ETOPO 1 database which is a 1 arc-minute global relief model of Earth's surface that integrates land topography and ocean bathymetry from numerous global and regional data sets (Amante and Eakins 2009).

Tropical cyclone simulations are performed in 2D mode with a time step of 30s. For
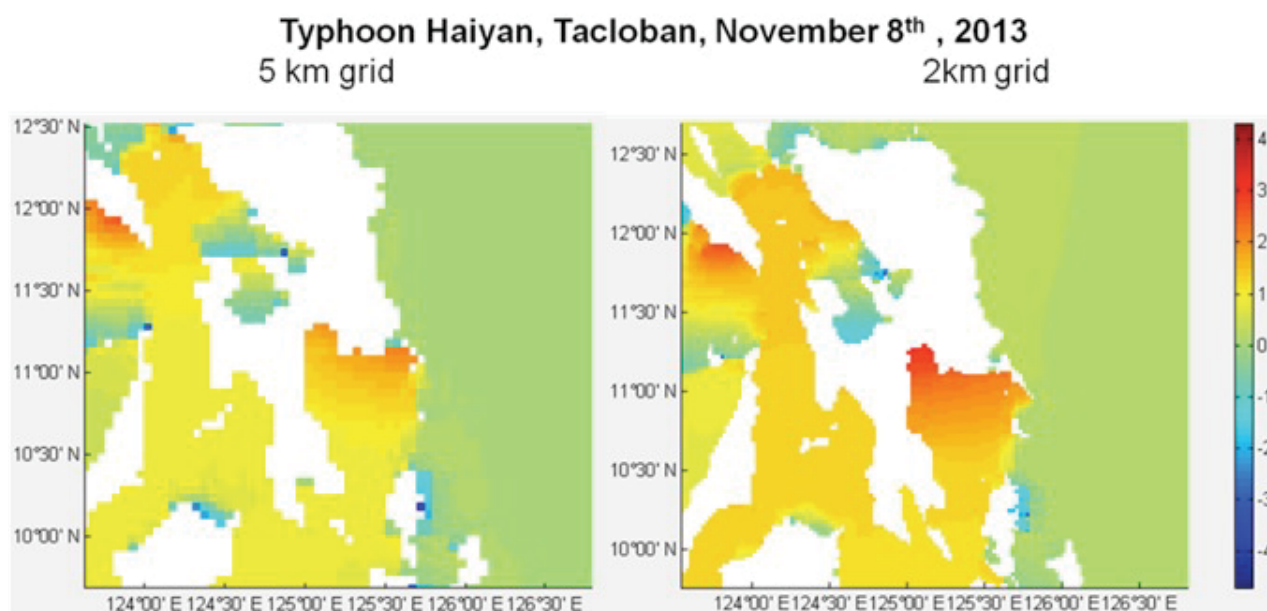
Figure 21 Effects of grid size on surge predictions. Differences between the maximum simulated surges in Tacloban generated by the Super Typhoon Haiyan using 5 km (left) and 2 km grids. Similar patterns are obtained with both grids with the difference of the slightly larger storm surge levels captured with 2 km grid
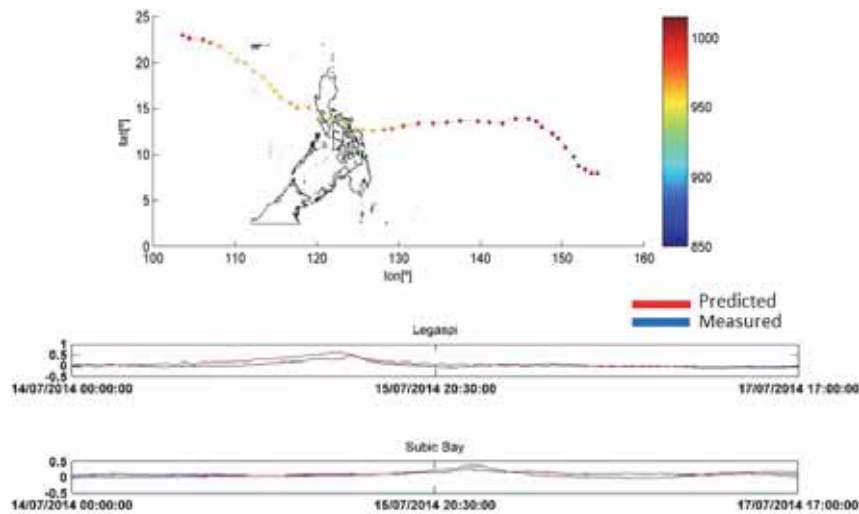
Figure 22 Validation of the simulated storm surge (in meters) of Typhoon Rammasun in Legaspi and Subic Bay tide gauges. The upper panel represent the cyclone track with the minimum pressure in hPa.
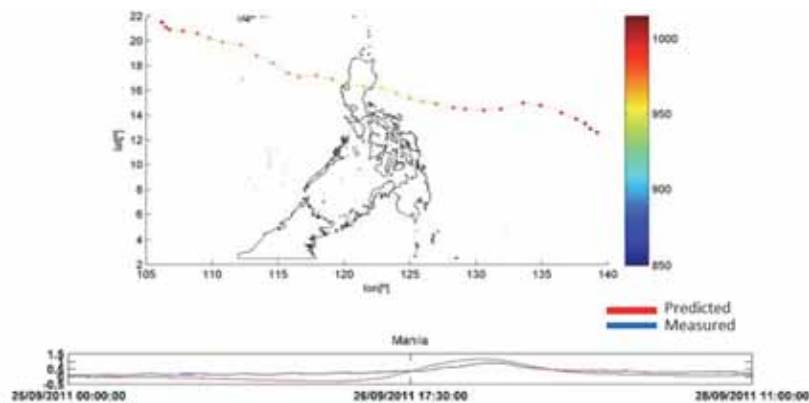
Figure 23 Validation of the simulated storm surge (in meters) of Typhoon Nesat in Manila tide gauge. The upper panel represent the cyclone track with the minimum pressure in hPa.

validation, boundary conditions have been defined throughout with harmonic constituents obtained from the TPXO7.2 Global Tide Model (Egbert and Erofeeva 2002). However, since we are more interested in the statistical distribution of the residuals, serial tropical cyclone simulations have been carried out using a Neumann type boundary condition in which a water level slope is defined rather than absolute water level. Tests showed that, at the selected mesh resolution, coupling the FLOW and WAVE modules did not result in any appreciable increase in model skill. Existing non-linearities in wave-current-sea level

interactions will be considered in the next step of the methodology in which a 1D profile WAVE-FLOW coupling is performed.

Finally, the simulations of offshore dynamics are validated against observations of historic storm events. Although Super Typhoon Haiyan remains the most severe event in term of storm surges and destruction in the Philippines, there are no available tide gauges in areas where this typhoon impacted to validate our model results. For this reason Typhoon Rammasun (July 2014, see Figure 22) and Typhoon Nesat (September 2011, see Figure 23) have been

chosen to validate the simulation of offshore dynamics.

We find that our model results align with observations, with only a few discrepancies of a few tens of centimeters found locally. It is unclear whether these differences are due to the model itself, the forcing data (track, intensity, radius of maximum winds, etc.), or local features of the observations. As an example, Figure 6.3 (Annex 1) shows the results of the maximum storm surge, significant wave height, and mean wave period produced by Super typhoon Haiyan. Higher resolutions might be necessary in some areas to account for local processes that can contribute significantly to the experienced surges. Due to the large extent analyzed, local processes will be solved in the next steps using a 1D profile wave-sea level coupled approach.

Even though no wave measurement is available for validating the simulated waves, there is a set of satellite missions (TOPEX, ERS, GFO, etc.) that provide altimetry measurements of the wave heights

worldwide (http://www.aviso.altimetry.fr/en/data.html). Altimetry data corresponding to November 8th, 2013, when Super Typhoon Haiyan made land fall, are shown in Figure 6. 4 (Annex 1). As can be seen, due to instrument limitations, there are no measurements in the eye of the tropical cyclone, nevertheless waves up to 12 m were observed at a short distance to the north. Measured values reasonably agree with those obtained throughout the simulation.

Figure 24 shows the expected storm surge height for the one in 50 year event across the Philippines. Most of the flood heights are below 1 m (note blue colors in Figure 24). However water levels are above 2.5 m in areas around Lamon (Calabarzon) and San Miguel (Bicolandia) Bays (note redder colors in Figure 24). This coastline is one of the most exposed to tropical cyclones in the Philippines, with a tropical cyclone occurring every 2 years on average, and the presence of pronounced bays and flat-gently-slopes contributes to storm surge amplification. Figure 6.5 (Annex 1) shows the water levels
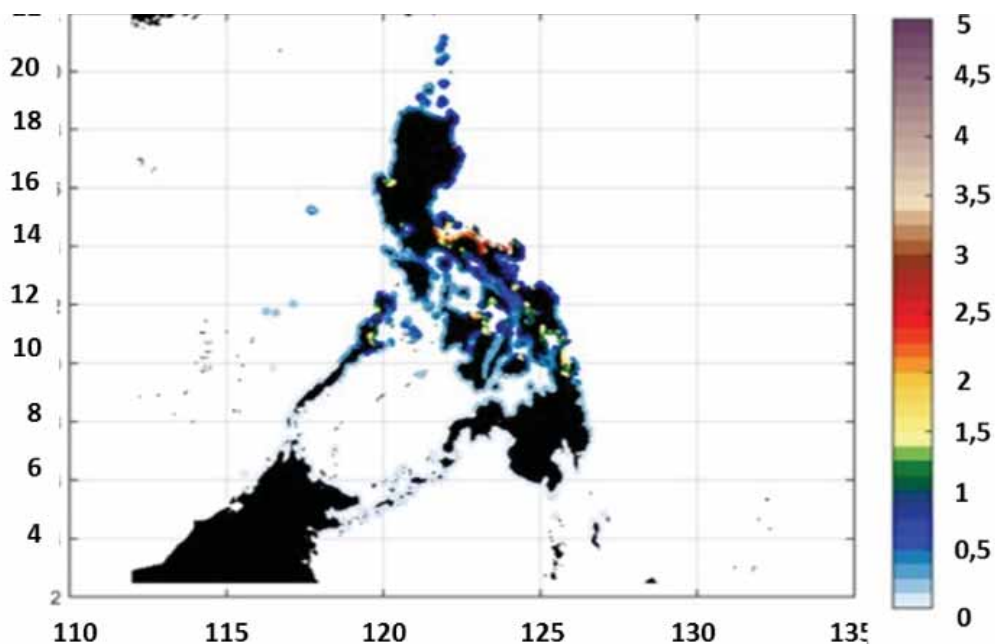
Figure 24 Storm surge (in meters above the mean sea level) due to wind set-up and the inverse barometer effect for 50 years return period.

for the other storm events including the 5, 10, 50 and 100 years return periods. Although the 100 year return period has higher water levels, there is only a slight increase in values with respect to the 50 year map, indicating that there are limits on the highest storm surge levels.

Figure 25 and Figure 6.6 (in Annex 1) show the same maps as above but for significant wave heights produced by tropical cyclones following a similar extreme analysis. Waves up to 10 m are observed in the most exposed coasts of the northeastern region, where no continental shelves exist to attenuate waves by breaking or bottom friction, for every 5 years. On the other hand, in the Subuyan, Visaya interior seas waves do not exceed 4 m due to fetch and depth limitations. For a return period of 100 years, tropical cyclones produce waves higher than 4 m in all the Philippines excluding the southernmost region. The most exposed coast in the east can experience waves up to 14 m in Siargao Island, increasing further towards the north

and exceeding 20 m heights in northeastern Luzon.

Once the tropical cyclone dynamics at the national scale are simulated, we then propagate these waves and sea levels towards the coast to assess the influence of mangrove forests in attenuating these storm surges. This step involves the coupling of high resolution wave and sea level models with a modification of the Manning's coefficient as a function of the bottom cover type, depending on the mangrove scenario being modelled. By coupling the wave and flow models, we translate wave radiation stress into a contribution to the Total Water Level at the coast, and we consider the storm surge duration as a factor in the attenuation potential of mangroves.

At the Pagbilao site, we apply a fully probabilistic approach by simulating 1,462 synthetic tropical cyclones, which represent 5,000 years of tropical cyclone activity (see Figure 6.7 in Annex 1). The stochastic tropical cyclone track modeling is able to completely
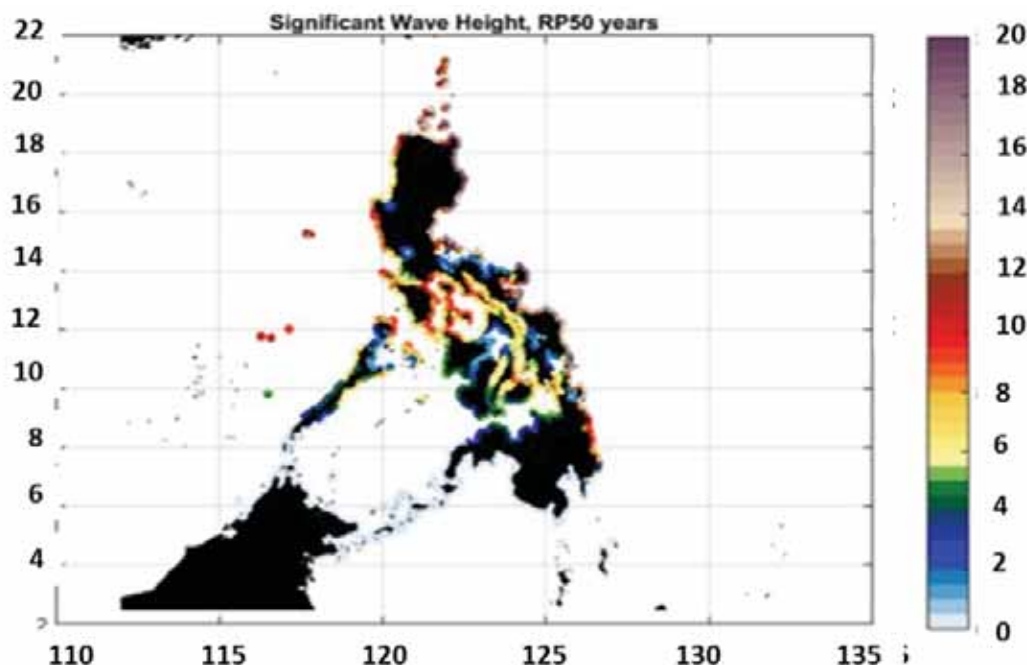
Figure 25 Significant wave heights (in meters) for 50 years return periods

cover the selected study area, thus accounting for a wide range of possibilities of tropical cyclone approach angles, land fall locations and intensities.

Despite the large number of simulated tropical cyclones, the maximum observed surge in the 5,000 year time period (considering only wind and inverse barometer effect) does not exceed 1.6 m, even for the most surge-prone synthetic track. As an example, Figure 26 shows a synthetic tropical cyclones that generates one of the highest surges. This fast moving severe typhoon has a south-north track when crossing Pagbilao. With minimum pressures of 890 hPa before reaching the Philippines, the tropical cyclone weakens when first making landfall in Moro Gulf, and then further intensifies to 930 hPa and 220 Km/h 10- min-averaged winds when crossing the warm Jolo Sea towards Pagbilao. This tropical cyclone generates high surges in Pagbilao, and it is able to transfer momentum to the

water surface all along the Tablas strait, causing the water to finally be piled up over the Tayabas Bay.

To compare statistical results from the historical and synthetic tracks, a general extreme value distribution was fitted to the storm surge data. As can be seen, both distributions are fairly similar, with the synthetic tracks being slightly higher. Results indicate little difference below the 100 year return period between the two distributions.

After defining offshore dynamics generated by each tropical cyclone, we propagate waves and sea levels over the previously defined 1D profiles. Two different scales will be analyzed with different inputs:

1. National scale: historical tropical cyclones.

2. Local scale: historical tropical cyclones + synthetic tropical cyclones
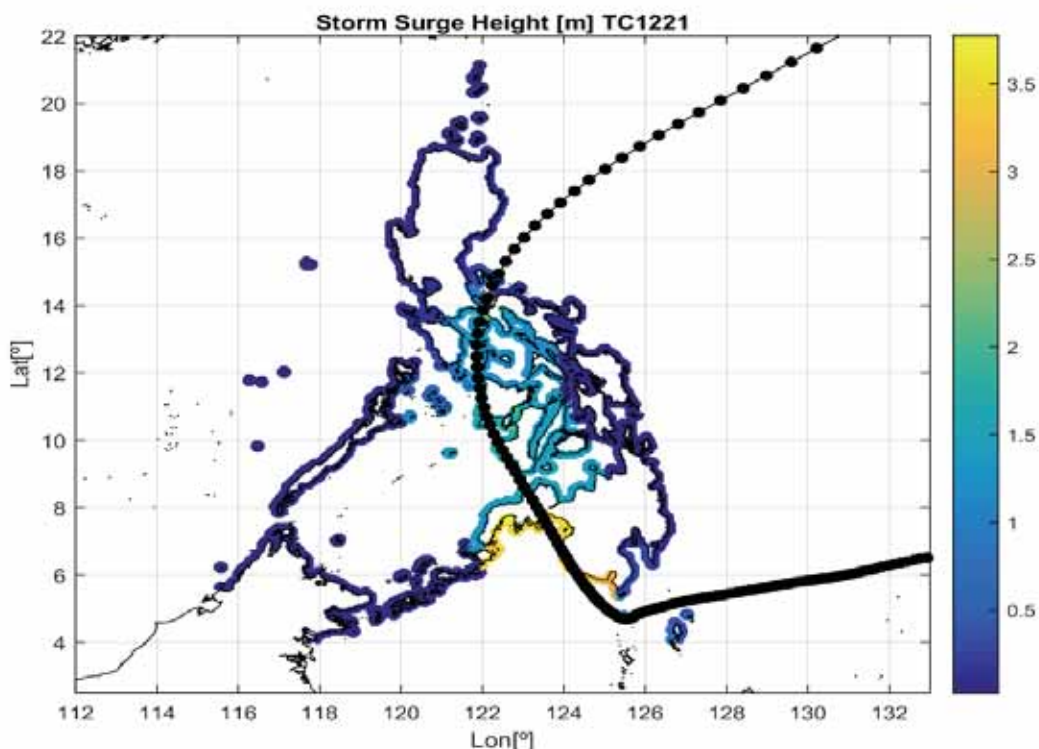
Figure 26 Storm surge generated by the synthetic tropical cyclone number 1221.

6.3 National Scale Nearshore Dynamics: Historical Tropical Cyclones

Offshore dynamics from 63 years of historical tropical cyclones (from 1951 to 2014) were obtained for the entire Philippines coast (548 events, 8.6 events per year). Waves and sea level are forced into a 5 km x 5 km mesh grid in the whole country with SWAN (for waves) and DELFT3D (for storm surge).

6.3.1 Classification of Tropical Cyclones

The closest points to the coastline of the coarse national numerical mesh (5x5km) are going to be used to feed the 1D numerical simulations over the vegetation fields (coral reefs and mangroves). In total, there are 3,225 points which contain the following hourly data time series:

- Significant wave height time series within each tropical cyclone

- Peak period time series within each tropical cyclone

- Storm surge time series within each tropical cyclone

However, storm surge is not the only component of Total Water Level offshore. Sea Level is obtained by adding the maximum Astronomical Tide to the storm surge time series at each location. It is crucial to consider the worst-case scenario in terms of Sea Level because of the sensitivity of the numerical model to water depth when propagating waves over coral reefs and mangroves.

Note that the average tropical cyclone duration is 8 hours, but the longest events could be 50 hours long.

Thus we have 3,225 points x 548 tropical cyclones x 8 h/tropical cyclone = 14,138,400

hourly data of Significant Wave Height, Peak Period and Storm Surge. These are reduced using the following approach:

1. First, each of the 548 historical tropical cyclone time series are reduced to the maximum values of 4 variables over the storm duration: Maximum Significant Wave Height; Peak Period associated to the maximum Significant Wave Height; Maximum Sea Level (i.e. Surge + Tide); and tropical cyclone duration. This reduces the data into 3,225 points x 548 tropical cyclone x 1 h/ tropical cyclone = 1,767,300 combinations of Hsmax, Tp, Sea Level and tropical cyclone duration.

2. Then, since not all areas of the country will experience these surges, maximum Storm Surges below 10 cm are excluded. The tropical cyclones producing significant storm surges comprise only 1% of the total dataset, or 17,673 combinations of Hsmax, Tp, Sea Level and tropical cyclone duration.

3. Finally, as with the profiles, statistical tools are applied to reduce the number of hydrodynamic cases to be simulated. A clustering technique, Maximum Dissimilarity Algorithm (MDA), was chosen for this purpose. In our clustering tests, MDA performed better than K-means inidentifying the minimum number of clusters required to capture the maximum wave height and storm surge.

The coastal profiles were classified into 250 families for each scenario with K-MEANS algorithm, or 750 theoretical profiles, representing the entire Philippine coast.

6.3.2   Habitat Pathway

The 50 selected tropical cyclones are propagated over the 750 theoretical profiles using DELFT 3D. In total, we have 50 x 750 = 37,500 simulations covering all bathymetry, bottom type and hydrodynamic combinations for the entire country.

The 37,500 1D simulations all consider the following:

- Flow and Waves modules are run simultaneously (coupling model): DELFT 3D propagates storm surge and astronomical tide induced flow and SWAN module propagates waves over the updated water depth.

- The computational time length is two times the tropical cyclone duration.

- Wave characteristics (Hs and Tp) are constant within the whole tropical cyclone

- Total Water Level discharge has triangular shape within the tropical cyclone event, with a peak equal to the maximum Sea Level (Sea Level= Storm Surge + Astronomical Tide 99%, corresponding to the worst case scenario) occurring at the mid-point of the tropical cyclone duration.

- Profile discretization: 10m resolution (2000 nodes/profile)

From these simulations, a final value of Total Water Level at the shoreline (i.e. Flood Height) is obtained for the entire Philippines coastline. With the 37,500 input variables combinations (Hs, Tp, Sea Level and tropical cyclone duration) from the hydrodynamic point of view, and mangrove length and mangrove average depth from the coastal habitat point of view, and the resulting 37,500 Flood Height values calculated by the model, we have created a "pick-up table" or "interpolation table" of 37,500 different combinations which allows us to interpolate the Flood Height for any scenario proposed.

6.3.2   Flood Height Reconstruction

We take the maximum Total Water Level at the coast (i.e. Flood Height) for each of the 37,500 simulations with the aim of reconstructing the Flood Height along the entire Philippine coastline, with the following steps:

- First we generate the interpolation tables with 5 columns (Hs, Tp, Sea Level and tropical cyclone duration as predictor variables and Flood Height as predicted variable) and 50 rows (the same as the number of representative tropical cyclones selected with MAXDISS clustering technique). We have one table per scenario and profile (3 scenarios x 250 profiles/scenario= 750 tables). Figure 6.11 in annex 1 shows a scheme of the interpolation datasets generated in the project.

- Next, for each profile we select the corresponding interpolation table for the 3 mangrove scenarios. Note that we had previously grouped each of the 171,888 profiles into 250 representative families.

- Then, the 548 historical tropical cyclones are reconstructed at each profile by interpolating in the mentioned tables. The interpolation technique is based on the Radial Basis Functions (Camus et al. 2011a). The methodology has been tested in case studies in different papers (Camus et al. 2011b, Nunes and Pawlak 2008). The methodology is not dependent on location, and is applicable globally

since the selection algorithm and reconstruction technique are solely dependent on the quality of the databases to be downscaled to the coast and the number of cases selected using the MDA.

- Once the 548 tropical cyclones at each profile are reconstructed, the extreme values analysis is performed. For that purpose, Peak Over Threshold selection method is applied to obtain the extreme regime of Flood Height. We fixed a threshold of 98%, corresponding to the strongest 2% tropical cyclones events over the total 548 registered between 1951 and 2014. The 2% most destructive events correspond to 11 tropical cyclones, resulting in 1 extreme tropical cyclone every 5 year, and consequently a minimum return period of 5 years.

- Three tables (one for each scenario) with 5, 6, 7, 8, 9, 10, 15, 20, 25, 30, 40, 50, 100, 150 and 200 years Return Period events of Flood Height are

obtained at each profile (for examples see Figure 6.11 in annex 1)

These tables are calculated for each profile (171,888 profiles for the entire Philippine coast) and three scenarios (1950, 2010 and no mangroves), providing the Flood Height for every 200 m of coastal line for 15 different return periods. Figure 27 shows the Flood Height for a 25 year return period under three scenarios as an example.

6.3.4 Comparing Flood Height for Different Scenarios

To understand the effect of mangrove forests on the propagation of Total Water Levels (and thus the resulting Flood Height), the extreme regime of Total Water Level offshore is compared with the resulting Total Water Level on the coast after passing through the mangroves. The selected profile contains a mangrove extension of 1 km. Two scenarios are shown: first, the current scenario of mangrove cover, and second, the hypothetical scenario of no mangrove cover (see Figure 6. 9 in Annex 1).
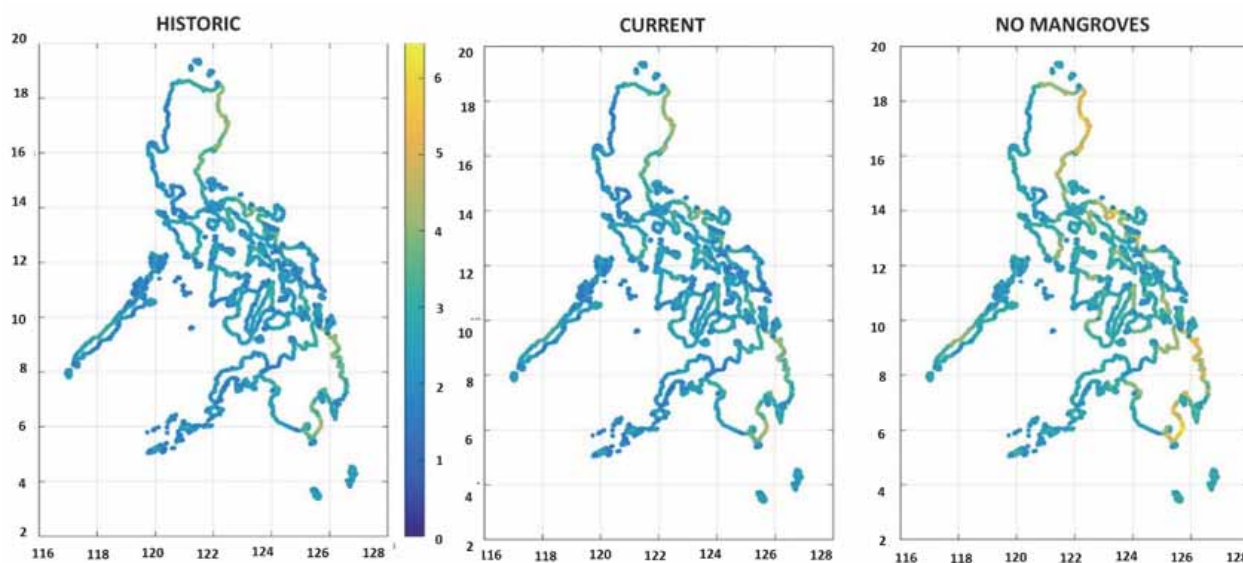
Figure 27 Flood height (m) in The Philippines for 25 year return period under tropical cyclone conditions, for scenarios with historical (1950) current (2010) and no mangrove cover.

Comparing scenarios allows us to evaluate the effect of mangroves in Total Water Level dissipation. Two comparisons can be done:

- Loss of protection between 1950 and 2010: How much did the Total Water Level increase from 1950 to 2010 due to mangrove loss?

- Current protection of mangroves: How much would the Total Water Level increase if we lose mangroves now?

Figure 28 shows both comparisons for the case of 50 year return period tropical cyclone event.

6.4 Regional Scale Nearshore Dynamics: Historical and Synthetic Tropical Cyclones in Pagbilao

For a high resolution analysis in a local area, the historical tropical cyclones database is not enough to statistically study the extreme regime of these events. This is because the number of "real" tropical cyclones in a small area is too small.

6.4.1 Synthetic Tropical Cyclones Generation

Of the total 548 tropical cyclones registered in The Philippines, only 37 tracks pass
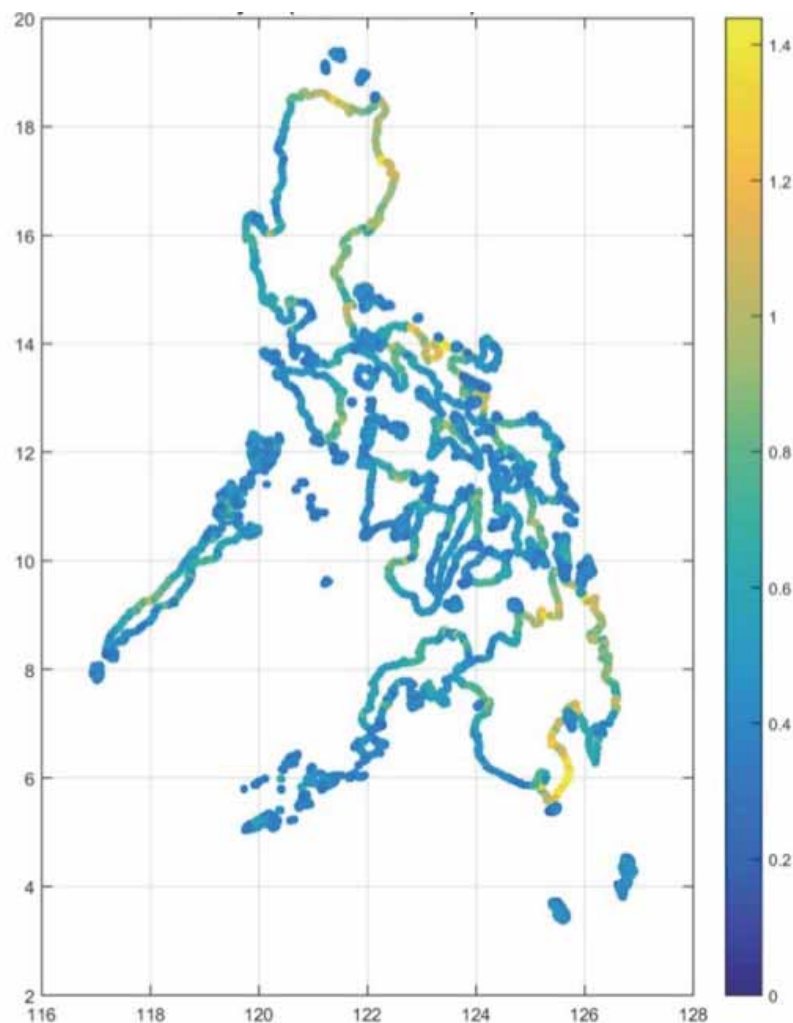
Figure 28 Current protection: Increase of Flood Height (m) for a 50 year return period under tropical cyclone conditions between current mangrove cover and a theoretical case of no mangroves cover

through the Pagbilao study site, one event every two years. This is insufficient for statistical analysis, so we developed a new and larger database based on the available historical information of the activity in the area. We used a stochastic Monte Carlo simulation to generate 1,462 synthetic cyclones in the whole country that are in statistical agreement with observations and represent 5,000 years of storm activity. Out of the 1,462 tropical cyclones simulated throughout the Philippines, 456 tropical cyclones pass through the Pagbilao study site.

Offshore dynamics for these 5,000 years (456 tropical cyclones) of synthetic tropical cyclones are obtained along the Pagbilao coast. As was done with the historical tropical cyclone at national scale, waves and sea level are forced in 5 km x 5 km mesh grid in the whole country with SWAN (for waves) and DELFT3D (for storm surge). The numerical simulations generated 546 combinations of waves (significant wave height, peak period and wave direction) and Storm Surge intensity and duration.

6.4.2 Flood Height Reconstruction

We evaluate the capacity of mangroves to attenuate waves and sea level, including the effect of different scenarios of mangrove cover on Flood Height, at the local scale. The national scale model already generated 37,500 cases of Flood Height covering a wide range of input combinations of wave height, peak period, sea level and tropical cyclone duration. With the aim of reducing the computational cost, these interpolation tables (for example see Figure 6.11 in Annex 1) for historical tropical cyclones were used to interpolate the Flood Height in Pagbilao.

The study site covers 232 km of coastline and includes 1,162 profiles for which the Flood Height will be reconstructed for 456

synthetic tropical cyclones for Pagbilao. This is done as follows:

- The Flood height is calculated at each profile (1,162 profiles in Pagbilao) by interpolating from the tables created with the 37,500 Delft3D model simulations for historical tropical cyclones. The input variables are (Hs, Tp, Sea Level max, tropical cyclone duration). Note that the previously generated interpolation tables are "profile-specific". Thus, we only have to directly associate each profile to the corresponding table and interpolating the Flood Height accordingly. However, to extend the methodology to other sites, two other variables, defining habitat characteristics, should be considered: mangroves length and mangrove average water depth.

- Once the 456 tropical cyclones are reconstructed at each profile, the extreme values analysis is performed, similar to the historical tropical cyclone analyses, using a Peak Over Threshold method with a 98% threshold. For Pagbilao, the 2% most destructive events correspond to 9 tropical cyclones, resulting in 1 extreme tropical cyclone every 550 years. This occurrence rate is so small that a new hypothesis is proposed to accomplish the extreme analysis: The 456 simulated (synthetic) tropical cyclones occur in the same period of time as the historical dataset, i.e. 1951-2014 (not 5,000 years, as originally modelled). Consequently, the occurrence rate is increased to one tropical cyclone event every 7 years. This allows a minimum return period of 7 years.

- Three tables (one for each scenario) with 7, 8, 9, 10, 15, 20, 25, 30, 40, 50, 100, 150 and 200 years Return Period events of Flood Height are obtained at each profile, shown in Figure 6.11 in annex 1. These tables are calculated for each profile (1,162 profiles in Pagbilao) and each scenario (historical, current, and no mangrove cover), providing the Flood Height level for every 200 m of coastal

line for 13 different return periods. The 25 and 50-years return period Flood Height are plotted as an example along the Pagbilao coastline for the three scenarios in Figure 29 and 30.

Figure 29 Flood height in Pagbilao for 25 year return period event under tropical cyclone conditions for the three scenarios of historical, current and no mangroves. The values are water or flood height at the coast ranging from ~1m (yellow) up to ~5m (blue).

Figure 30 Flood height in Pagbilao for 50 year return period event under tropical cyclone conditions for the three scenarios of historical, current and no mangroves. The values are water or flood height at the coast ranging from ~1m (yellow) up to ~5m (blue).

7 | Coastal Impacts: Flooding Mask Calculation in the Philippines

7.0   Section Overview

This section describes how we translated flood heights at the coastline to inland flood extents, at both the national scale and at the local scale in Pagbilao and compares the results at these different scales. The flood extent estimates are done nationwide for 'regular' waves and historic tropical cyclones, and in Pagbilao for historic and synthetic tropical cyclones. Flood extents are estimated for three mangrove scenarios- historic, current and total loss. At the national scale, the flood extents are estimated using a simple hydraulically-connected bath-tub model and a 30 m elevation database. In Pagbilao, a much higher resolution database at 5 m resolution allows for the use of a more sophisticated flooding model (the Rapid Flood Spreading Methodology), which provides better estimates of inland flood extents.

7.1 National Scale Results (30 m resolution)

At the national level, we used a flooding model with a 30 m resolution. In Figures 33 to 37, we show the results of this model at specific sites in South Manila and Roxas for a 50 year return period event under water levels predicted under 'regular conditions' and 'extreme conditions' (or tropical cyclone conditions).

7.2 Local Scale Results in Pagbilao and Busuanga (5m resolution)

At the local scale, in the Pagbilao and Busuanga sites, high resolution elevation data is available (IFSAR 5m), which allows for more detailed flooding analyses. The following figures show the mangrove cover at each location (Pagbilao in Figure 36 and
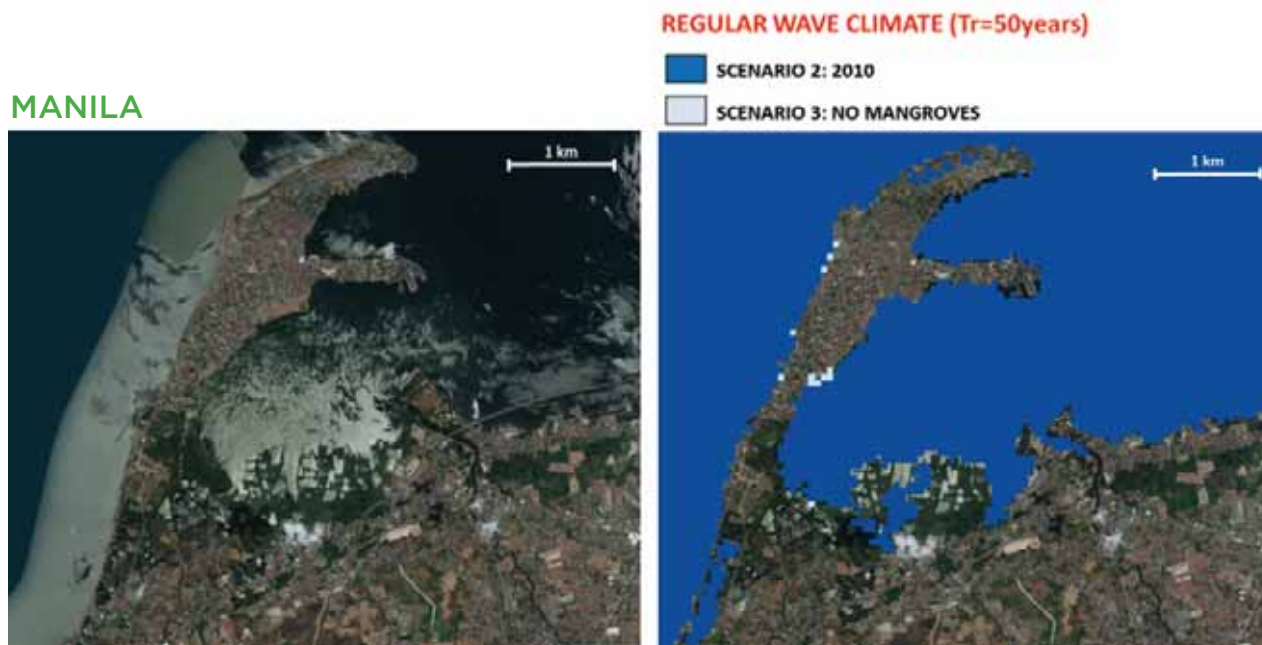
Figure 31 Flooding in South Manila for 50 year return period event under regular conditions. Blue and grey colors indicate flooding extent under current mangroves (2010) and no mangroves.
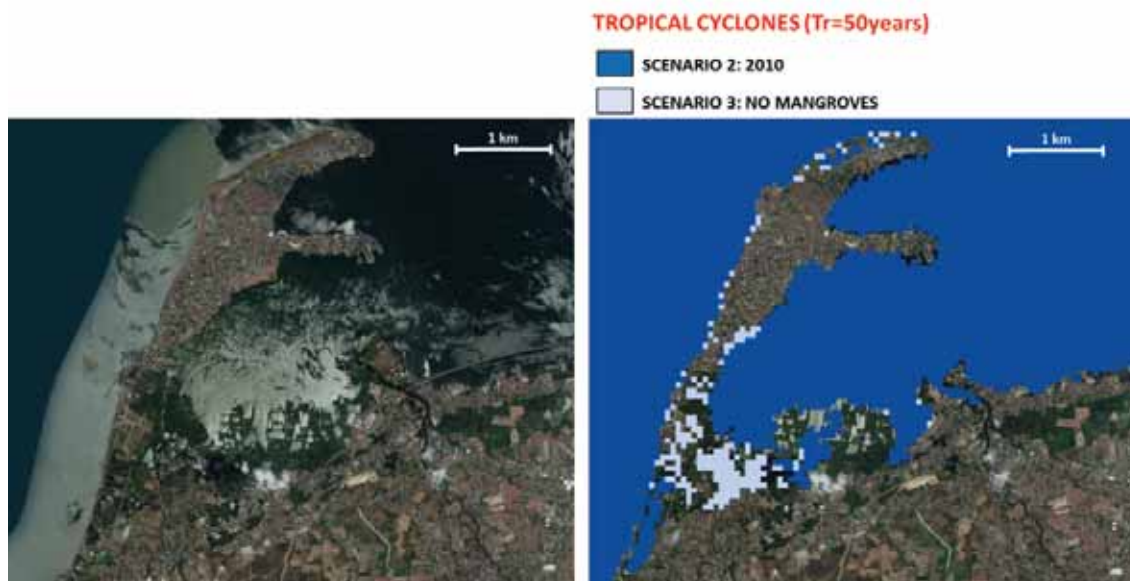
Figure 32 Flooding in South Manila for 50 year return period under tropical cyclone conditions. The light and dark blue polygons indicate flooding extent under the different scenarios of current mangroves (2010) and no mangroves.

ROXAS

Figure 33 Roxas study site: mangrove cover in 2010 appears in green on the right.
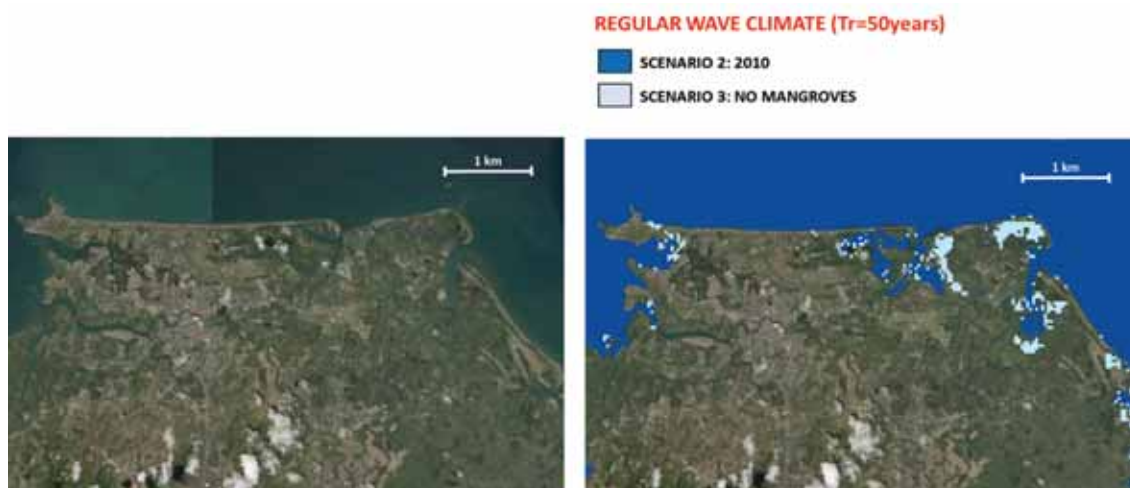
Figure 34 Flooding in Roxas for 50 year return period under regular conditions. The light and dark blue polygons indicate flooding extent under the different scenarios of current mangroves (2010) and no mangroves.

Figure 35 Flooding mask in Roxas for 50 years return period event in the Tropical Cyclones data. The light and the dark blue polygons in the figure on the right represent water and flooding of land under the two different scenarios.

PAGBILAO

Figure 36 The left image shows the location of Pagbilao in the Philippines. The right image shows the mangrove cover in 1950 and 2010.
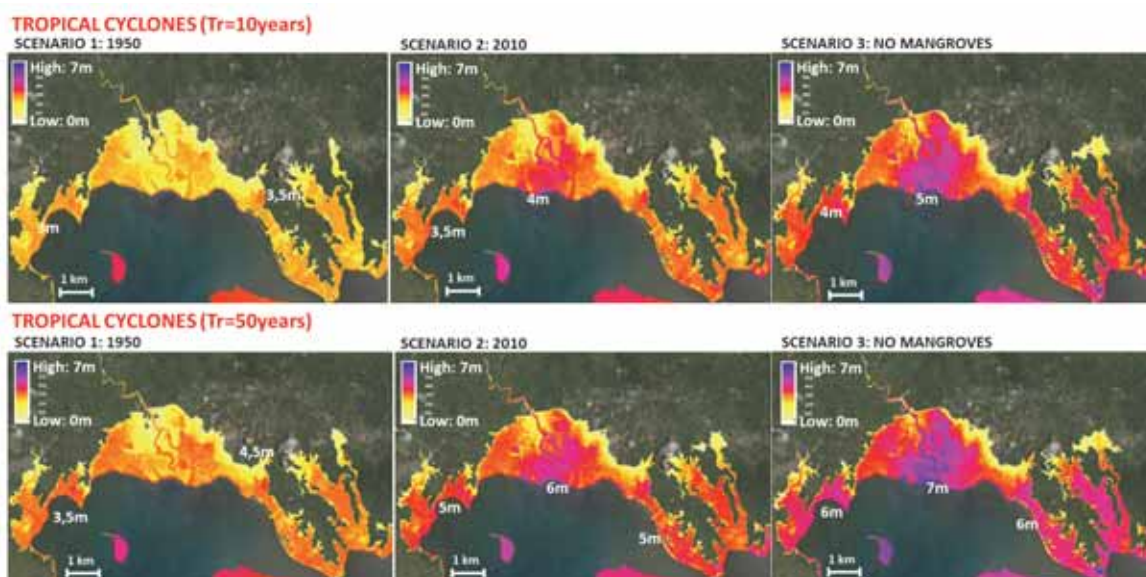
Figure 37 Flood extent and water depth in Pagbilao for 1 in 10 and 1 in 50 years return period event under tropical cyclone conditions under three different mangrove scenarios, Historical (1950), Current (2010) and No Mangroves.

BUSUANGA

Figure 38 The left image shows the location of Busuanga in the Philippines. The right image shows the mangrove cover in 1950 and 2010.
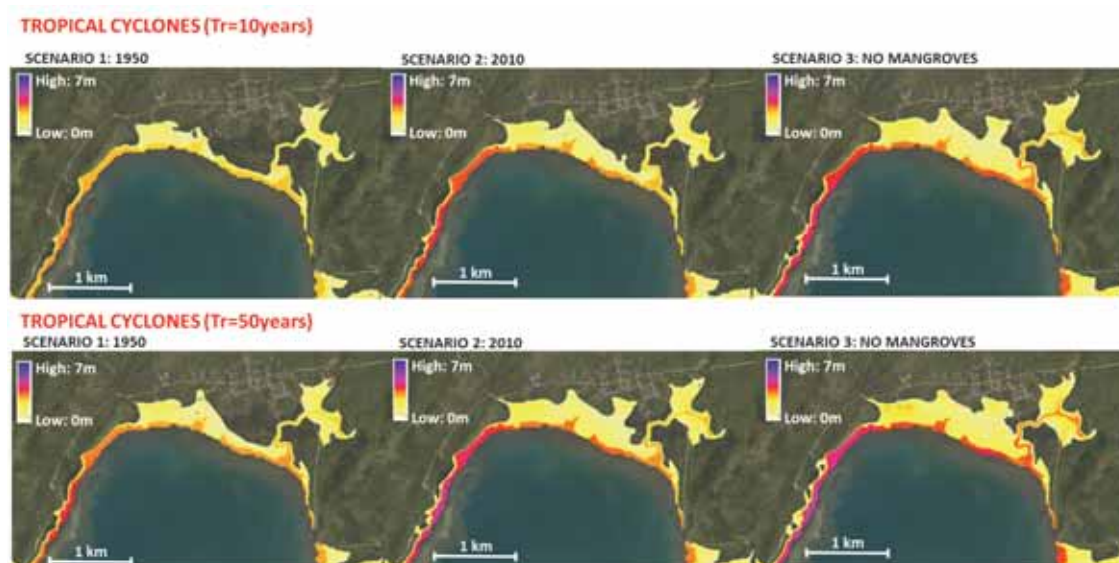
Figure 39 Flood extent and water depth in Busuanga for 1 in 10 and 1 in 50 year return period event under tropical cyclone conditions under three different mangrove scenarios: Historical (1950), Current (2010) and No Mangroves.

Busuanga in Figure 38) and the flooding extent and water depth for three scenarios (historical, current and no-mangroves) and two storm return periods, 10 and 50 years (Pagbilao in Figure 37 and Busuanga in Figure 39). These results are from flooding levels predicted from extreme, or tropical cyclone, conditions.

8 | Assessing the Benefits of High Resolution Data and Flooding Models

8.0 Section Overview

In this section we assess the potential of high resolution data and models for assessing flooding and flood protection benefits. There are 2 key messages from this assessment for the present and future work.

1. Flood estimates are greatly improved with higher resolution elevation data. At the national level, the best available data was of low resolution. Our comparisons with higher resolution site-based data suggest that we underestimate the actual flooding levels.

2. With high resolution elevation data, flood estimates can be improved by using better Rapid Flood Spreading Models (RFSM) instead of hydraulically connected bathtub flooding models. The RFSM models provide lower site-based flooding envelopes. However, even with a more accurate model, the low resolution data available still lead us to underestimate flooding in our national analyses.

8.1 Comparing the Effects of Higher and Lower Resolution Elevation Data

8.1.1 Regular Wave Climate

For regular wave climate, we compared two Digital Terrain Model (DTM) databases: National DTM SRTM30 PLUS, with 30m resolution (available across the Philippines) and the regional DTM IFSAR with, 5 m resolution (only available in Pagbilao). The two DTM databases are compared by using the same flooding method, i.e., a hydraulically-connected bathtub algorithm, which consists of connecting cells below the Coastal Total Water Level. Other more sophisticated flooding methods, like RFSM-EDA (Rapid Flood Spreading Model-Explicit Diffusion waves with Acceleration), cannot be applied with such coarse elevation data. This comparison shows the high sensitivity of the flooding model to the DTM resolution. The 30 m elevation data provides lower quality results and underestimates coastal flooding, while the 5 m resolution database provides more detailed flooding maps. (see Figure 40 and 41.)
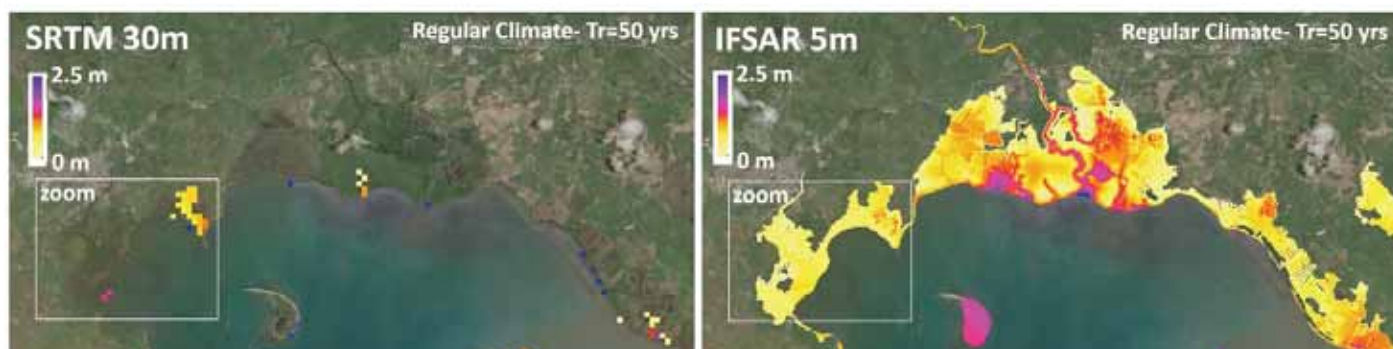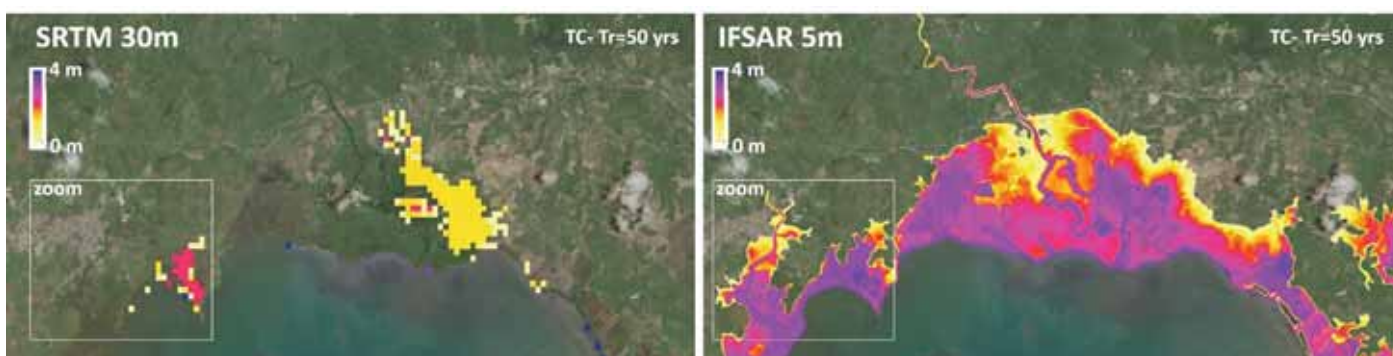

Figure 40 Flood Height in Pagbilao for 50 year return period event under regular conditions with current mangrove cover. The left image shows the SRTM 30m, the right image shows IFSAR 5m.
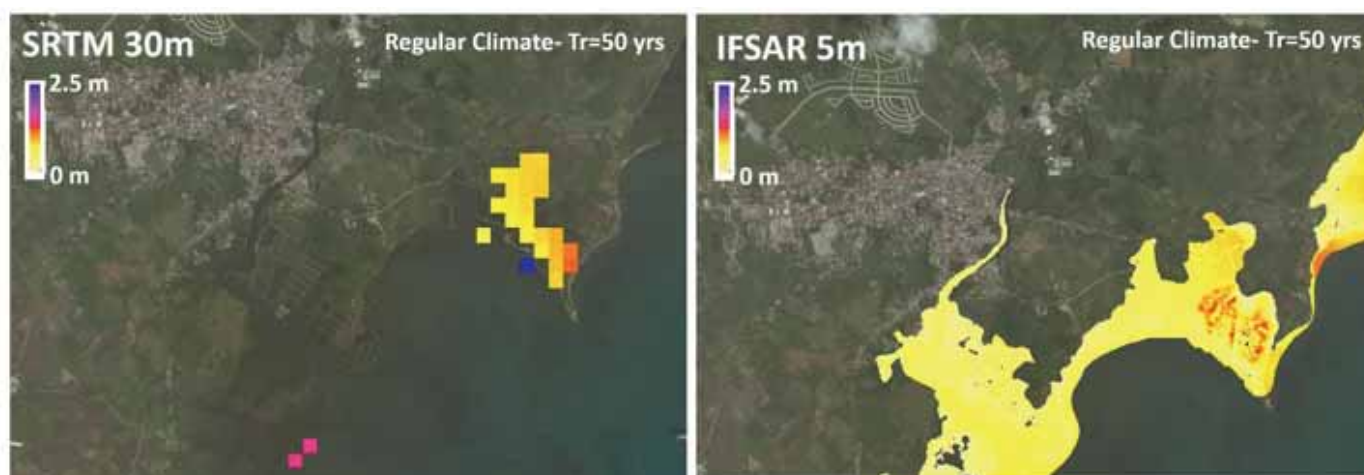
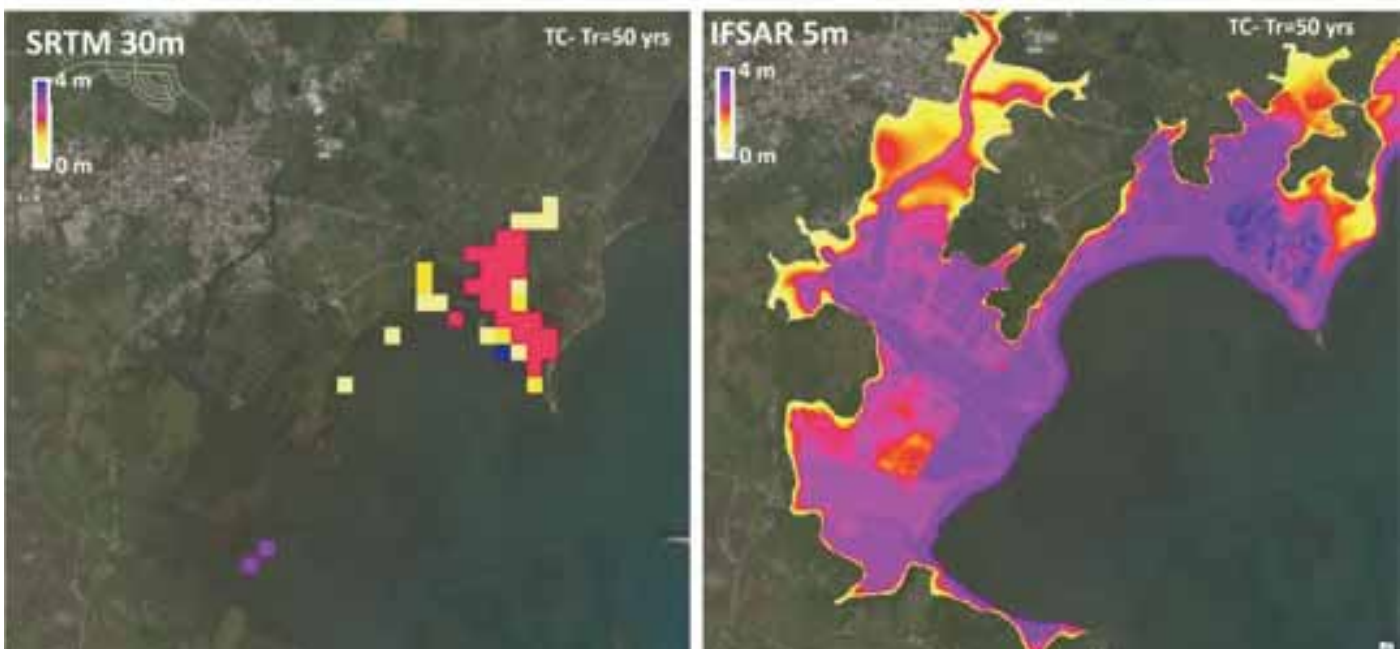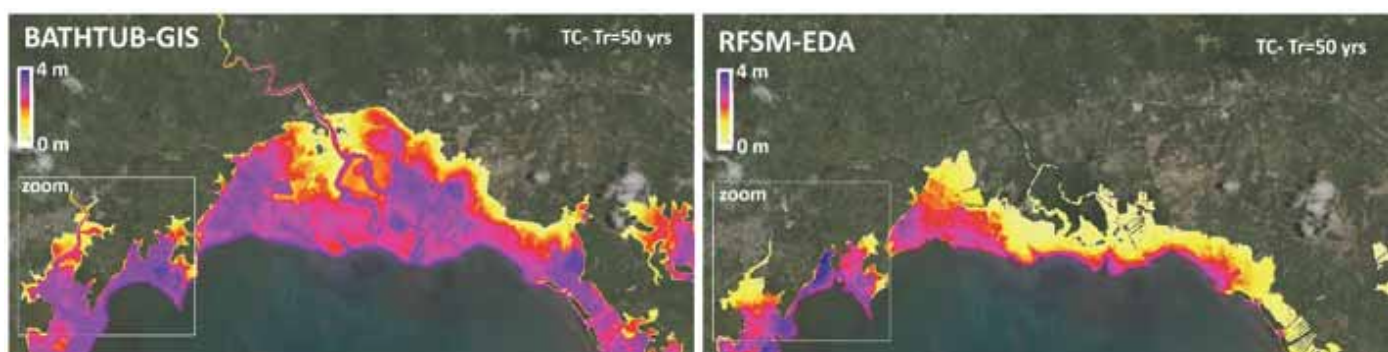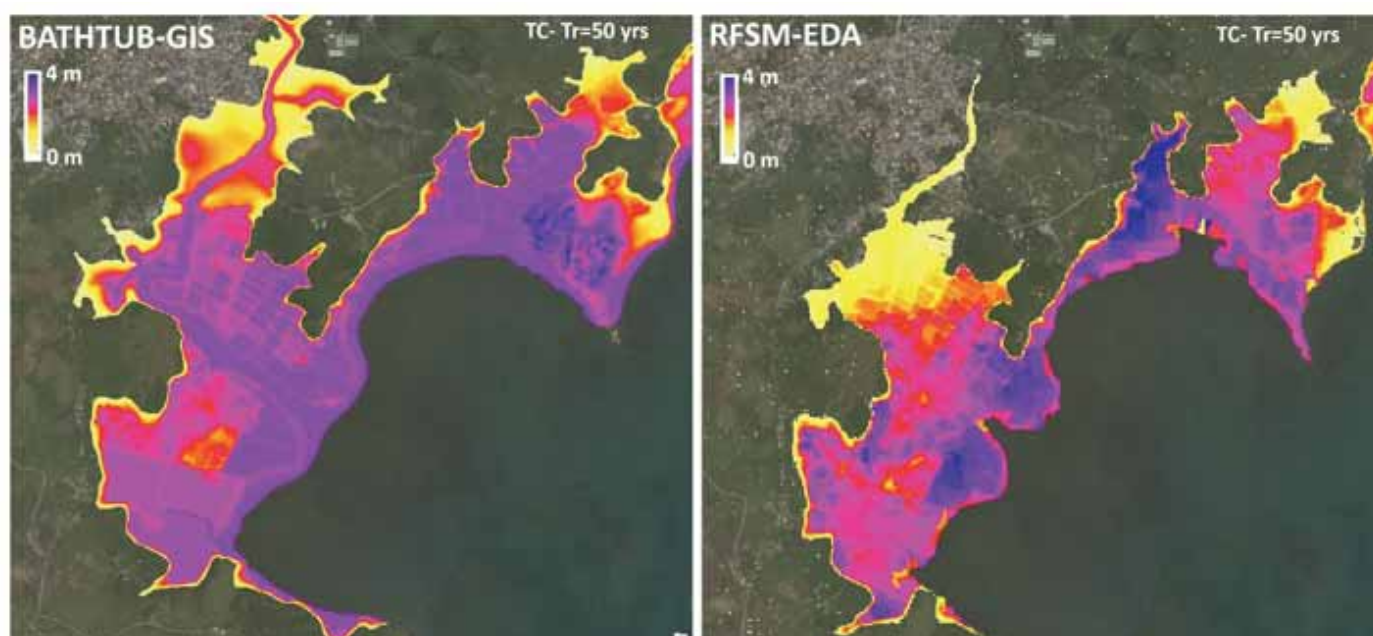**Figure 41** Flood Height in the most populated area of Pagbilao for 50 year return period under regular conditions for current mangrove cover. The left image shows the SRTM 30m, the right image shows IFSAR 5m.

8.1.2 Cyclone Data

The same comparison explained in Section 8.1.1 was performed for tropical cyclones events. Both DTM resolutions, SRTM30 PLUS and IFSAR 5 m, are tested for tropical cyclones, and the same conclusions are reached: a minimum of 5 m DTM resolution is required if we want an accurate Flood Height map. The 30 m DTM is too coarse for regional or local studies, but it is the highest resolution available at the national (or larger) scale. (See Figure 42 and 43.)

8.2 Flooding Methods: Hydraulically Connected Bathtub (5m) vs RFSM (5m)

The two flooding methodologies were compared at the local scale in Pagbilao using the flood levels from the tropical cyclone data. The DTM is IFSAR 5 m resolution, which clearly improves the SRTM30 PLUS (30 m resolution). The hydraulically connected bathtub methodology shows an overestimation of the flooding extent with respect to RFSM-EDA model. This could be due to the differences in the flooding method:

- The hydraulically-connected bathtub algorithm is based on the hydraulic

Figure 42 Flood Height in Pagbilao for 50 year return period event under tropical cyclone conditions for current mangrove cover. The left image shows the SRTM 30m, the right image shows IFSAR 5m.

Figure 43 Flood Height in the most populated area of Pagbilao for 50 year return period event under tropical cyclone conditions for current mangrove cover. The left image shows the SRTM 30m, the right image shows IFSAR

connectivity between cells and assumes that coastal flooding is stationary. The flooding mask given by this method is the maximum envelope within a sea state considering a constant landward flow. Additionally, no soil friction or porosity is considered (no water loss by infiltration) and all connected cells below the Flood Height are filled with water.

- RFSM-EDA is a high resolution hydraulic model which considers the flow rate within the tropical cyclone event. In this case, a triangular water discharge is

assumed with the peak of the flow equal to the Flood Height associated to a given return period. Furthermore, the model allows to include water inlets (rainfalls or river flows), and outlets (water infiltration, evapotranspiration).

In summary, the hydraulically connected bathtub model provides the envelope of a constant flooding within the whole TC duration and, consequently, it overestimates the flooding mask (which may be useful from the perspective of flood warnings where it can be better to over estimate flood levels).

Figure 44 Flooding Height in Pagbilao region for 50 year return period event under tropical cyclone conditions for current mangrove cover. The left image shows the Hydraulically-connected Bathtub method, the right image shows the RFSM-EDA method.

Figure 45 Flood Height in the most populated area of Pagbilao for 50 year return period event under tropical cyclone conditions for current mangrove cover. The left image shows the Hydraulically-connected Bathtub method, the right image shows the RFSM-EDA method.

In contrast, the RFSM-EDA model provides the punctual flooding associated to the peak of the Tropical Cyclone event. Figure 44 and Figure 45 show the differences in the flooding mask for both methods in Pagbilao, by using the same mangrove layer corresponding to current scenario. Fifty years return period flooding event has been plotted with flood heights reaching 4 meters in most of Pagbilao coast. The most affected area seems to be the West side of the bay where an additional zoom has been made, in order to notice the differences of both methodologies (see Figure 44 and Figure 45).

9 | Damages and Benefits

9.0 Section Overview

This section describes the process for estimating flooding exposure, the resulting damages to people and property, and the estimation of risk and probability based on event return periods, for each of the three mangrove cover scenarios, at the national and local scales. Available global, national and local databases are used to estimate the population, population below poverty level, residential stock, industrial stock, and length of roads for the country. This information is combined with empirical damage curves for population, stock and roads to estimate the damage from flooding under different return periods. Finally, the damages to population, stock and roads are compared for 'regular' conditions, historic tropical cyclones and synthetic tropical cyclones across the three mangrove cover scenarios, at the local and national scales. We did not apply discount rates because we are only estimating current expected benefits; we are not, for example, estimating the future flood reduction benefits from measures such as mangrove restoration, for which a discount rate would be applied.

The differences in damages across the three mangrove cover scenarios give the benefits of mangroves for risk reduction in terms of annual expected monetary benefits and in terms of people protected. The section also describes the process of annualizing the risk reduction benefits so that these mangrove values can ultimately be included in national ecosystem service accounts.

9.1 Exposure, Damage Curves and the Estimation of Risk Probability

9.1.1 Exposure of Assets: People and Stock

As discussed in section 2, we assessed the consequences of flooding across five key variables across the Philippines, which have total national values of:

1. Population: 100,234,428 people

2. Population below poverty level: 20,371,701 people

3. Residential Stock: $US 129,506,000,000

4. Industrial Stock: $US 87,475,000,000

5. Roads: 217,456 km

9.1.2 Damage Curves

We followed existing approaches for assessing the damages to built capital as a function of the level of flooding. We calculated the percentage of built capital that has been damaged (D) for a given flooding level and a certain coefficient that must be calibrated as $D(h) = h/(h +k)$. This curve indicates that as flooding level increases, the percent of damages to built capital also increases.

These functions are different for each category (i.e. population, stock, road) and can be different within the same category (i.e. different types of residential stock). We were not able to access damage curve data that may exist for all portions of the Philippines, so we used curves derived from the common database of damage functions in US HAZUS. HAZUS is a set of models and data developed by the Federal Emergency Management Agency of the United States of America that considers potential losses from natural disasters such as earthquakes, floods, and hurricanes.

We tested the use of various damage curves for population, residential and industrial stock and roads from HAZUS in the Philippines, and we found that the results were not significantly different from approaches using simpler curves.

To define case-specific semi-empiric damage functions for the Philippines we used a damage function for all categories, i.e. population and population below poverty level, residential and industrial stocks, and road network (see Figure 9. 1 in Annex1).

9.1.3 Assessing Risk – Combining Spatial Results

We assessed flood heights along each coastal profile and then identified the area flooded within each coastal study unit. We extended the flood heights inland by ensuring hydraulic connectivity between points at a 30m resolution, a significant advancement over more common bathtub approaches in earlier global flooding models. From the flooding levels and flooding extent, we calculated the total area of land affected and damages at each study unit. Flooding maps were also intersected with population data after resampling from the original 100 m resolution to the 30 m of the digital elevation model. In addition to assessing risk and damages for particular events (e.g., 100 year storm event), we also examined average annual expected damages and benefits provided by mangroves.

To estimate annual risk, we integrated the values under the curve that compares built capital damaged by storm return period, i.e., the integration of the expected damage with the probability of the storm events. This step helps us define the spatial and temporal distribution of the risk level borne by society.

The magnitude of risk is determined by the damage probability distribution existing at different areas and sectors. Assessing the risk borne by society requires the combination of all the variables presented into a set of synthetic indicators presenting the probabilistic distribution of impacts.

In summary, we combine the flooding information for different return periods with the exposure and vulnerability of people and property to obtain the damage associated with different probabilities.

In terms of the spatial summation of the risk results, for each asset (population, population below poverty, residential stock, industrial stock and road network) we did the following:

1. Raster layers from flooding and exposure were loaded. We homogenized their projection systems and resolutions (if necessary).

2. Raster layers were transformed into matrices. Zero and NA values were normalized to avoid possible errors in following steps.

3. For each matrix element, the damage function was applied and the damage was obtained.

4. Matrices were then transformed to raster layers and saved.

5. The damage for the Philippines was obtained by summing all matrices or raster layers values.

Due to technical and computational limitations, to perform the described methodology, the Philippines was divided into 71 sections. A buffer zone was defined for each section to ensure data continuity and avoid contour problems. The processes described were executed for each of these 71 sections, and then results were merged into single layers (see Figure 9. 2 Annex 1).

9.2   National Scale Results

The results help understand the expected benefits provided by mangroves for flood reduction to people and property annually and for catastrophic events. The benefits provided by mangroves are assessed as the flood damages avoided by them. We examine the benefits provided by current mangroves, and the additional benefits that could be provided if mangroves were restored to their 1950 distribution. We provide results in absolute terms and terms relative to the total economy, population and
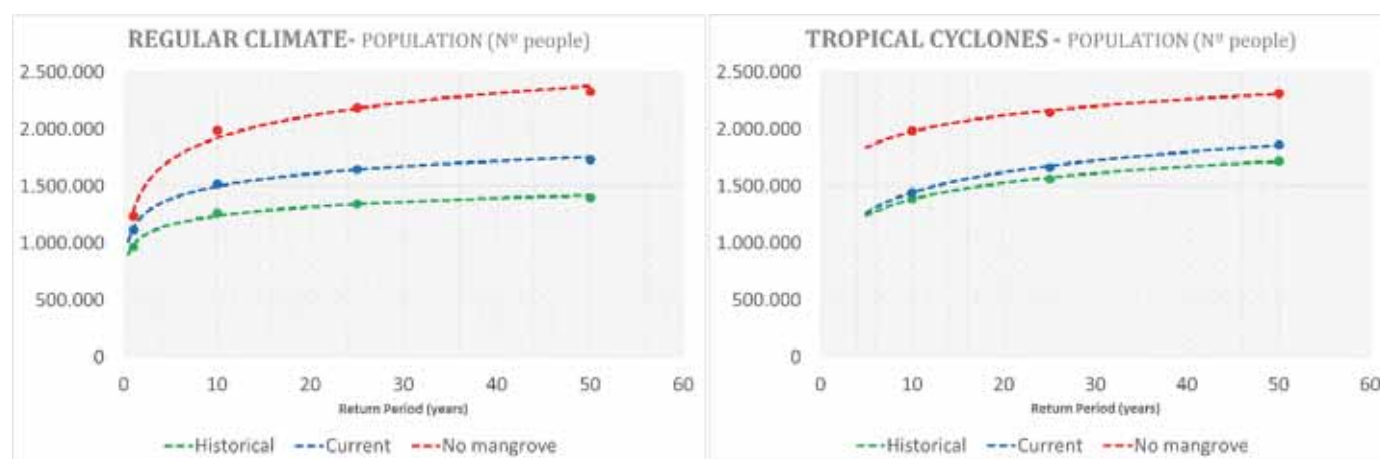
Figure 46 People affected in the Philippines. Reg. Climate (left) and Tropical Cyclones (right)
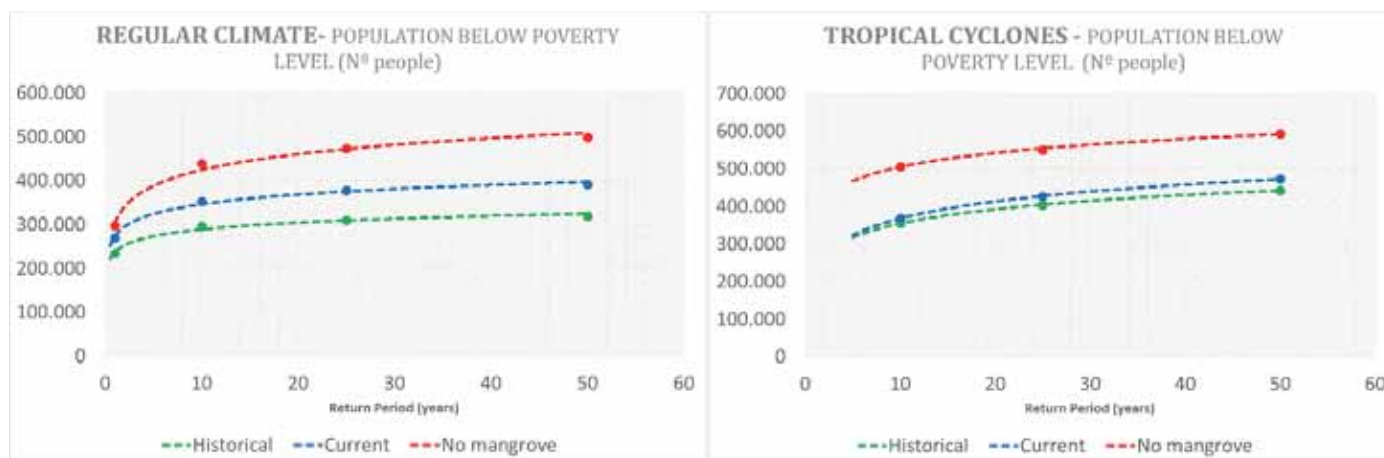
Figure 47 Poor people affected in the Philippines. Reg. Climate (left) and Tropical Cyclones (right)
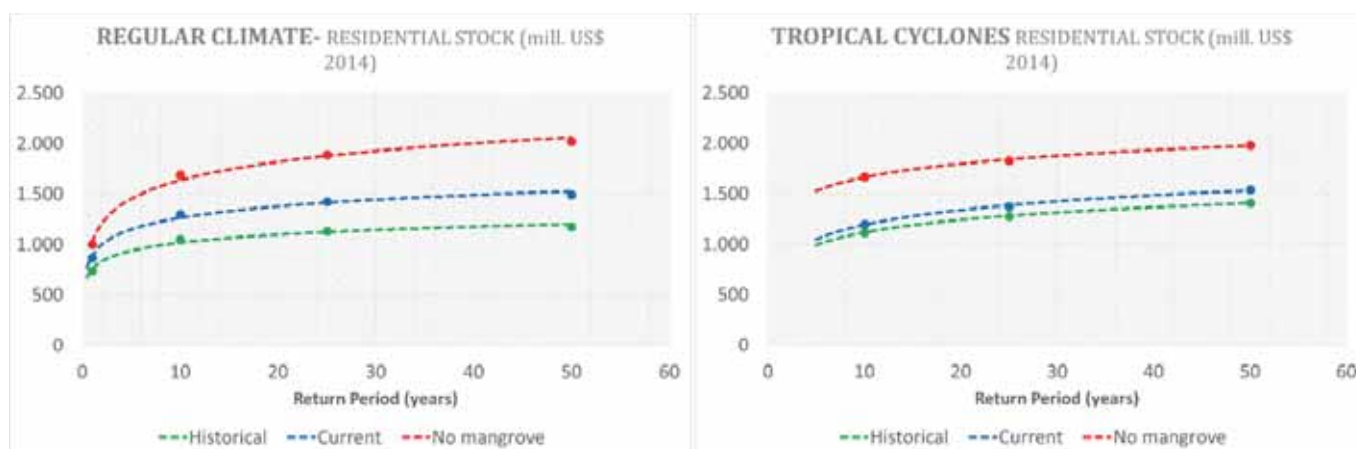
Figure 48 Residential stock damaged in the Philippines. Reg. Climate (left) and Tropical Cyclones (right)
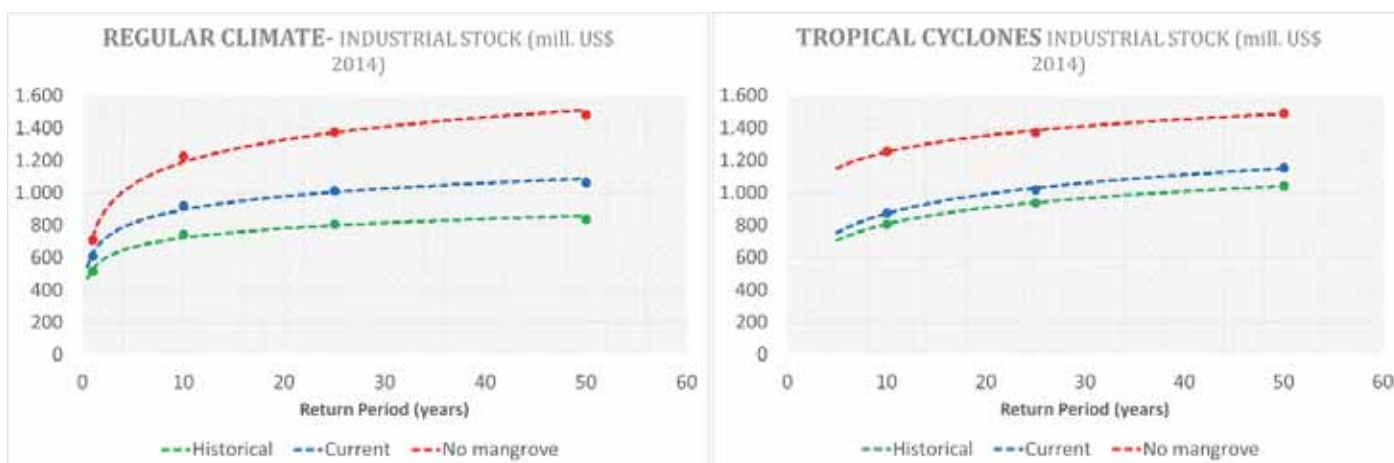
Figure 49 Industrial stock damaged in the Philippines. Reg. Climate (left) and Tropical Cyclones (right)

Figure 50 Total stock (residential + industrial) damaged in the Philippines. Reg. Climate (left) and Tropical Cyclones (right)
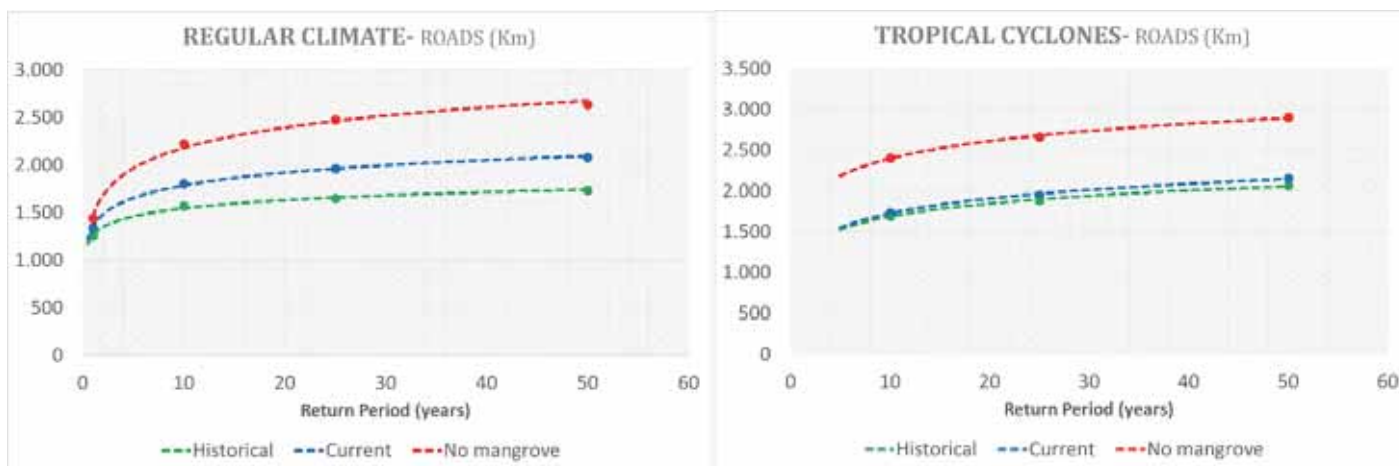
Figure 51: Roads network damaged in the Philippines. Reg. Climate (left) and Tropical Cyclones (right)

hectares of mangrove. We recognize that relative benefits vary spatially. The benefits per hectare may be important to consider in cost effectiveness analyses for restoration.

9.2.1 Damages vs Return Period

The core results are summarized in Figure 46 to Figure 51, which show the consequences of flooding in terms of people and infrastructure flooded for the different storm return periods. The annual expected damages, i.e., flooding of people and property, are calculated via the integration of each curve. The curves show expected damages by storm return period for the three different habitat scenarios of current mangroves, historical mangroves and no

mangroves. For these results, we show the curves for the two types of flood data from the regular wave models and the cyclone models.

9.2.2 Expected Damages: Annual and by Return Period

The expected damages from flooding for each scenario of mangrove cover are in Table 3. They are given as annual expected damages, and as damages per return period.

		TOTAL DAMAGE (Annual Expected Damage)
POPULATION (nº people)	Historical	2,253,954
	Current	2,521,004
	No Mangrove	3,134,465
POPULATION BELOW POVERTY (nº people)	Historical	558,009
	Current	619,488
	No Mangrove	761,915
RESIDENTIAL STOCK (millions US $ 2014)	Historical	1,816
	Current	2,073
	No Mangrove	2,637
INDUSTRIAL STOCK (millions US $ 2014)	Historical	1,308
	Current	1,503
	No Mangrove	1,940
TOTAL STOCK	Historical	3,124
	Current	3,577
	No Mangrove	4,577
ROADS (Km)	Historical	2,784
	Current	2,990
	No Mangrove	3,757

Table 3 Annual Expected Damage in the Philippines in terms of people, stock and km of roads

		ANNUAL EXPECTED BENEFITS OF MANGROVES FOR FLOOD REDUCTION
POPULATION (nº people)	Current Benefits	+613,431
	Potential Restoration Benefits	+267,050
POPULATION BELOW POVERTY (nº people)	Current Benefits	+142,428
	Potential Restoration Benefits	+61,479
RESIDENTIAL STOCK (millions US $)	Current Benefits	+564
	Potential Restoration Benefits	+257
INDUSTRIAL STOCK (millions US $)	Current Benefits	+437
	Potential Restoration Benefits	+195
TOTAL STOCK (millions US $)	Current Benefits	+1,001
	Potential Restoration Benefits	+452
ROADS (km)	Current Benefits	+767
	Potential Restoration Benefits	+206

Table 4 Annual Expected Benefits provided by mangroves in the Philippines

9.2.3 Expected Benefits: Annual and by Return Period

The annual expected benefits provided by mangroves are estimated by comparing scenarios. The annual expected benefits received from current mangroves are the difference in damages between the Current (2010) and No Mangrove scenarios. (see Table 4).

We can also estimate how many more flood reduction benefits could potentially be gained by restoring mangroves to their distribution in 1950. This is the difference between expected benefits from Historic (1950) and Current (2010) mangroves. Caution should be applied when making assumptions about the potential benefits of mangrove restoration, because many of the

areas that have lost mangroves may have been developed in ways that prevent the restoration of previously existing mangroves.

9.2.4 Annual Expected Benefits per Ha of mangroves

Given that there are currently 310,000 ha of mangroves in the Philippines, we can provide a figure for the average current annual benefits per hectare of mangrove. Across the Philippines, each 10 hectares of mangrove reduces flooding for 20 people of which 5 are below the poverty level, and provides more than US $32,000 in prevented damages to built stock annually. If mangroves were restored to their 1950 distribution, each 10 hectares of mangroves would reduce flooding for an additional 9 people, 2 of them below poverty level, and

		ANNUAL EXPECTED BENEFITS OF MANGROVES FOR FLOOD REDUCTION (each 10 Ha of Mangroves)
POPULATION (nº people/10ha)	Current Benefits	+20
	Potential Restoration Benefits	+9
POPULATION BELOW POVERTY (nº people/10ha)	Current Benefits	+5
	Potential Restoration Benefits	+2
RESIDENTIAL STOCK (millions US $ 2014/10ha)	Current Benefits	+18,161
	Potential Restoration Benefits	+8,290
INDUSTRIAL STOCK (millions US $ 2014/10ha)	Current Benefits	+14,097
	Potential Restoration Benefits	+6,323
TOTAL STOCK	Current Benefits	+32,258
	Potential Restoration Benefits	+14,613
ROADS (Km/10ha)	Current Benefits	+25
	Potential Restoration Benefits	+7

Table 5 Annual Expected Benefits provided by each 10 Ha of mangroves in the Philippines

would avoid more than US $14,000 in damages to built stock annually.

9.2.5 Catastrophic Benefits (100 years return period event)

Analyzing the most extreme events gives us information about the maximum current benefits and the maximum potential restoration benefits provided by mangroves in the Philippines. Across the Philippines, for a 100 year return period event (i.e., a catastrophic event), mangroves would reduce flooding for 1,290,308 people; 277,157 of them below the poverty level, and would prevent US $2,046 million in damages to built stock. If mangroves were restored to their 1950 distribution, each 10 hectares of mangroves would reduce flooding for an additional 503,297 people, 108,516 of them below poverty level, and would avoid US $866 million in damages to built stock annually.

		CATASTROPHIC BENEFITS (100 years return period event)
POPULATION (nº people)	Current Benefits	+1,290,308
	Potential Restoration Benefits	+503,297
POPULATION BELOW POVERTY (nº people)	Current Benefits	+277,157
	Potential Restoration Benefits	+108,516
RESIDENTIAL STOCK (millions US $ 2014)	Current Benefits	+1,147
	Potential Restoration Benefits	+496
INDUSTRIAL STOCK (millions US $ 2014)	Current Benefits	+900
	Potential Restoration Benefits	+370
TOTAL STOCK	Current Benefits	+2,046
	Potential Restoration Benefits	+866
ROADS (Km)	Current Benefits	+1,566
	Potential Restoration Benefits	+498

Table 6 Catastrophic benefits provided by mangroves in the Philippines against 100 year return period event

9.2.6 National Maps of Annual Expected Benefits

CURRENT BENEFITS: POPULATION
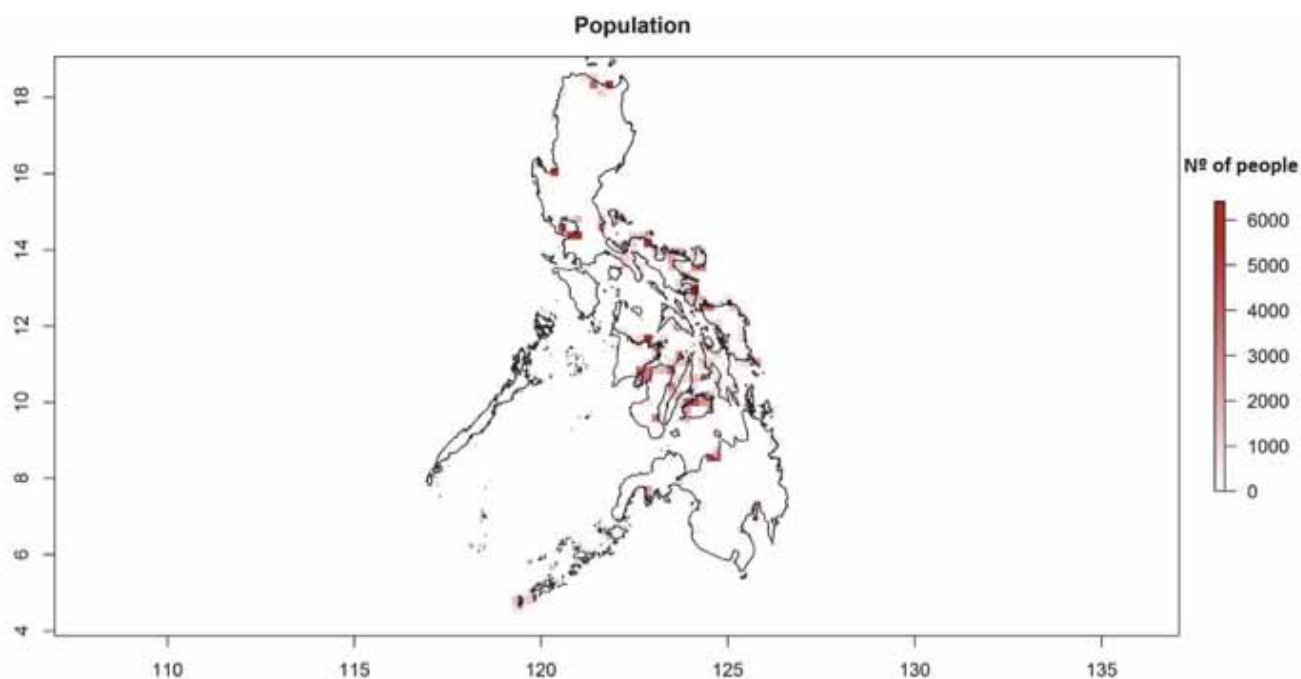
Figure 52 National distribution of the Annual Current Benefits provided by mangroves to people in the Philippines (25 km aggregation units)

CURRENT BENEFITS: POPULATION BELOW POVERTY
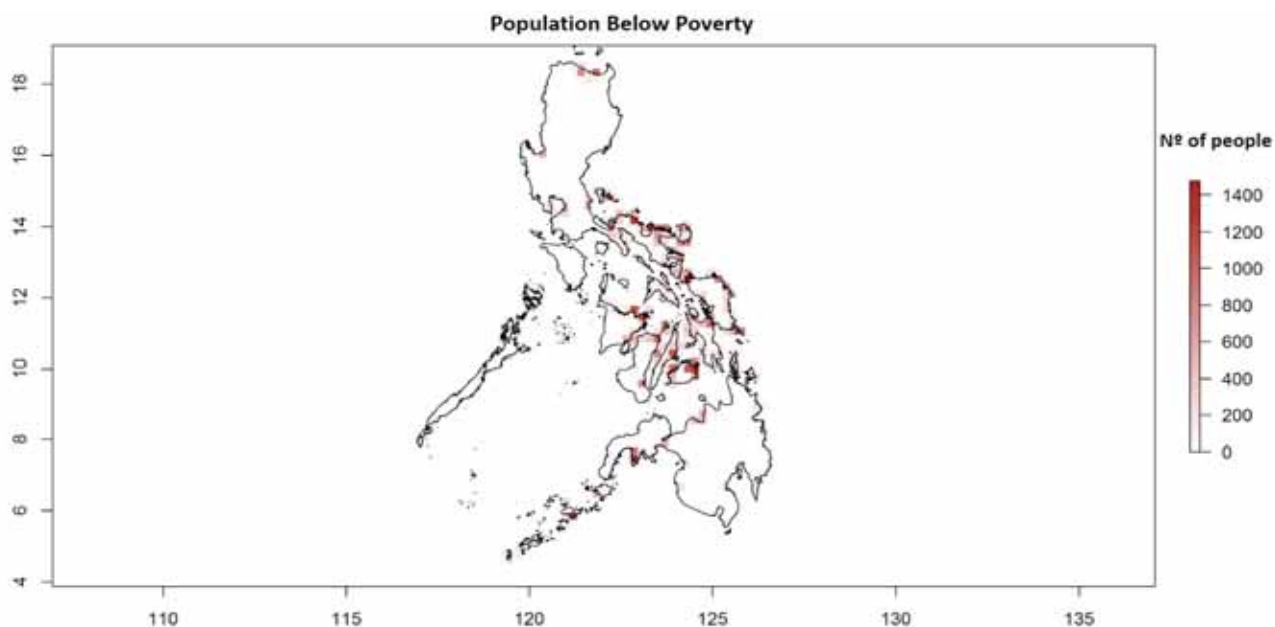
Figure 53 National distribution of the Annual Current Benefits provided by mangroves to people below poverty in the Philippines (25 km aggregation units)

CURRENT BENEFITS: TOTAL STOCK:
INDUSTRIAL + RESIDENTIAL STOCK
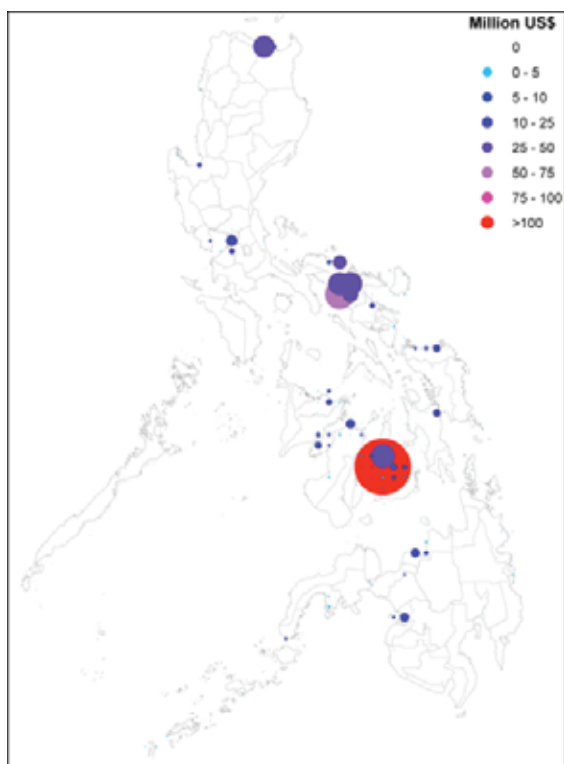
Figure 54 National distribution of the Annual Current Benefits provided by mangroves to the total stock (industrial + residential) in the Philippines (25 km aggregation units)

CURRENT BENEFITS: KM OF ROADS
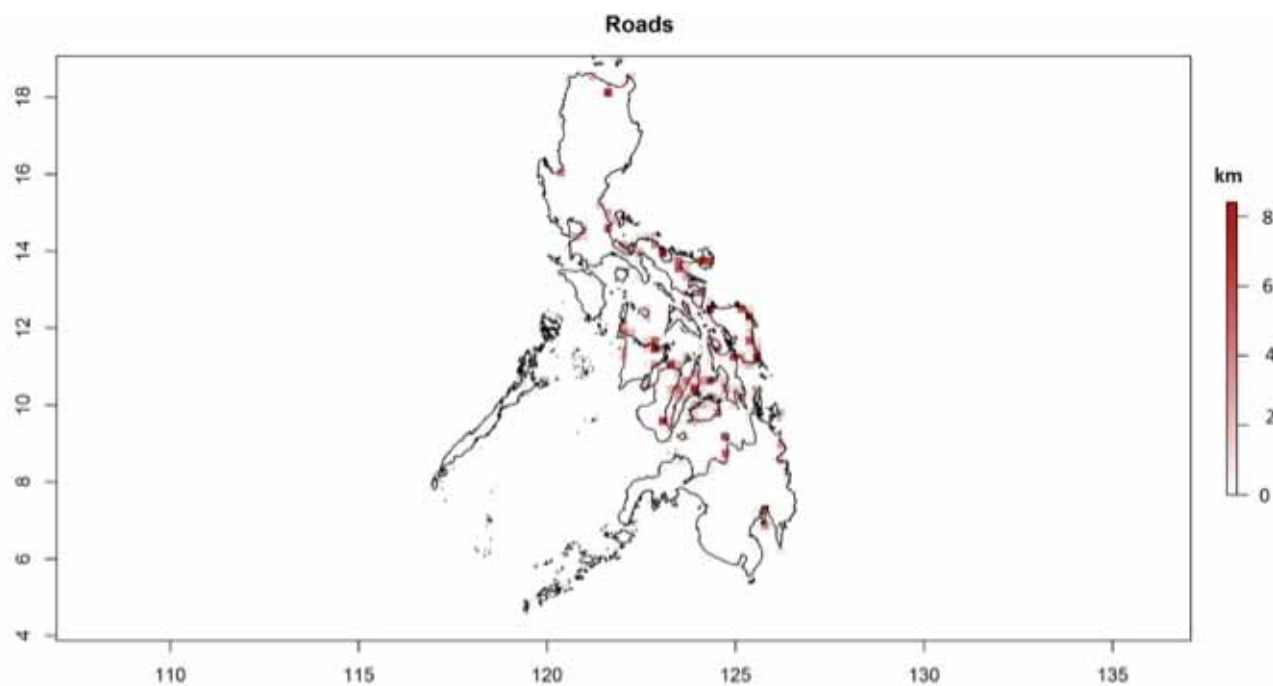
Figure 55 National distribution of the Annual Current Benefits provided by mangroves to roads in the Philippines (25 km aggregation units)
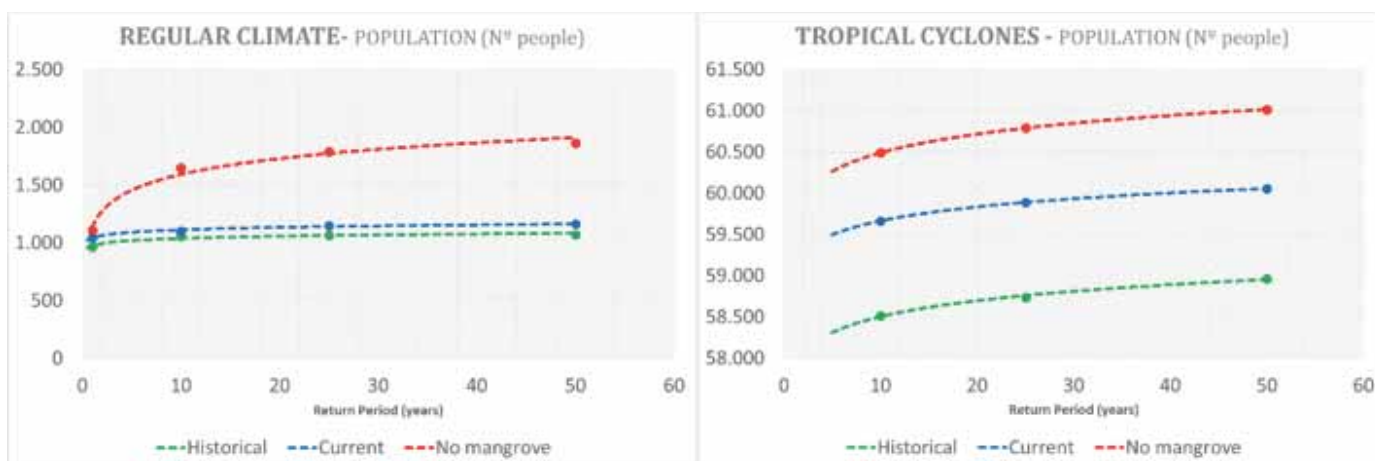
Figure 56 People flooded in Pagbilao. Reg. Climate (left) and Tropical Cyclones (right)
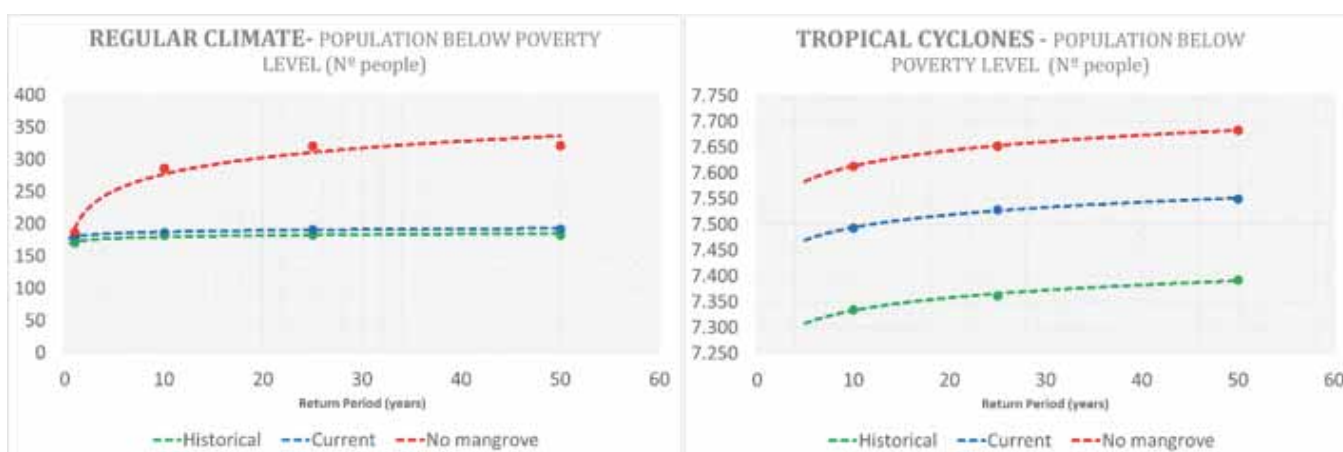
Figure 57 People below poverty flooded in Pagbilao. Reg. Climate (left) and Tropical Cyclones (right)
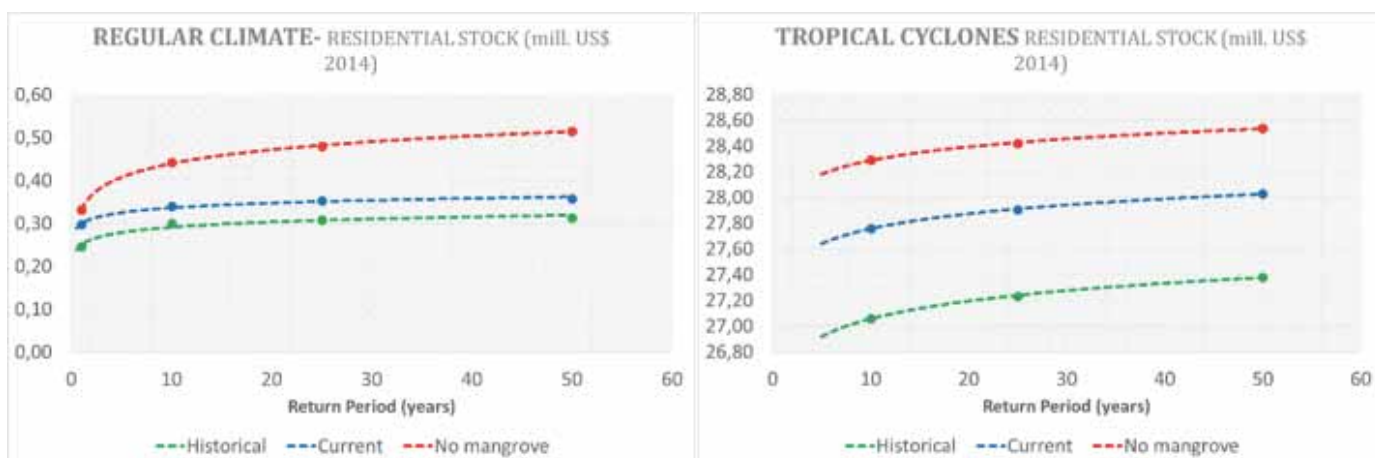
Figure 58 Residential stock damage in Pagbilao. Reg. Climate (left) and Tropical Cyclones (right)

9.3 Local Scale Results: Pagbilao

The spatial distribution of benefits differs along the coastline of the Philippines. As noted above, high resolution elevation data is available for Pagbilao, which allowed us to compare flood mapping results for high and lower resolution analyses. Below using the highest resolution elevation data and flood model, we provide high resolution estimates
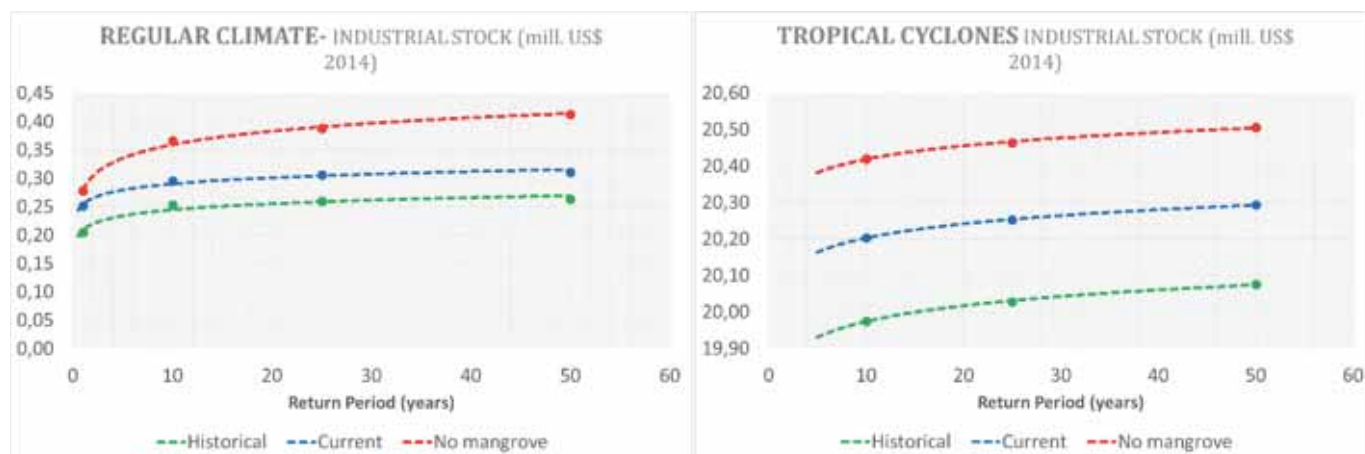
Figure 59 Industrial stock damaged in Pagbilao. Reg. Climate (left) and Tropical Cyclones (right)

Figure 60 Total stock (residential + industrial) damaged in Pagbilao. Reg. Climate (left) and Tropical Cyclones
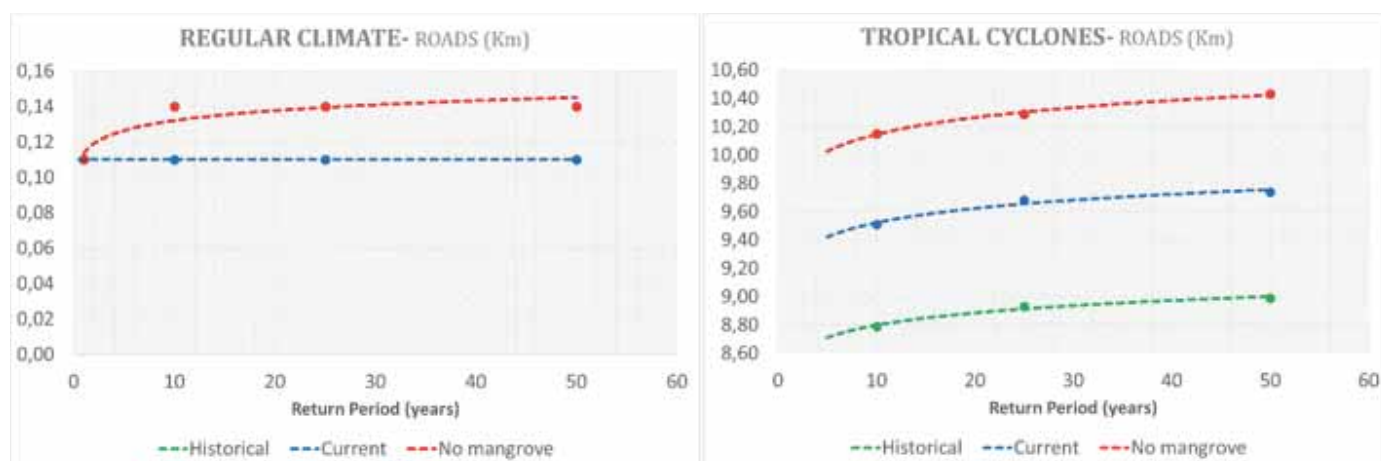
Figure 61 Roads damaged in Pagbilao. Reg. Climate (left) and Tropical Cyclones (right). Note that the curves for roads flooded under regular wave climate are overlapped for historical and current mangroves.

of the flood protection benefits from mangroves.

9.3.1 Damages vs Return Period

The core results are summarized in Figure 56 to Figure 61, which show the consequences of flooding in terms of damages to people

and infrastructure for the different storm return periods. The curves show expected damages for habitat distribution scenarios of current mangroves, historical mangroves and no mangroves. The annual expected damages- i.e., flooding consequences to people and property- are the integration of each curve. For these results we show the curves for the two types of flood data from the regular wave models and the cyclone models.

9.3.2 Annual Expected Damage

Three scenarios were analyzed: mangrove level at 1950, mangrove level at 2010 and no mangroves. The annual expected damage for Pagbilao for each scenario was obtained.

		TOTAL DAMAGE (Annual Expected Damage)
POPULATION (nº people)	Historical	57,814
	Current	59,145
	No Mangrove	60,414
POPULATION BELOW POVERTY (nº people)	Historical	7,285
	Current	7,462
	No Mangrove	7,655
RESIDENTIAL STOCK (millions US $ 2014)	Historical	26,41
	Current	27,26
	No Mangrove	27,94
INDUSTRIAL STOCK (millions US $ 2014)	Historical	19,79
	Current	20,09
	No Mangrove	20,37
TOTAL STOCK	Historical	46,21
	Current	47,35
	No Mangrove	48,31
ROADS (km)	Historical	82,34
	Current	89,55
	No Mangrove	96,79

Table 7 Annual Expected Damage in Pagbilao in terms of people, stock and km of roads

9.3.3 Annual Expected Benefits

The annual expected benefits received from current mangroves is the difference in damages between the Current and No Mangrove scenarios. We can also estimate how many more flood reduction benefits could potentially be gained by restoring mangroves to their distribution in 1950.

9.3.4 Annual Expected Benefits per 10 Ha of mangroves

There are currently 4,560 ha of mangroves in Pagbilao. Each 10 hectares of mangroves reduce flooding for 2.92 people, 42% of them below poverty level, and avoid more than US $2,107 in damages to built stock annually. In

		ANNUAL EXPECTED BENEFITS OF MANGROVES FOR FLOOD REDUCTION
POPULATION (nº people)	Current Benefits	+1,269
	Potential Restoration Benefits	+1,332
POPULATION BELOW POVERTY (nº people)	Current Benefits	+193
	Potential Restoration Benefits	+178
RESIDENTIAL STOCK (millions US $ 2014)	Current Benefits	+0.681
	Potential Restoration Benefits	+0.847
INDUSTRIAL STOCK (millions US $ 2014)	Current Benefits	+0.280
	Potential Restoration Benefits	+0.298
TOTAL STOCK	Current Benefits	+0.961
	Potential Restoration Benefits	+1.145
ROADS (Km)	Current Benefits	+7,241
	Potential Restoration Benefits	+7,211

Table 8: Annual Expected Benefits provided by mangroves in Pagbilao

		ANNUAL EXPECTED BENEFITS OF MANGROVES FOR FLOOD REDUCTION (each 10 Ha of Mangroves)
POPULATION (nº people/10ha)	Current Benefits	+2.92
	Potential Restoration Benefits	+2.78
POPULATION BELOW POVERTY (nº people/10ha)	Current Benefits	+0.42
	Potential Restoration Benefits	+0.39
RESIDENTIAL STOCK ((millions US $ 2014)/10ha)	Current Benefits	+1,493
	Potential Restoration Benefits	+1,857
INDUSTRIAL STOCK ((millions US $ 2014)/10ha)	Current Benefits	+614
	Potential Restoration Benefits	+654
TOTAL STOCK	Current Benefits	+2,107
	Potential Restoration Benefits	+2,511
ROADS (Km/10ha)	Current Benefits	+15.88
	Potential Restoration Benefits	+15.81

Table 9 Annual Expected Benefits provided by each 10 Ha of mangroves in Pagbilao

		CATASTROPHIC BENEFITS (100 years return period event)
POPULATION (nº people)	Current Benefits	+1,741
	Potential Restoration Benefits	+1,135
POPULATION BELOW POVERTY (nº people)	Current Benefits	+286
	Potential Restoration Benefits	+164
RESIDENTIAL STOCK (US $ millions 2014)	Current Benefits	+0.643
	Potential Restoration Benefits	+0.642
INDUSTRIAL STOCK (mill. US$ 2014)	Current Benefits	+0.313
	Potential Restoration Benefits	+0.252
TOTAL STOCK ($US Millions)	Current Benefits	+0.955
	Potential Restoration Benefits	+0.895
ROADS (Km)	Current Benefits	+6,728
	Potential Restoration Benefits	+7,532

Table 10 Catastrophic Benefits provided by mangroves in Pagbilao against 100 years return period event

1950, there were 6,652 ha of mangroves. If mangroves were restored to their 1950 distribution, each 10 hectares of mangroves in Pagbilao would reduce flooding for an additional 2.78 people, 39% of them below poverty level, and would avoid more than US $2,511 million in damages to built stock annually.

9.3.5 Benefits for catastrophic events (100 year return period event)

Analyzing the most extreme events gives us information about the maximum current benefits and the maximum potential restoration benefits provided by mangroves in Pagbilao. Across Pagbilao and for a 100 year return period event (i.e., a catastrophic event), mangroves would reduce flooding for 1,741 people, 286 of them below poverty level, and avoid US $955,000 of damages to in built stock.If mangroves were restored to their 1950 distribution, they would reduce flooding for an additional 1,135 people, 164 of them below poverty level, and would avoid

US $895,000 million in damages to built stock annually.

10 | Conclusions

Mangrove conservation and restoration can be an important part of the solution for reducing coastal risks. This Report provides a social and economic valuation of mangroves that can inform the policy and practice of many Philippine agencies, businesses and organizations across development, aid, risk reduction and conservation sectors as they seek to identify sustainable and cost-effective approaches for risk reduction. By showing the spatial variation of the flood reduction benefits provided by mangroves, these results can identify the places where mangrove management may yield the greatest returns. By valuing these coastal protection benefits in terms used by finance and development decision-makers (e.g., annual expected benefits), these results can be readily used alongside common metrics of national economic accounting, and can inform risk reduction, development and environmental conservation decisions in the Philippines.

In the Philippines, many opportunities exist for the application of these results:

- These results can help identify priority sites for mangrove conservation and restoration for coastal protection, either as 'stand-alone' solutions, or part of hybrid approaches that combine natural defenses, like mangroves, with built infrastructure. Numerous programs can incorporate these results into their plans and analysis, including: the National Greening Program; Integrated Area Development, Risk Resilience and Sustainability Program; Green Climate Fund and People Survival Fund; and the Comprehensive Land Use Plans of local governments.

- PAGASA[10] and Local Government Units may use these results to inform and improve their risk assessment and flood risk mapping.

- These results can be considered in insurance industry risk models, which may potentially influence insurance premiums in the Philippines.The results may inform the development of innovative finance mechanisms, including catastrophic hazard bonds, resilience bonds, and blue bonds, which could better account for the value and potential premium reductions associated with mangrove conservation and restoration.

- In the past nature-based measures for coastal protection, such as mangrove restoration, were not assessed for their cost effectiveness for risk reduction, because rigorous values of their coastal protection benefits were missing. Now we can rigorously value these services, and we can inform cost-benefit analyses and comparisons of different coastal protection options, including natural defenses, built defenses and hybrid approaches.

Annex 1 | Figures
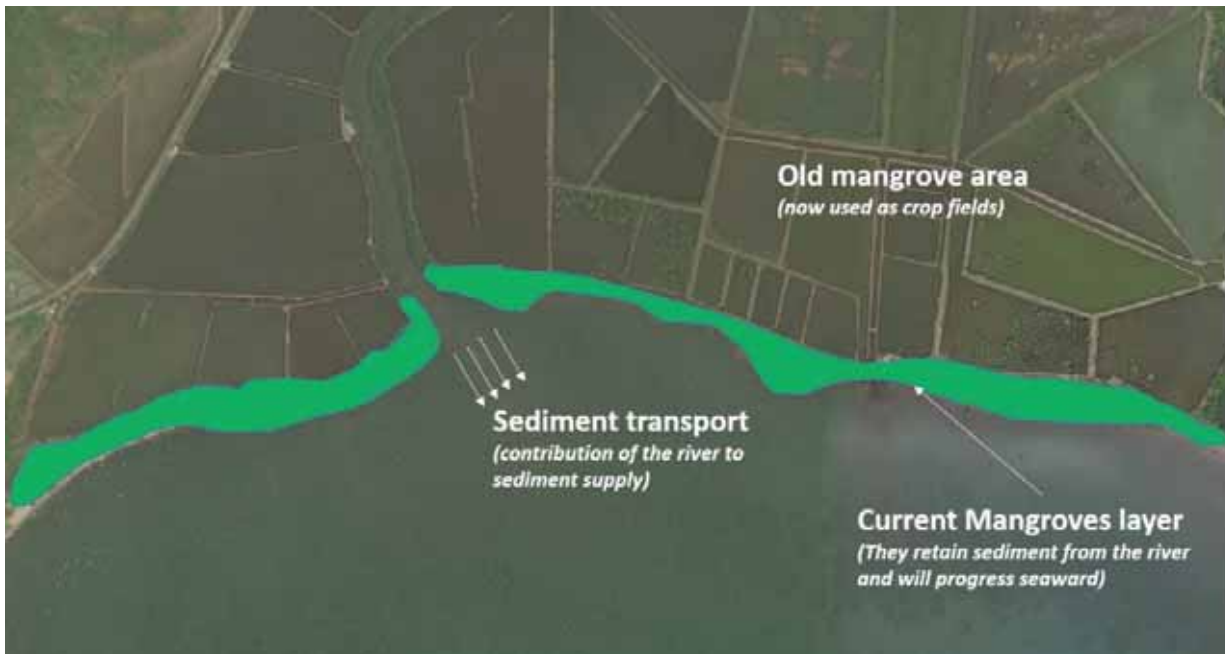
Figure 1.1 Example of land cover and land use change in Pagbilao Bay. Previously existing mangrove forests have been converted to agriculture Mangroves continue to propagate on the new coastline.
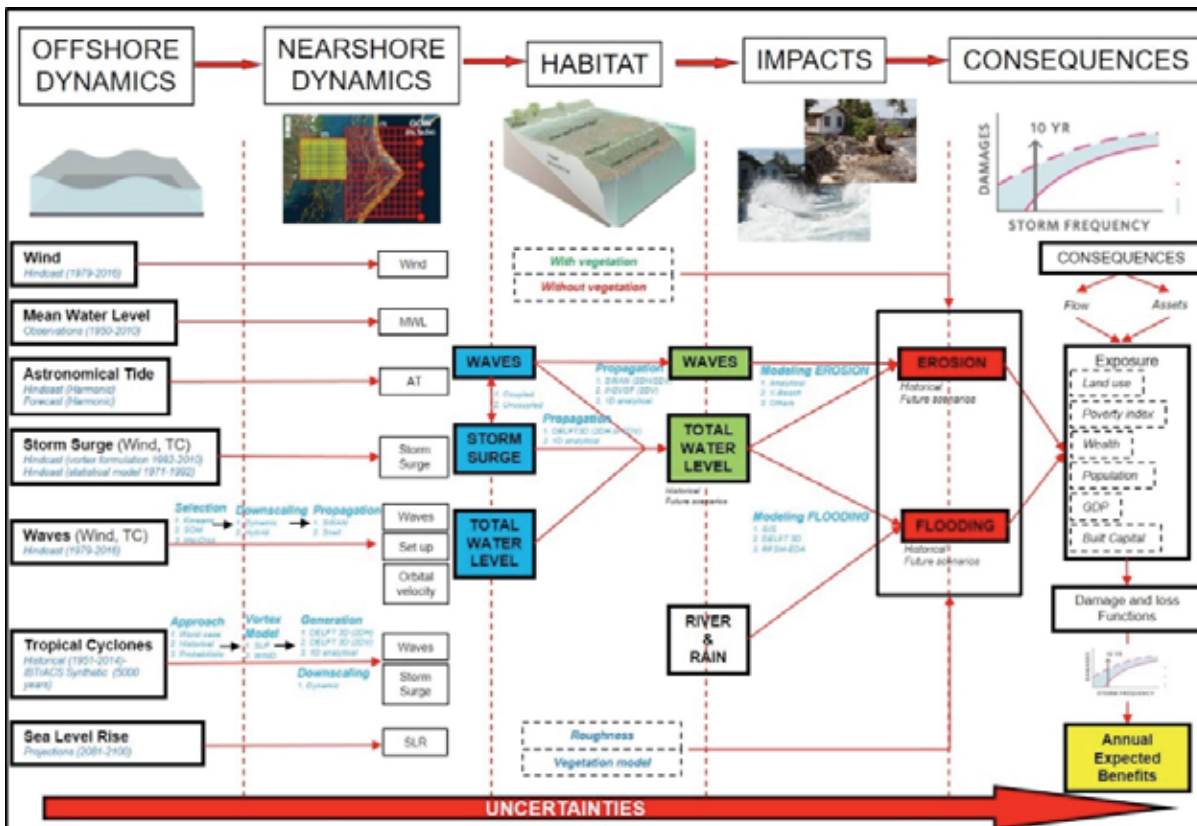
Figure 1.2 General view of the methodology to evaluate coastal protection services of ecosystems like coral reefs and mangroves.
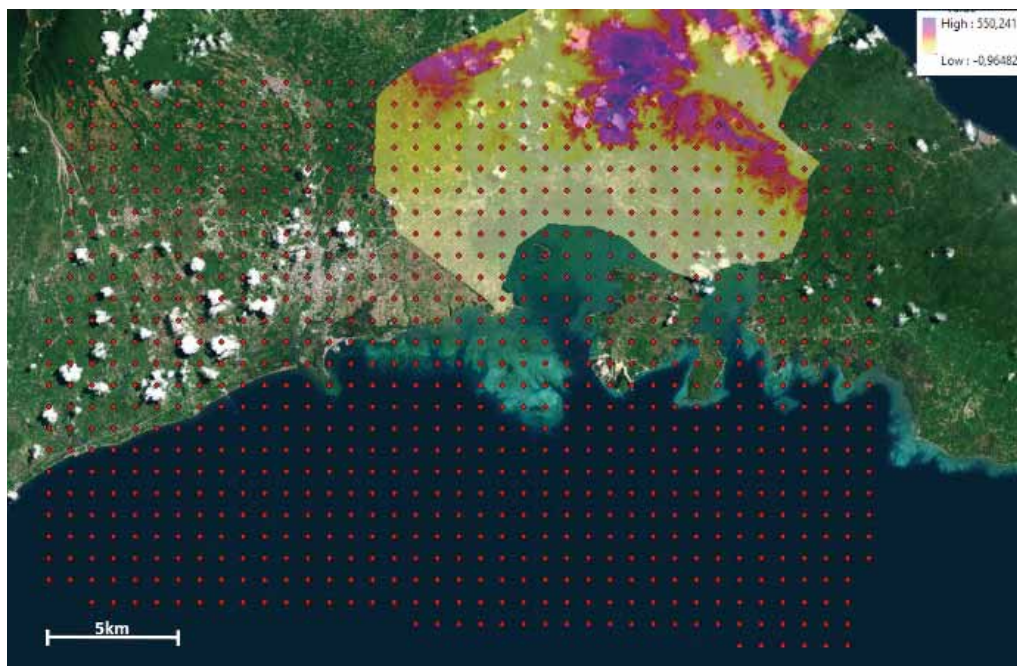
Figure 2.1 Topography IFSAR 5m resolution (colored area) and the ensemble Topography (ETOPO) and bathymetry (SEAWIFS) with 1km resolution (red dots) in Pagbilao.
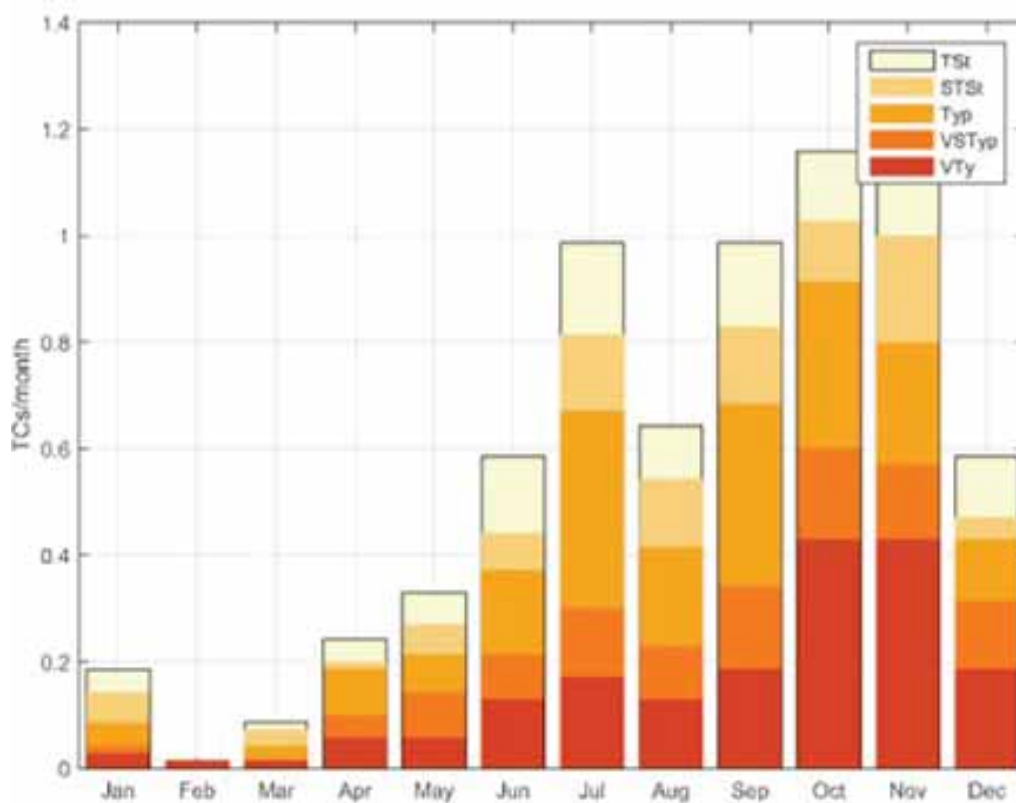
Figure 2.2 Monthly climatology of tropical cyclone activity.
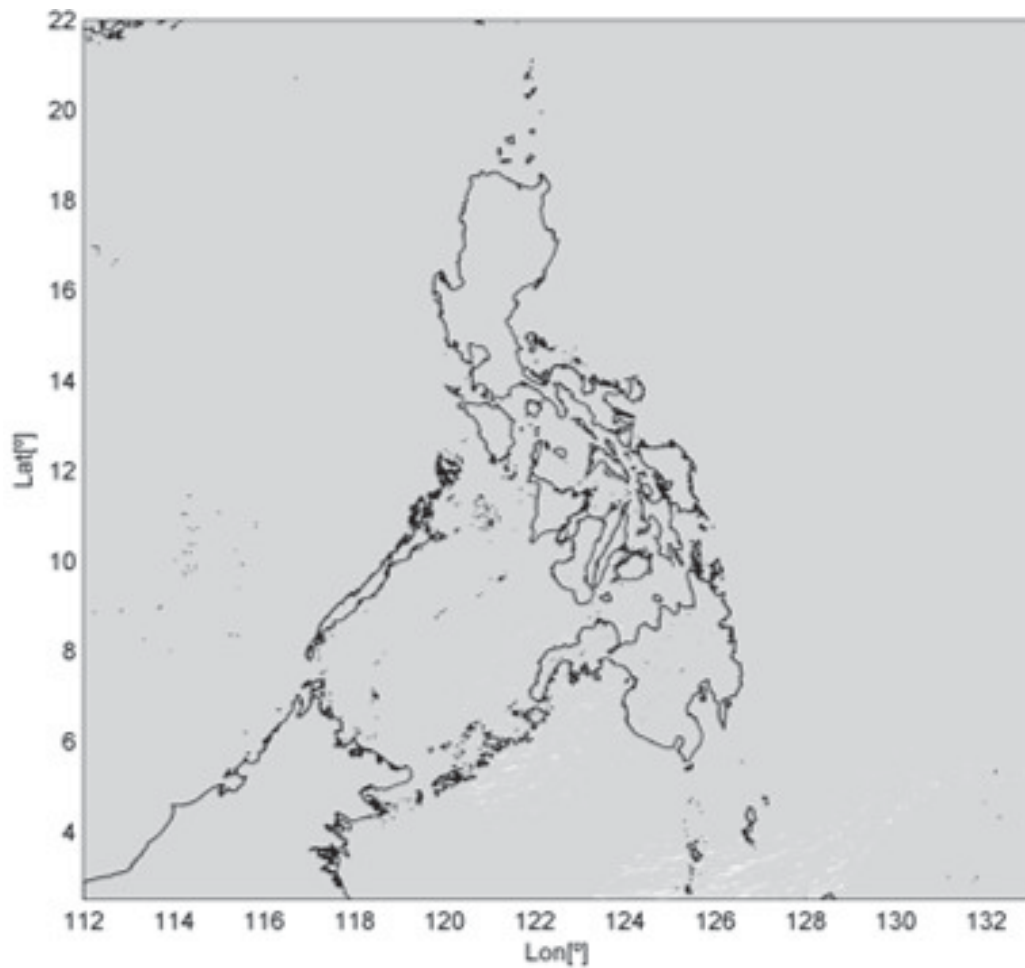
Figure 2.3 Tropical Cyclone tracks in the 5,000 year synthetic dataset.
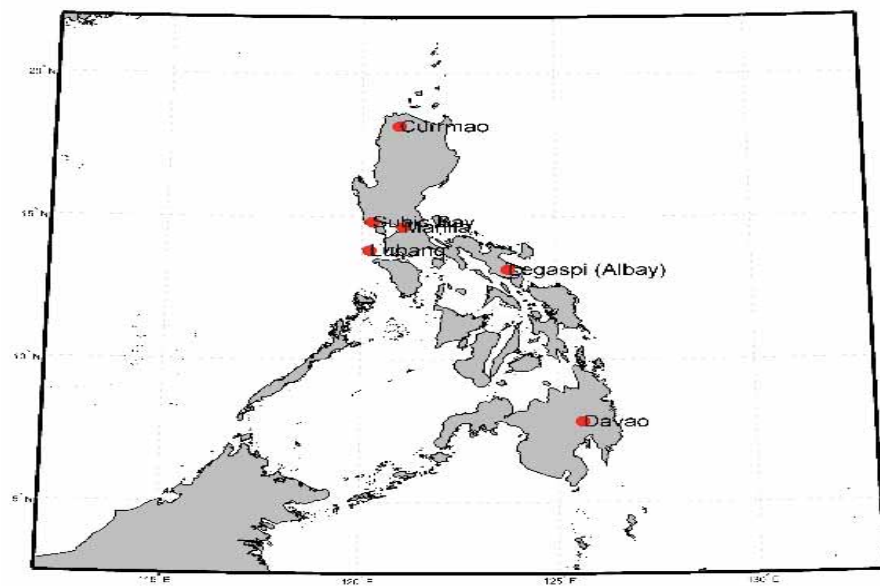
Figure 2.4 Location of the six tide gauges used in this study.
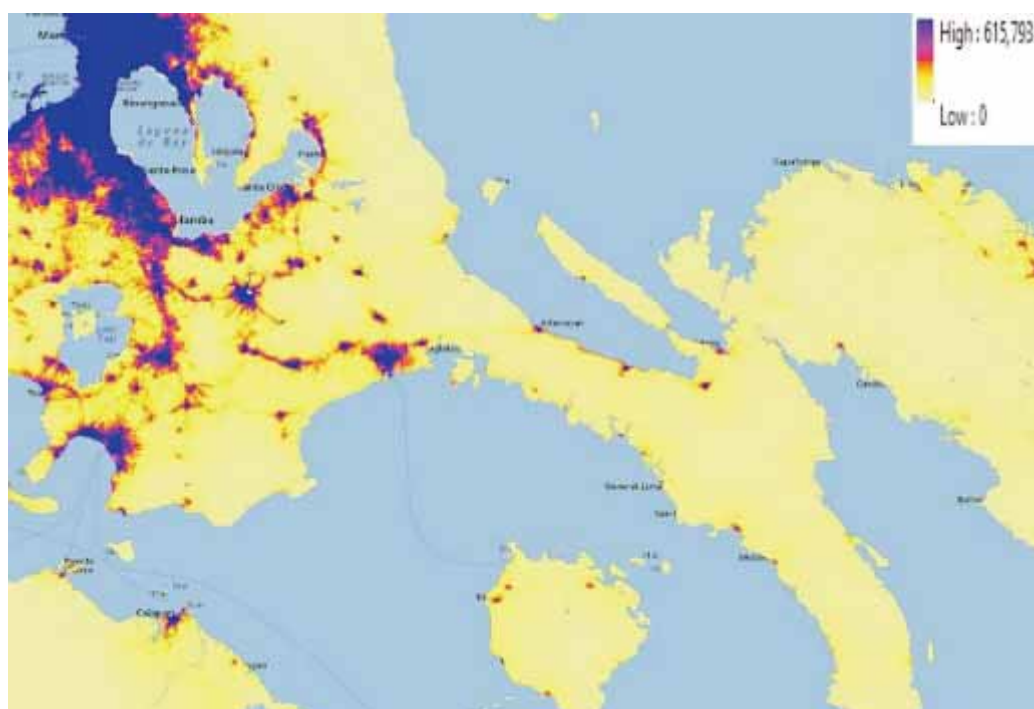
Figure 2.5 Example of WorldPop layer in Pagbilao and Manila areas in The Philippines in 2010 (People per hectare).

	STEP 0 (Coastal segmentation)	STEP 1 (Climatic Hazards Selection)	STEP 2 (Waves + Surge Propagation)	STEP 3 (Total Water Level Reconstruction)	STEP 4 (Flooding mask calculation)	STEP 5 (Socio-economic consequences)
REGULAR CLIMATE *(Whole Philippines)*	Profile construction and selection process (KMEANS)	Historical wave climate and Sea Level selection process nearshore (KMEANS)	Waves and Sea Level propagation over the habitat (1D profiles with DELFT3D)	TWL reconstruction in coast for 1, 10, 25 and 50 years return period events	Coastal flooding mask (bathtub flooding methodology with GIS) for 3 scenarios (mangrove cover 1950, mangrove cover 2010 and no mangroves)	Socio-economic consequences of coastal flooding
HISTORICAL TROPICAL CYCLONES *(Whole Philippines)*	Profile construction and selection process (KMEANS)	Nearshore Waves and Sea Level generated by historical TC (SWAN+DELFT3D). Selection process of representative TC (MAXDISS)	Waves and Sea Level propagation over the habitat (1D profiles with DELFT3D)	TWL reconstruction in coast for 10, 15, 20, 25, 30, 40, 50, 100, 150 and 200 years return period events	Coastal flooding mask (buthtub flooding methodology with GIS) for 3 scenarios (mangrove cover 1950, mangrove cover 2010 and no mangroves) and 4 Return Periods: 10, 15, 25 and 50 years	Socio-economic consequences of coastal flooding
SYNTHETIC TROPICAL CYCLONES *(Only Pagbilao coast)*	Profile construction and selection process (KMEANS)	Nearshore Waves and Sea Level generated by synthetic TC in Pagbilao (SWAN+DELFT3D). Selection process of representative TC (MAXDISS)	No propagation over 1D profile. We will use the interpolation database generated with the "Historical Tropical Cyclones" to interpolate TWL in coast in the following step	TWL interpolated for each of the synthetic tropical cyclones.	TWL interpolated for each of the synthetic tropical ciclones with a high resolution model (RFSM-EDA) and for 10, 15, 20, 25, 30, 40, 50, 100, 150 and 200 years return period	Socio-economic consequences of coastal flooding

Figure 3.1 Specific methodology to evaluate the coastal protection provided by mangroves against regular wave climate and Tropical Cyclones events in The Philippines. Step 0 has been additionally included to explain the pre-processing work in coastal segmentation. This step is specific of this projects and it has not been included in the general methodology (Figure 3 and Figure 1. 2 in the Annex)

71
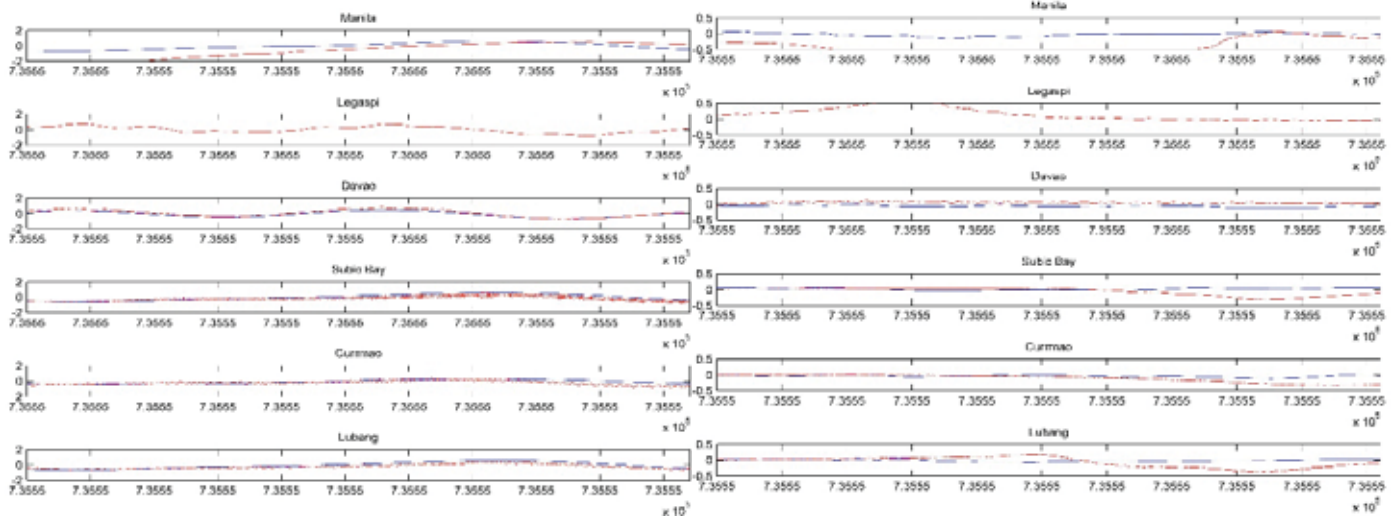
Figure 4.1 Validation of TWL generated by Haiyan Tropical Cyclone forced with Astronomical Tide+Wind+Waves (left). Validation of Storm Surge generated by Haiyan Tropical Cyclone forced with Wind (right). Red lines are the numerically simulated TWL and blue line are the field measurements of the TWL
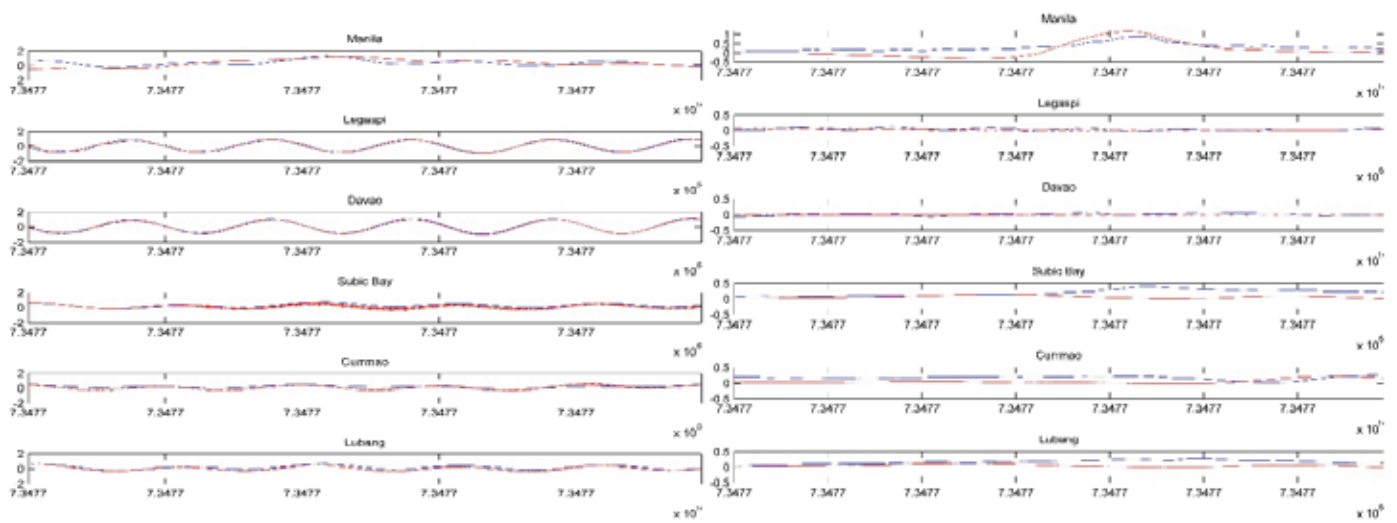
Figure 4.2 Validation of TWL generated by Nesat Tropical Cyclone forced with Astronomical Tide+Wind+Waves (left). Validation of Storm Surge generated by Nesat Tropical Cyclone forced with Wind (right). Red lines are the numerically simulated TWL and blue line are the field measurements of the TWL
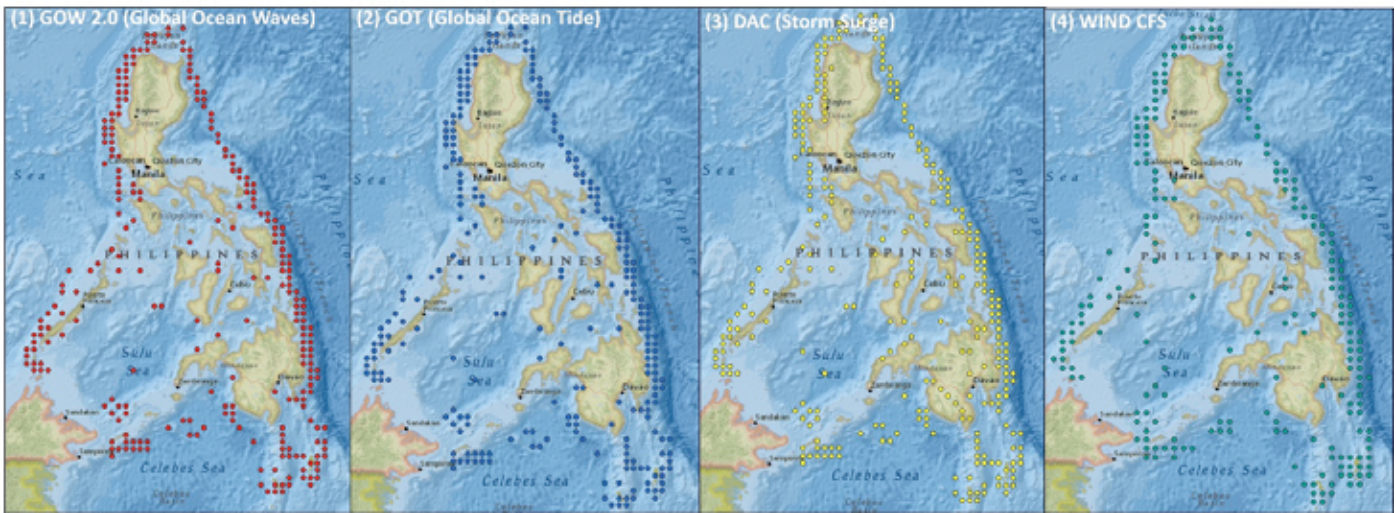
Figure 5.1 Offshore Ocean Dynamics database points: (1) Waves, (2) Astronomical Tide, (3) Storm Surge and (4) Wind
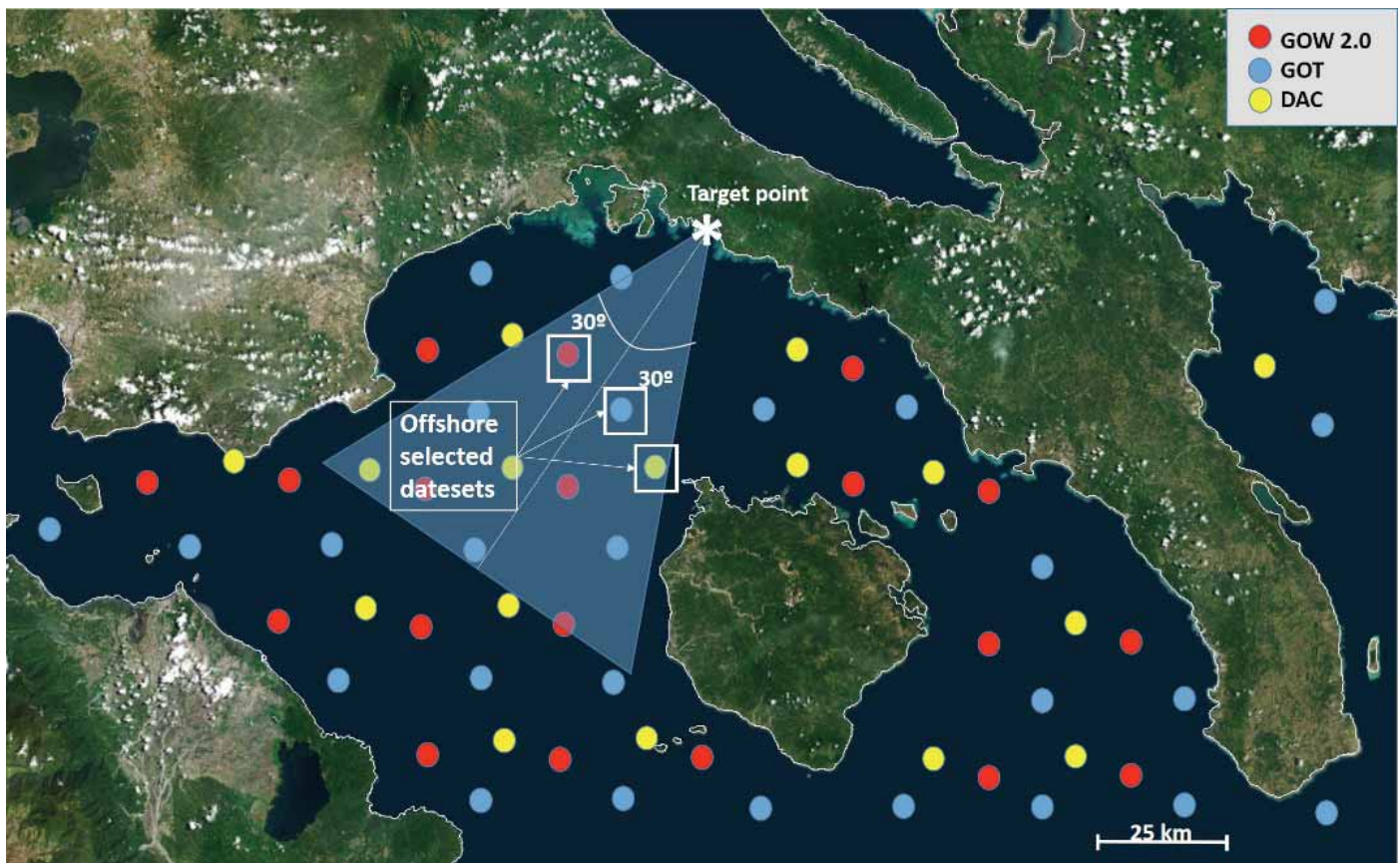
Figure 5.2 Offshore dynamics datasets selection method. Example of one point in the coast of Pagbilao
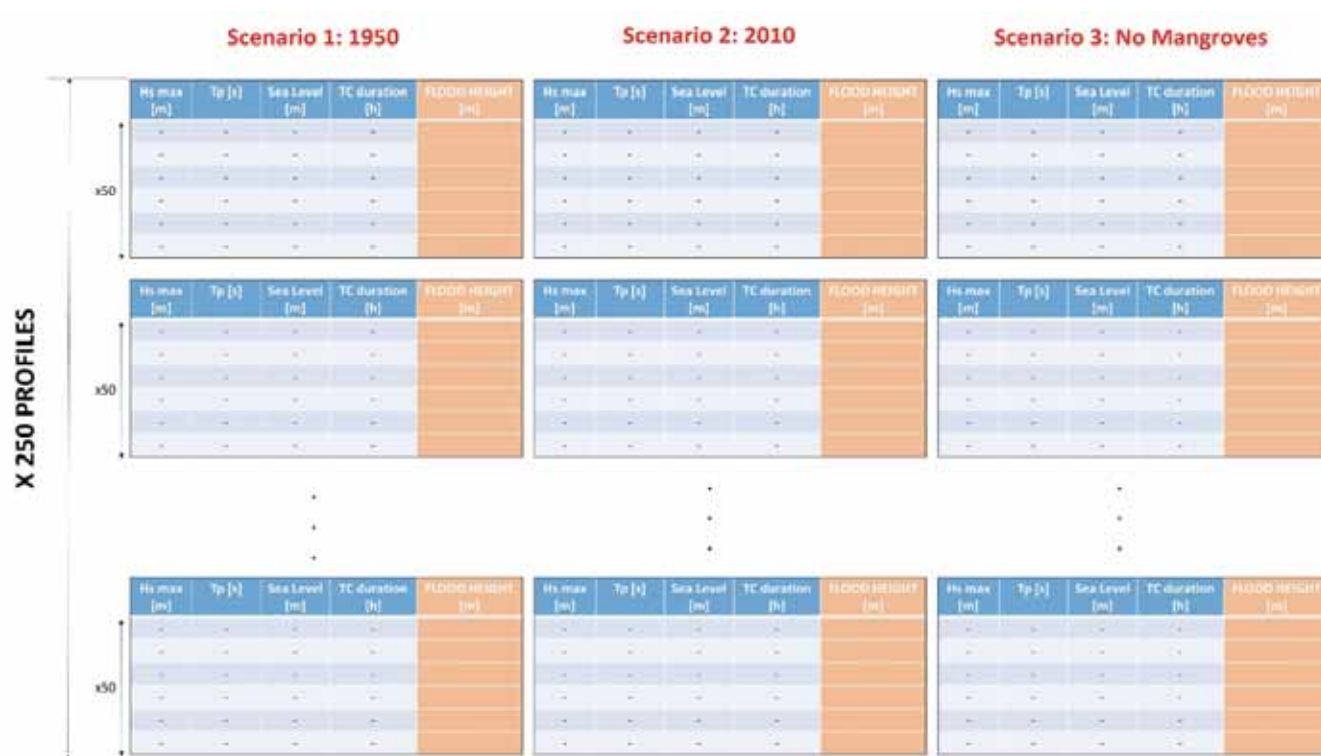
Figure 5.3 Interpolation table for Flood Height estimation. Values obtained from the maximum Total Water Level in coast provided by DELFT 3D runs. Note – to be completed later.
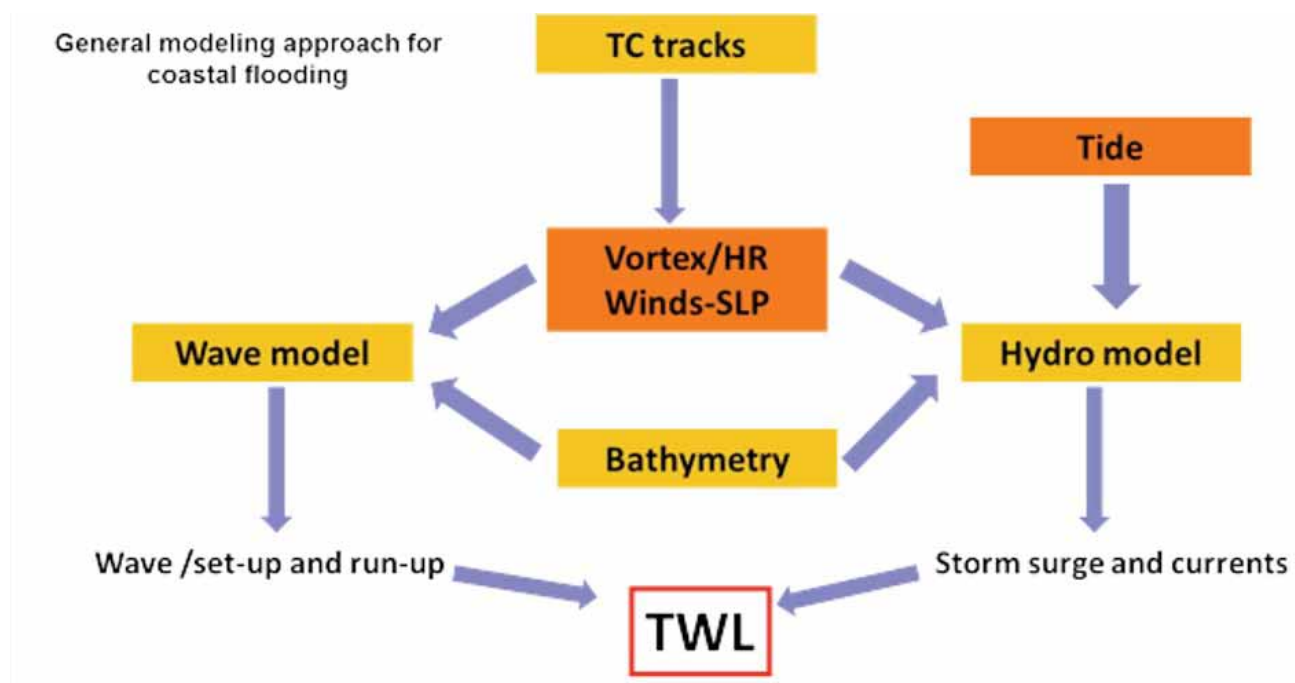
Figure 6.1: General scheme of the methodology used to obtain offshore total water level estimations.

Figure 6.2 The 5 Km grid used for the baseline storm surge study, coastal points where waves and sea levels are obtained are highlighted in cyan.
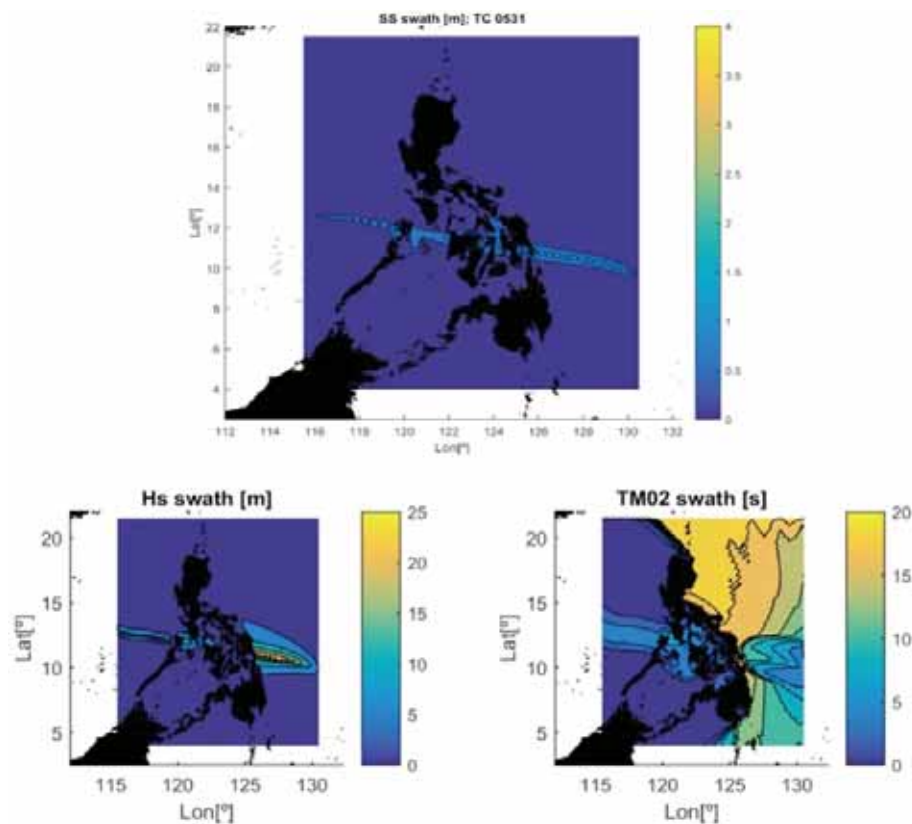
Figure 6.3 Maximum simulated storm surge produced by the Super Typhoon Haiyan (upper panel), significant wave height (bottom left panel) and wave mean period (bottom right panel).
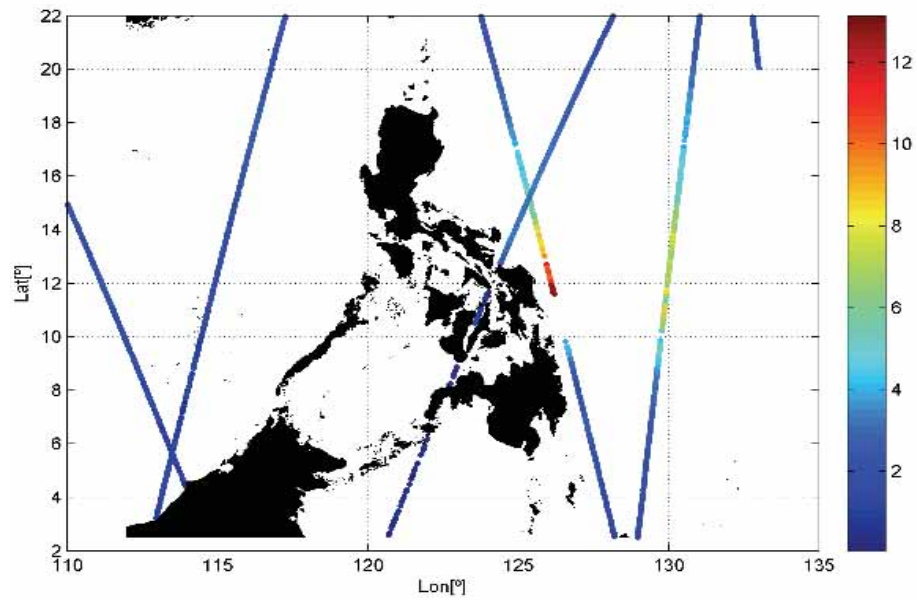
Figure 6.4 Altimeter significant wave heights (in meters) measured on November 8th, 2013
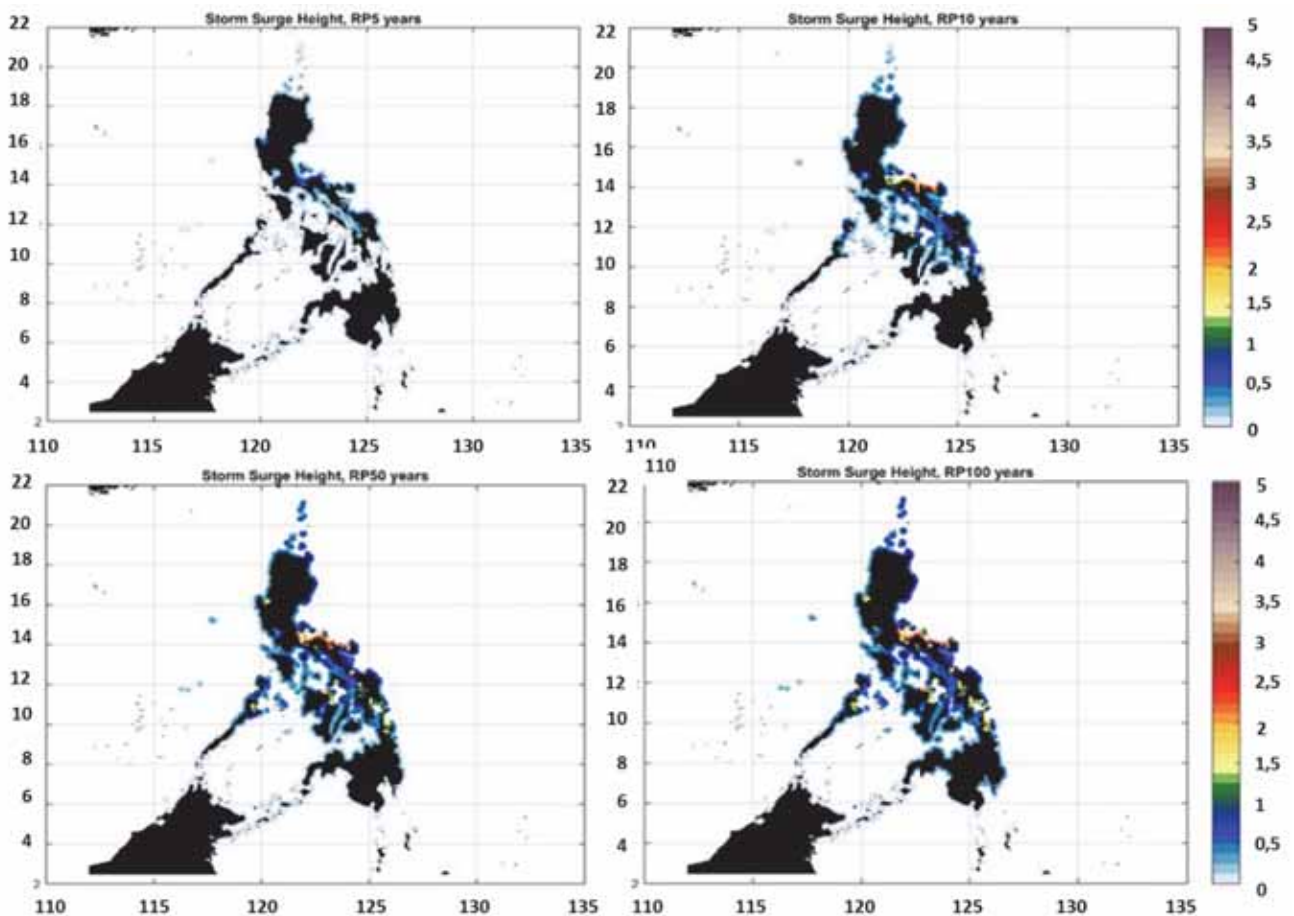
Figure 6.5 Storm surge (in meters above the mean sea level) due to wind set-up and the inverse barometer effect for 5, 10, 50 and 100 years return period.
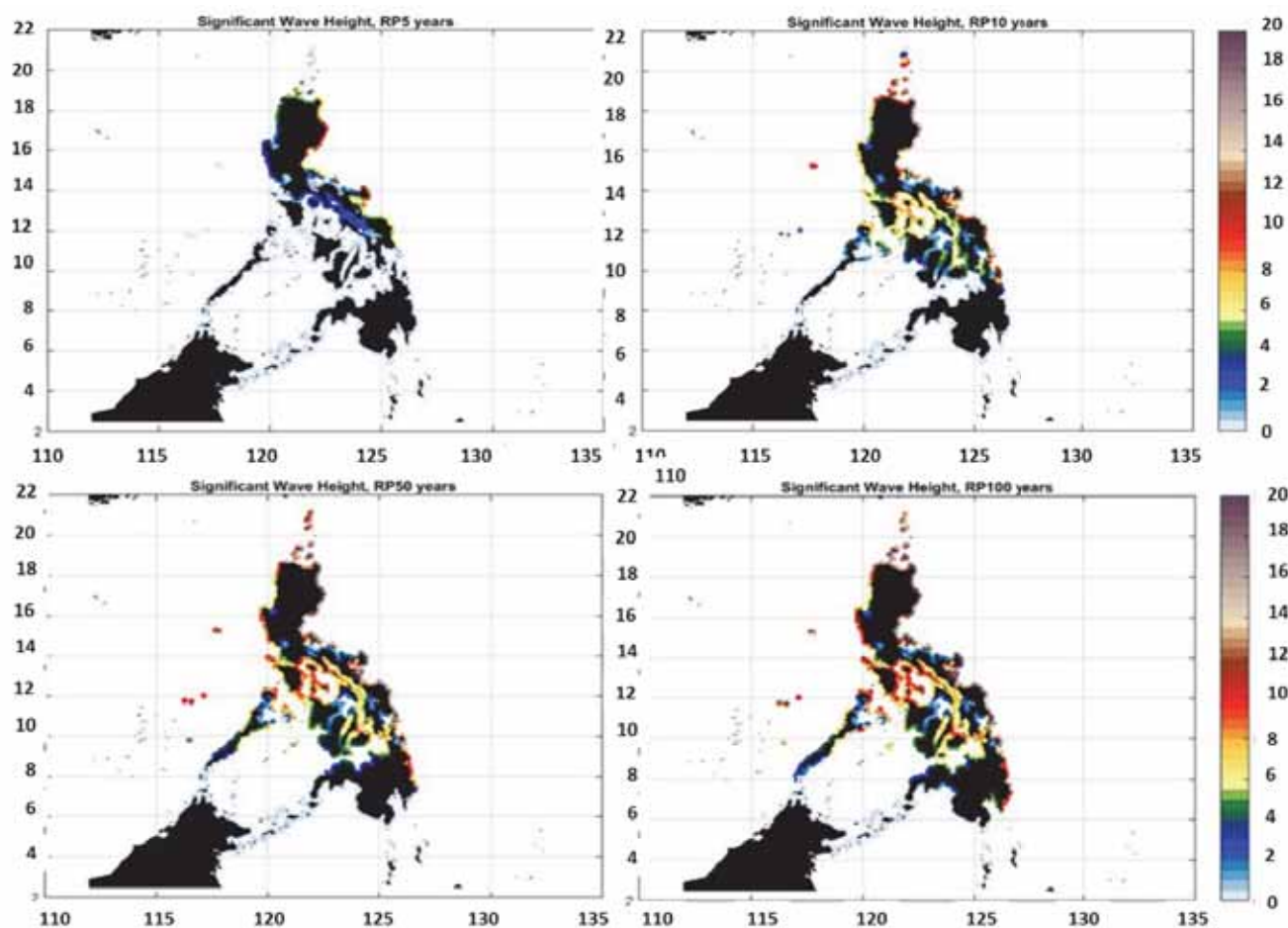
Figure 6.6 Significant wave heights (in meters) for 5, 10, 50 and 100 years return periods
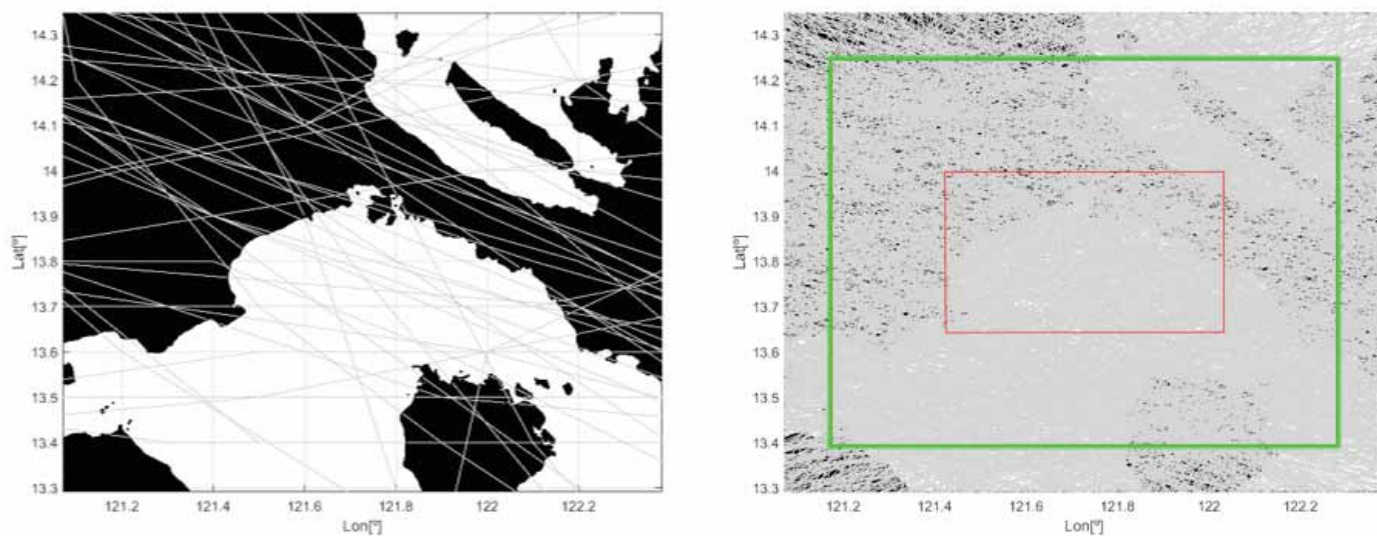
Figure 6.7 Comparison of the historical available tropical cyclone tracks against synthetic in Pagbilao
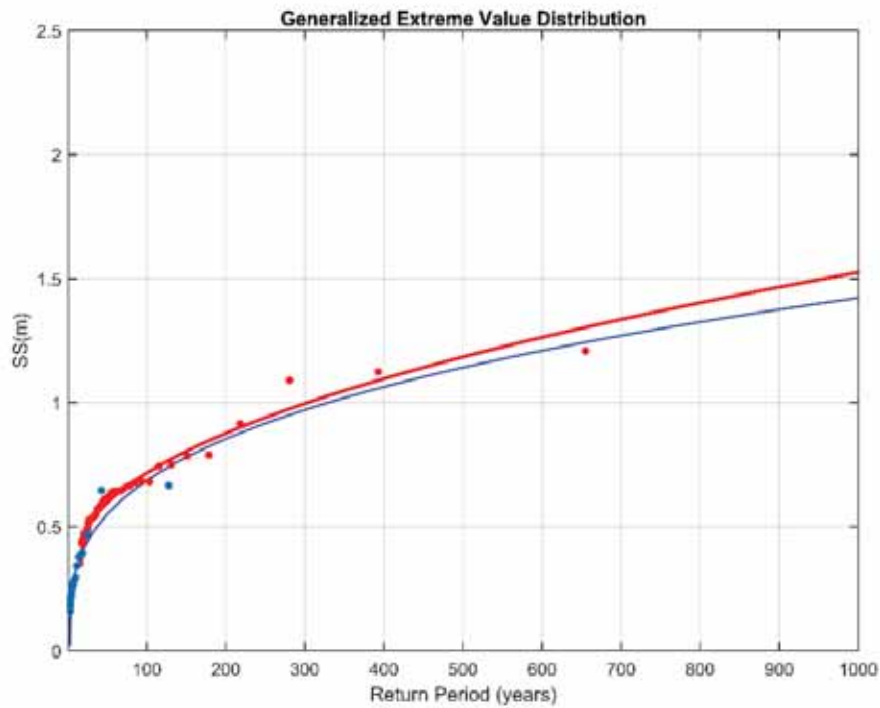
Figure 6.8 Comparison the generalized extreme value distributions in Pagbilao fitted to the historical data (blue dots and line) and synthetic (red dots and line).
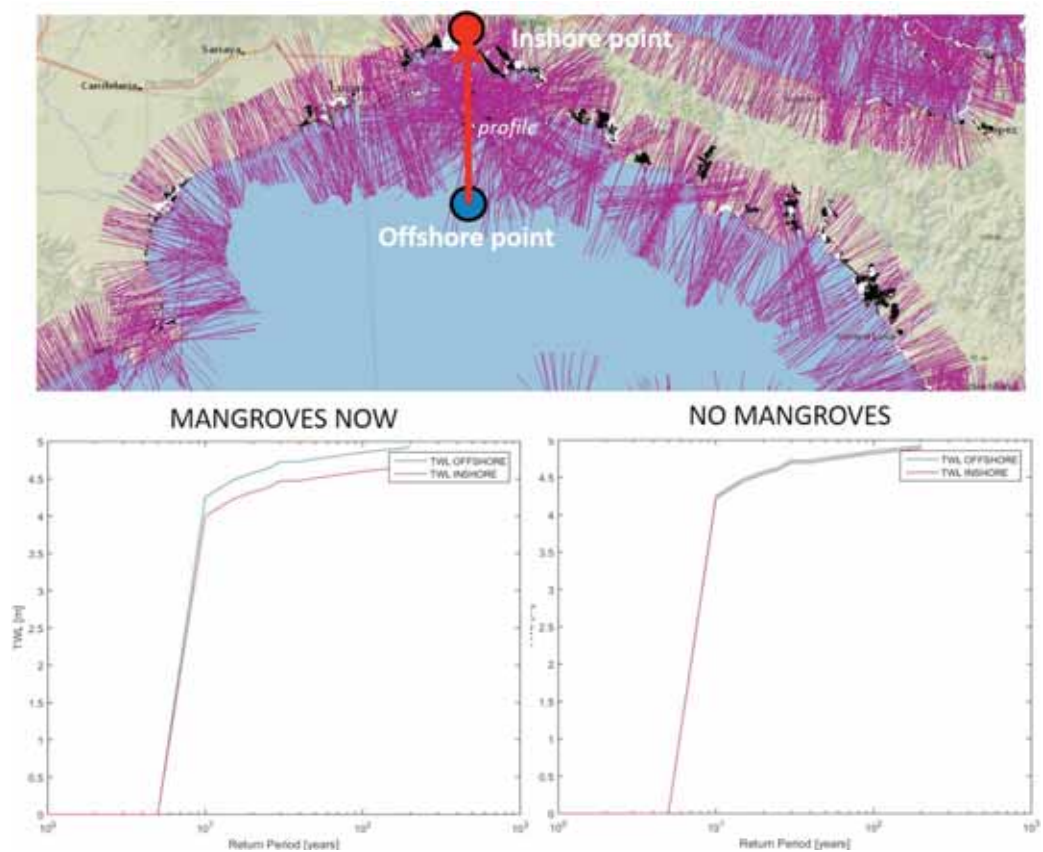
Figure 6.9 Total water level WL offshore versus Total Water Level inshore in one 1D profile of Pagbilao
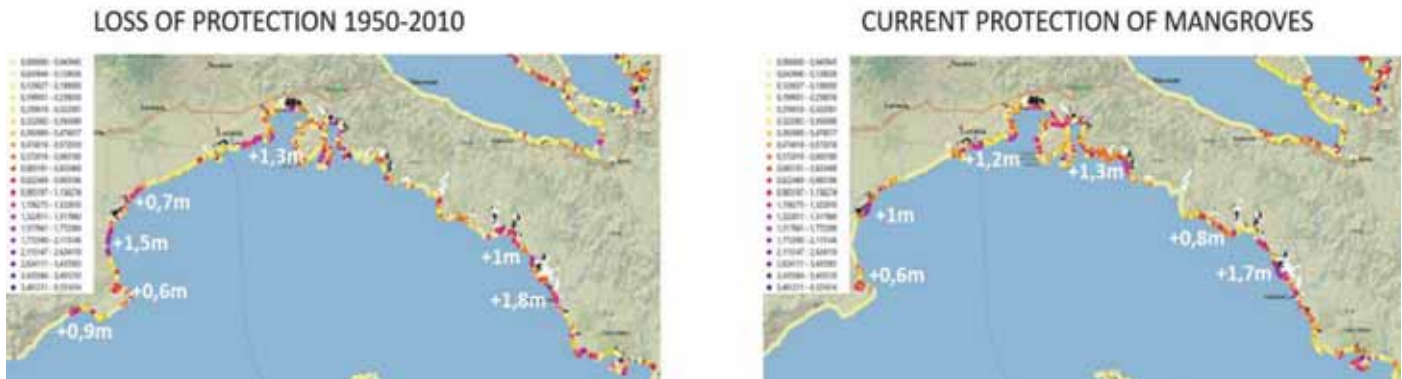
Figure 6.10 Predicted increase in Flood Height (1) Between Historical and Current Mangrove distribution and (2) Between Current and a No Mangroves scenario for a 25 year return period event considering tropical cyclone events.

Figure 6.11 Interpolation table for Flood Height estimation. Values obtained from the maximum Total Water Level in coast provided by DELFT 3D runs. NOTE – this table to be completed later.
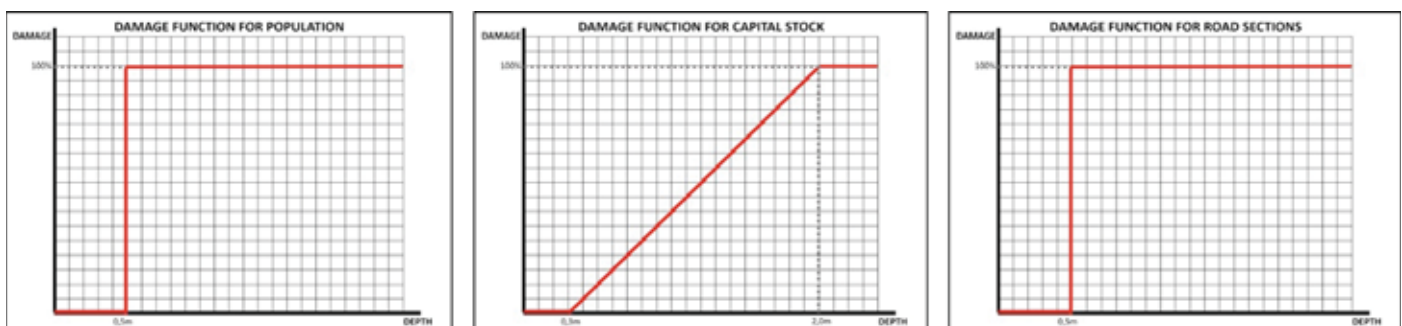

Figure 9.1 Damage functions of people and people below poverty level (left), residential and industrial stock (middle) and road network (right). They represent the percentage of damage at each flooding height level
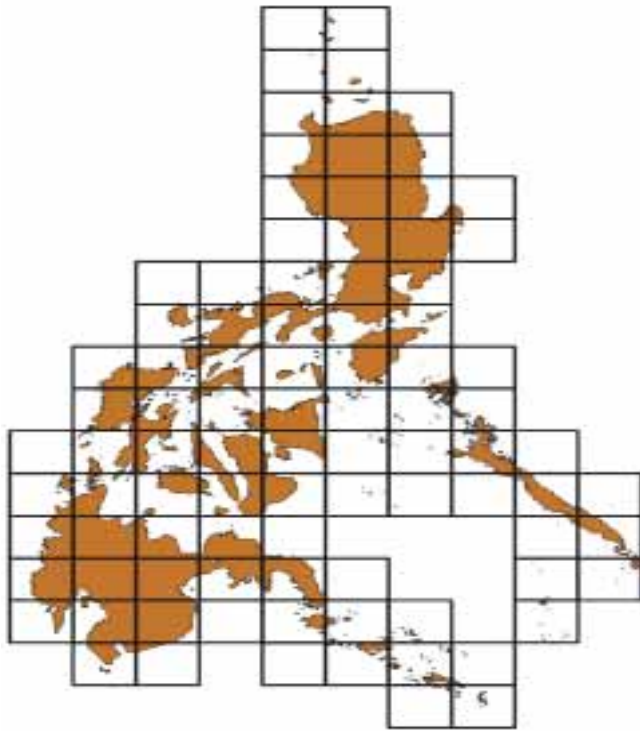
Figure 9.2 The Philippines sections in which the country was divided for optimize the computation cost

Figure 9.3 National distribution of the Annual Potential Benefits provided by mangroves to people in the Philippines (25 km aggregation units)

Figure 9.4 National distribution of the Annual Potential Benefits provided by mangroves to people below poverty in the Philippines (25 km aggregation units)

Figure 9.5 National distribution of the Annual Potential Benefits provided by mangroves to the total stock (industrial + residential) in the Philippines (25 km aggregation units)

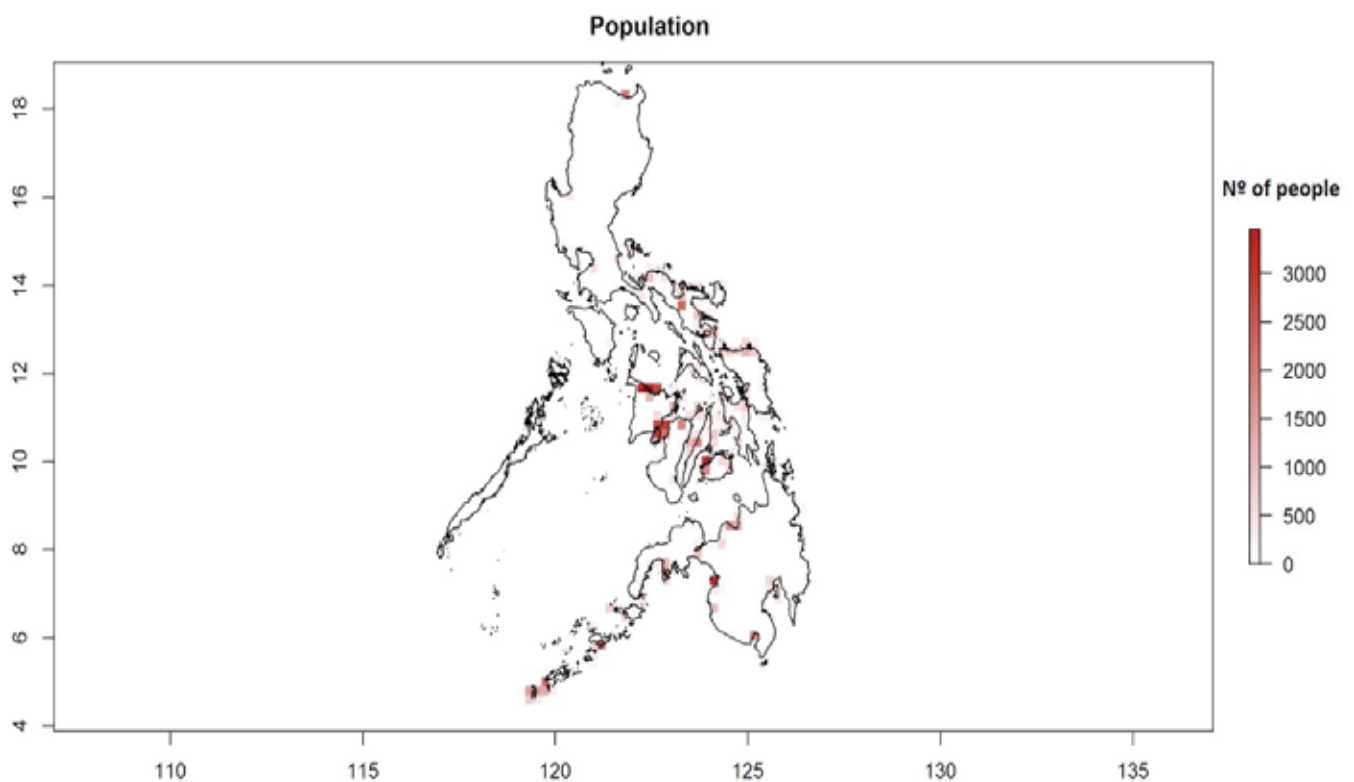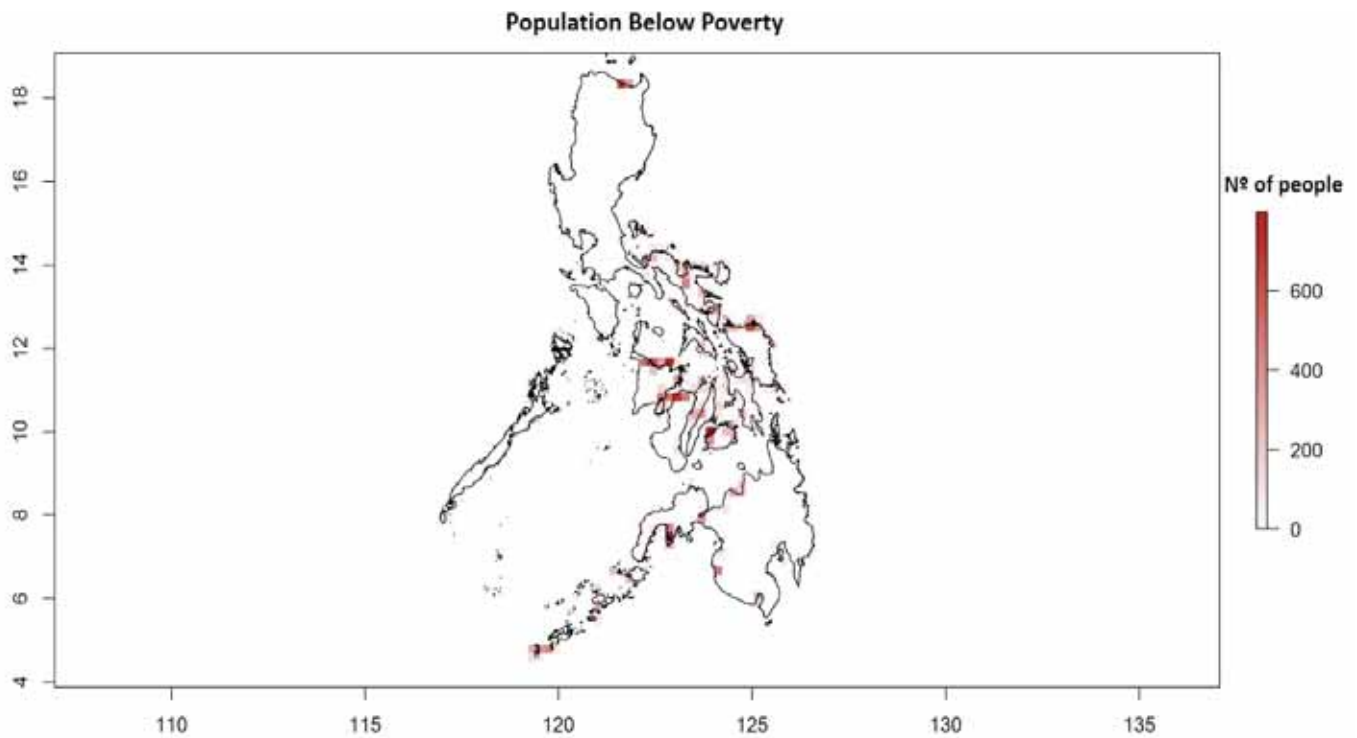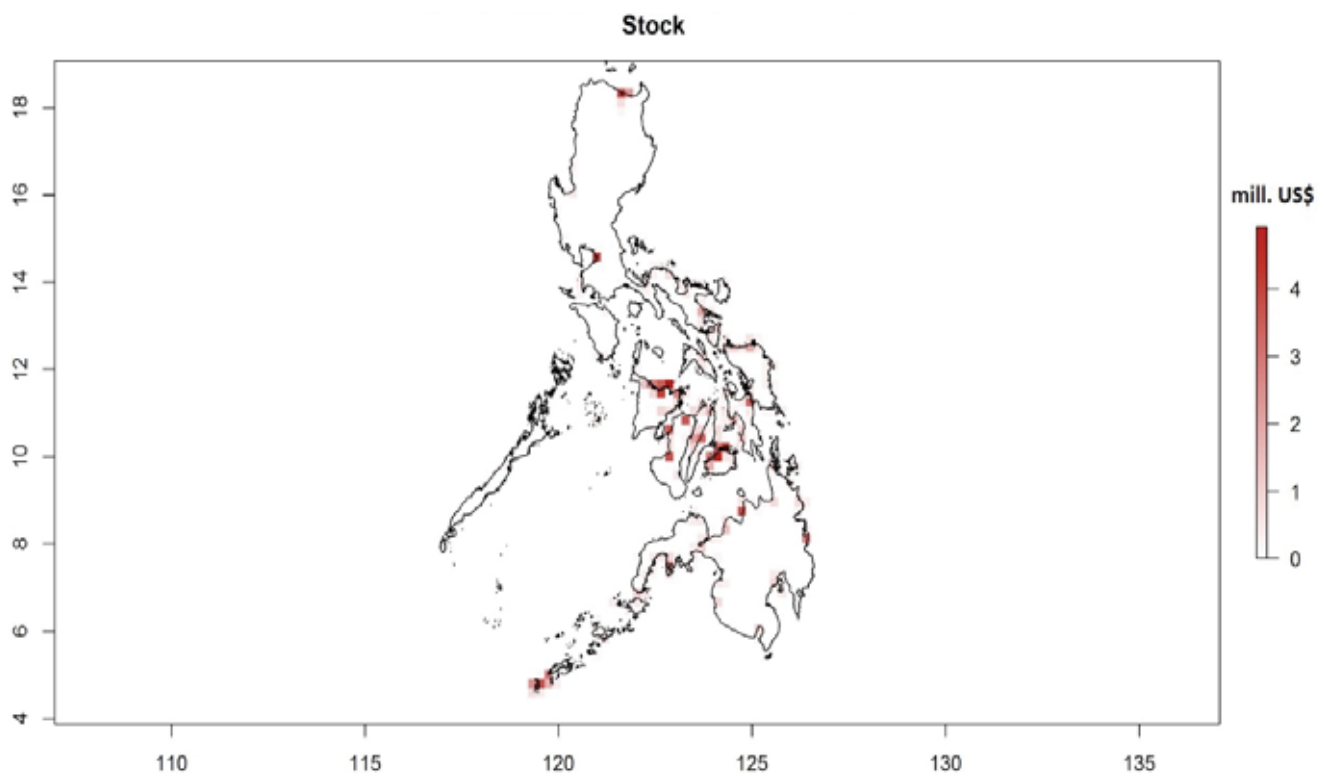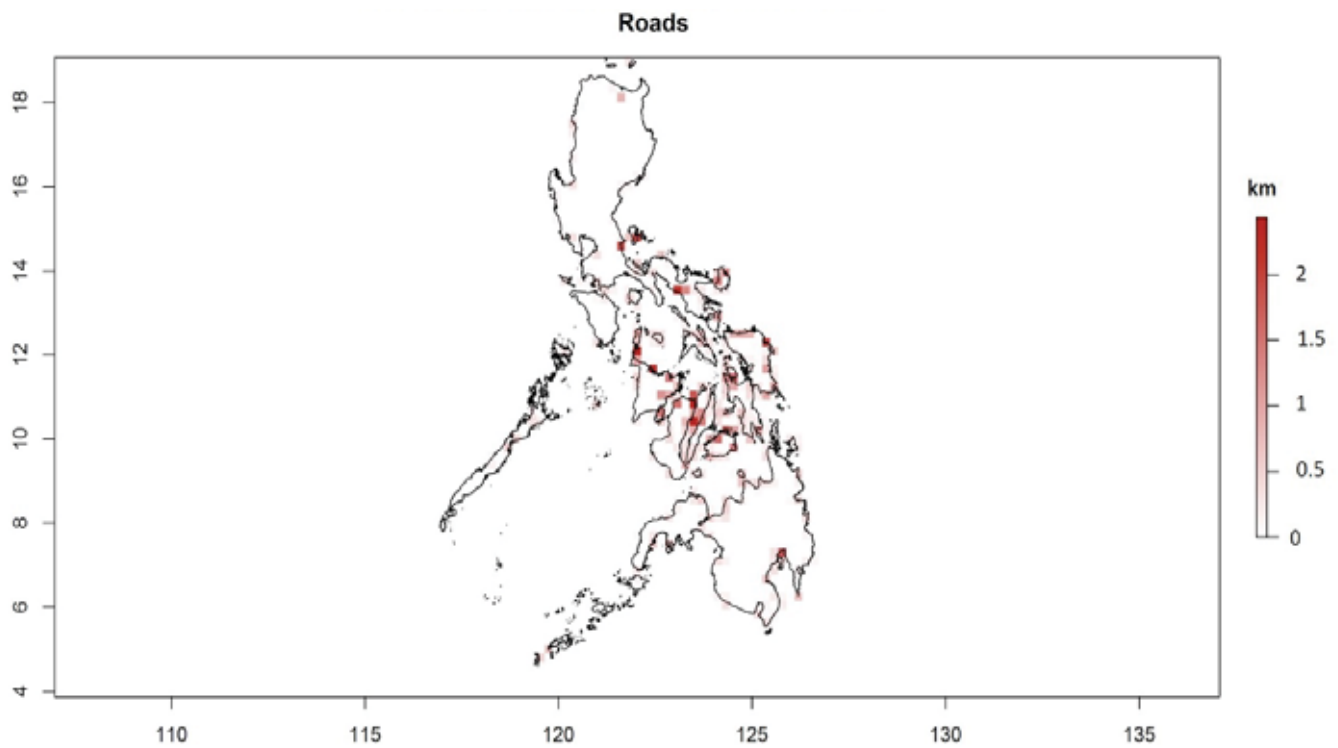**Figure 9.6** National distribution of the Annual Potential Benefits provided by mangroves to roads in the Philippines (25 km aggregation units)

Annex 2 | Physics and Governing Equations

Delft 3D model has been used in this project to propagate waves and storm surge induced by Tropical Cyclones and regular storms in the Philippines. The Delft3D modeling suite is composed of several modules of which this study utilizes the Delt3d-FLOW and Delft3d-WAVE modules.

The FLOW module has been implemented to calculate the contribution of the storm surge and astronomical tide to the Total Water Level. It has been externally forced with the offshore water level calculated at the beginning of each profile (offshore water level is the linear summation of offshore storm surge and astronomical tide). The FLOW module assumes shallow water Boussinesq approach to solve the Navier Stokes equations for incompressible fluid (depth average continuity equations and momentum equations are simultaneously solved in 2D mode).

WAVE module has been implemented to calculate wave set-up contribution to the Total Water Level in the coast. Wave radiation stresses and their gradients are computed and shared to the hydro dynamic model on the same mesh used in the hydrodynamic simulation. A wide range of validation cases (explained in the following sections), support Delft3D model.

In this project, flow and waves are simultaneously simulated by coupling SWAN model (waves) with DELFT 3D (flow). The wave computation uses flow characteristics from a completed Delft3D-FLOW computation, so that the effect of flow on waves is accounted for.

Coupled Delft 3D model (flow+wave) account for the following physics:

- Wave refraction over a bottom of variable depth and/or a spatially varying ambient current

- Depth and current-induced shoaling

- Wave generation by wind

- Wave dissipation by white capping

- Dissipation by depth-induced breaking

- Dissipation due to bottom friction (three different formulations)

- Nonlinear wave-wave interactions (both quadruplets and triads)

- Wave blocking by flow

- Transmission through, blockage by or reflection against obstacles

- Diffraction

The governing three-dimensional equations describing free-surface flows can be derived from the Navier-Stokes equations after averaging over turbulence time-scales (Reynolds-averaged Navier-Stokes equations). Such equations express the physical principle of conservation of volume, mass and momentum.

In this section, we describe the shallow water equations, for which the depth is assumed to be much smaller than the horizontal length scales of flow and bathymetry. Under the further assumption that the vertical accelerations are small compared to the horizontal ones the shallow water assumption is valid. This means that the vertical momentum equation is reduced to the hydrostatic pressure relation. The equations in case of a non-hydrostatic pressure are described in a separate section. In the latter case, non-hydrostatic pressure terms are added to the shallow water equations, which make the equations practically equivalent to the

incompressible Navier-Stokes equations. This means that in Delft3D-FLOW the user has the possibility to either apply a hydrostatic or a non-hydrostatic pressure model.
The three-dimensional hydrostatic shallow water equations, which for convenience of presentation are given in Cartesian rectangular coordinates in the horizontal and V-coordinates in the vertical, are described by:

$$\frac{\partial u}{\partial t} + u\frac{\partial u}{\partial x} + v\frac{\partial u}{\partial y} + \frac{w}{d+\zeta}\frac{\partial u}{\partial \sigma} - f_v = -\frac{1}{\mu}P_u - F_u + \frac{1}{(d-\zeta)^2}\frac{\partial}{\partial \sigma}\left(v\frac{\partial u}{\partial \sigma}\right) \qquad (5.1)$$

$$\frac{\partial v}{\partial t} + u\frac{\partial v}{\partial x} + v\frac{\partial v}{\partial y} - \frac{w}{d+\zeta}\frac{\partial v}{\partial \sigma} - f_u = -\frac{1}{\mu}P_r + F_r + \frac{1}{(d+\zeta)^2}\frac{\partial}{\partial \sigma}\left(v\frac{\partial v}{\partial \sigma}\right) \qquad (5.2)$$

$$\frac{\partial w}{\partial \sigma} = -\frac{\partial \zeta}{\partial t} - \frac{\partial[(d+\zeta)u]}{\partial x} - \frac{\partial[(d+\zeta)v]}{\partial y} + H(q_{in} - q_{out}) + P - E \qquad (5.3)$$

Where are the three directional components of velocity, is the local water depth, is the water level oscillation with respect the mean water level, is the coriolis coefficient, is the total water depth (), are the local source and sink per unit volume and is the hydrostatic pressure.
The vertical velocities Z in the V-coordinate system are computed from the continuity equation, where the global source or sink per unit area and are the depth-average velociety in x-direction and y-direction.

$$\frac{\partial \zeta}{\partial t} - \frac{\partial[(d+\zeta)U]}{\partial x} + \frac{\partial[(d+\zeta)V]}{\partial y} = Q \qquad (5.4)$$

by integrating in the vertical from the bottom to a level. The (comparatively small) vertical velocity w in the x-y-z Cartesian coordinate system can be expressed in the horizontal velocities, water depths, water levels and vertical velocities according to:

$$w = \omega + u\left(\sigma\frac{\partial H}{\partial x} - \frac{\partial \zeta}{\partial x}\right) + v\left(\sigma\frac{\partial H}{\partial y} + \frac{\partial \zeta}{\partial y}\right) + \left(\sigma\frac{\partial H}{\partial t} - \frac{\partial \zeta}{\partial t}\right) \qquad (5.6)$$

Annex 3 | Computational Cost and Hard Disk Memory Required

An additional analysis of DELFT 3D was carried out, consisting in measuring the computational cost and the memory required to save results under different forcing conditions. The test case characteristics are the following:

- 4 days length Tropical Cyclone (Haiyan)

- 56 control points with time records every minute

- Time records every hour in the whole mesh (302x352 =106304 cells)

Case	Computational cost (min)	Memory (MB)
Astronomical Tide	5	793
Wind	7	1200
Wind+ Astronomical Tide	7	1200
Wind+Astronomical Tide +Waves(swell)	104	1600
Wind+Astronomical Tide +Waves(wind)	104	1600
Wind+Waves(wind)	104	1600

Table 12 Computational cost and memory required for Natianal scale 2D simulations with Delft 3D under different forcing methods

References Cited

Amante C, Eakins BW. 2009. ETOPO1 1 arc-minute global relief model: procedures, data sources and analysis. National Oceanic and Atmospheric Administration.

Beck MW. 2014. Coasts at Risk: An assessment of coastal risks and the role of environmental solutions. Narrangansett.

Beck MW, Losada I, Menendez O, Reguero BG, Diaz Simal P, Fernandez F. In review. The global flood protection savings provided by coral reefs. Nature Communications.

Burke L, Reytar K, Spalding M, Perry A. 2011. Reefs at risk revisited. WRI.

Camus P, Mendez FJ, Medina R. 2011a. A hybrid efficient method to downscale wave climate to coastal areas. Coastal Engineering 58:851-862.

Camus P, Mendez FJ, Medina R, Cofiño AS. 2011b. Analysis of clustering and selection algorithms for the study of multivariate wave climate. Coastal Engineering 58:453-462.

Carrère L, Lyard F. 2003. Modeling the barotropic response of the global ocean to atmospheric wind and pressure forcing - comparisons with observations. Geophysical Research Letters 30:DOI: 10.1029/2002GL016473.

Cid A, Castanedo S, Abascal AJ, Menéndez M, Medina R. 2014. A high resolution hindcast of the meteorological sea level component for Southern Europe: the GOS dataset. Climate Dynamics 43:1-18.

Cid Carrera A. 2015. Modelado Numérico y Estadístico de la Componente Meteorológica del Nivel del Mar a Escala Regional y Global. Numerical and Statistical Modelling of the Atmospheric Surge at Regional and Global Scale.

De Bono, Andrea, Bruno Chatenoux. 2015. A Global Exposure Model for GAR 2015, UNEP/Grid, Geneva. Background Paper prepared for the 2015 Global Assessment Report on Disaster Risk Reduction. Geneva, Switzerland: UNISDR.

DRR Platform. 2014. Disaster Risk Reduction and Management in the Philippines. A desk study conducted by the Swiss NGO DRR Platform following Typhoon Haiyan, Luzerne, July 2014. Available at http://www.drrplatform.org/images/DocPub/RiskAssessment.pdf

Egbert GD, Erofeeva SY. 2002. Efficient inverse modeling of barotropic ocean tides. Journal of Atmospheric and Oceanic Technology 19:183-204.

Hamilton LS, Dixon JA, Miller GO. 1989. Mangrove forests: an undervalued resource of land and the sea. Pages 254-288 in Borgese EM, Ginsburg N, Morgan JR, eds. Ocean Yearbook 8, University of Chicago Press,.

Myers N. 1998. Environmental degradation and some economic consequences in the Philippines. Environmental Conservation 15:205-214.

NEDA. 2017. Philippine Develpoment Plan 2017-2022. Pasig City. Report no.

Nunes V, Pawlak G. 2008. Observations of bed roughness of a coral reef. Journal of Coastal Research 24:39-50.

Perez, J., Menendez, M., Losada, I.J. 2017 GOW2: A global wave hindcast for coastal applications.
Coastal Engineering, 124: 1-11.

Primavera JH. 1991. Intensive prawn farming int he Philippines: ecological, social and economic implications. Ambio 20:28-33.

---. 1995. Mangroves and brackish water pond culture in the Philippines. Hydrobiology 295:303-309.

Spalding MD, Kainuma M, Collins L. 2010. World mangrove atlas. Earthscan.

UNISDR. 2011. Global assessment report on disaster risk reduction revealing risk, redefining development. UN.

---. 2015a. Annual Report 2014. United Nations Office for Disaster Risk Reduction.

---. 2015b. Making development sustainable: the future of disaster risk management, global assessment report on disaster risk reduction. United Nations Office for Disaster Risk Reduction.

---.2015c Global assessment report on disaster risk reduction 2015. GAR Global Risk Assessment: Data, Methodology, Sources and Usage.

Walters BB. 1997. Human ecological questions for tropical restoration: experiences from planting native upland trees and mangrove in the Philippines. Forest Ecology and Management 99:275-290.

World Bank. 2016. Managing coasts with natural solutions: Guidelines for measuring and valuing the coastal protection services of mangroves and coral reefs. (eds M. W. Beck, G-M Lange). Washington, DC: World Bank. Report no.

World Risk Report. 2016. World Risk Report: Logistics and infrastructure. Berlin. Report no.

Zedler JB, Kercher S. 2005. Wetland resources: status, trends, ecosystem services, and restorability. Annual Review of Environment and Resources 30:39-74.

Zhang K, Liu H, Li Y, Xu H, Shen J, Rhome J, Smith Iii TJ. 2012. The role of mangroves in attenuating storm surges. Estuarine, Coastal and Shelf Science 102–103:11-23.